**UNIVERSITÉ DE BLIDA 1**

**Faculté de Technologie**
Département d'Automatique et Électrotechnique

# THÈSE DE DOCTORAT

en Automatique

# Contrôle de la formation de plusieurs robots mobiles à roues non holonomes

Par
**ALLAEDDINE YAHIA DAMANI**

Devant le jury composé de:

| | | |
|---|---|---|
| A. FERDJOUNI | Professeur, U. de Blida 1 | Président |
| A. MADDI | MCA, U. de Blida 1 | Examinateur |
| A. HOCINE | MCA, U. de Khemis Miliana | Examinateur |
| Z.A BENSELAMA | Professeur, U. de Blida 1 | Directeur de thèse |
| R. HEDJAR | Professeur, U. de Roi SAOUD | Co-directeur de thèse |

U. Blida 1, 14/04/2024

# DEDICATION

I dedicate this work to my dear father *MEHANI* and my kind aunt *OUMELKHIR* who supported me in the whole course of my life, until the last day of their lifes. May **ALLAH** have mercy on their precious souls and grant them paradise.

Also, I dedicate this modest work as a sign of my great respect to my dear mother, *NAIL ZOULIKHA*, for all her sacrifices, love, tenderness, support, and prayers throughout my studies. May **ALLAH** protect your health and grant you a long life.

To my brothers, sister, grandparents, uncles, aunts, friends and colleagues who shared their words of advice and encouragement to finish this PhD work.

# ACKNOWLEDGEMENT

First and foremost, I thank **ALLAH** almighty, all powerful, to have given me the strength to survive, as well as the audacity and the patience to overcome all the difficulties.

The work presented in this thesis was carried out at the University of Blida 1, Department of Automation and Electrotechnics, Faculty of Technology, Blida, Algeria, under the supervision of Mr. **BENSELAMA ZOUBIR ABDESALEM**, Professor at the University of Blida 1, who supervised me throughout this thesis and who shared with me his brilliant intuitions. May he also be thanked for his availability and for the numerous encouragements that he lavished on me.

My heartfelt thanks to Mr. **HEDJAR RAMDANE** Professor at the University of King SAUD for sharing his experience and valuable suggestions and for his greatest help and guidance throughout this research journey.

I express my gratitude to Mr. **FERDJOUNI ABDELAZIZ**, Professor at the University of Blida 1, who agreed to chair the jury of this thesis.

My thanks also go to Mr. **HOCINE ABDELFETTAH**, professor at the University of Khemis Miliana, and Mr. **MADDI ABDELKADER**, professor at the University of Blida 1, who agreed to be examiners.

# ABSTRACT

Formation control of wheeled nonholonomic mobile robots has advanced significantly in the past few decades, and currently is regarded as a crucial research subject in the domains of multi-agent systems and robotics. This resulted from its potential in a wide range of real-world applications, including search and rescue operations, exploration and large object transportation. Where it has be proven that it can be more efficient in achieving such complex missions compared to using a single robot, as it allows for parallel execution of tasks and increased overall system capabilities.

However, formation control of nonholonomic wheeled mobile robots can face several challenges. For example, the nonholonomic constraints that restricts the robot's motion, which require careful consideration in the modeling phase and during the control design. As well as, the presence of uncertainties and disturbances in the robot's dynamics which require the design of robust and adaptive control strategies.

In this thesis, the formation control problem is investigated by proposing three different control approaches. Firstly, we explore the leader-follower formation strategy via fuzzy fractional integral sliding mode control. This control scheme enables the follower robots to accurately track the leader and achieve the desired formation pattern, despite the presence of external disturbances and uncertainties.

Secondly, an adaptive distributed fractional fast terminal sliding mode control is introduced. This controller aims to accomplish a rapid and finite-time convergence of the robot towards the desired formation. The controller is developed using the consensus approach, which make it suitable for large multi robot systems as it requires less communication links between the robots.

Lastly, a discrete predictive sliding mode control is developed for formation control of nonholonomic robots. Such control synthesis can lead to a well accomplished formation with a robust, chattering free and constrained control laws.

To demonstrate the effectiveness and efficiency of the proposed controllers, comparative studies are conducted. The results highlight improved formation tracking, robustness to uncertainties and disturbances, and ability to achieve complex formation patterns.

# RESUME

Le contrôle de formation des robots avec roues non holonomes a considérablement progressé au cours des dernières décennies et est actuellement considéré comme un sujet de recherche crucial dans les domaines des systèmes multi-agents et de la robotique. Cela résulte de son potentiel dans un large éventail d'applications réelles, notamment les opérations de recherche et de sauvetage, l'exploration et le transport de gros objets. Il a été prouvé que le contrôle de la formation peut être plus efficace pour réaliser des missions aussi complexes que l'utilisation d'un seul robot, car il permet l'exécution parallèle de tâches et augmente les capacités globales du système.

Cependant, le contrôle de la formation de robots mobiles à roues non holonomes peut être confronté à plusieurs défis. Par exemple, les contraintes non holonomiques qui limitent le mouvement du robot, qui nécessitent une attention particulière lors de la phase de modélisation et lors de la conception du contrôle. Ainsi que la présence d'incertitudes et de perturbations dans la modéle dynamique du robot qui nécessitent la conception de stratégies de contrôle robustes et adaptatives.

Dans cette thèse, trois différentes approches de contrôle sont proposé pour étudié le problème de contrôle de la formation. Premièrement, nous explorons la contrôle de formation on ultilisant la stratégie leader-suiveur via un controlleur robuste basé sur la logique flou, calcule fractionnaire et intégral mode glissant. Ce système de contrôle permet aux robots suiveurs de suivre avec précision son leader et d'obtenir le configuration de formation souhaité, malgré la présence de perturbations et d'incertitudes externes.

Deuxièmement, une commande distribué adaptatif de fractionnaire mode glissant est introduit. Ce contrôleur vise à réaliser une convergence rapide et en temps fini du robots vers la formation souhaitée. Le contrôleur est développé en utilisant l'approche consensuelle, ce qui le rend adapté aux grands systèmes multi-robots car il nécessite moins de communication entre les robots.

Finalement, une commande prédictive discrète en mode glissant est développée pour le contrôle de formation de robots non holonomes. Une telle synthèse de contrôle peut

conduire à une formation bien accomplie avec une performance de taux de convergence rapide et sans broutement.

L'efficacité des méthodes de contrôle proposées dans cette thèse sont démontrées à travers des études comparatives. Les résultats mettent en évidence un suivi amélioré des formations, une robustesse aux incertitudes et aux perturbations, ainsi que la capacité à réaliser des modèles de formation complexes.

# الملخص


لقد تطور التحكم في تشكيل الروبوتات المتنقلة غير الشاملة ذات العجلات بشكل ملحوظ في العقود القليلة الماضية، ويعتبر حاليًا موضوعا بحثيًا حاسما في مجالات الأنظمة متعددة الوكلاء والروبوتات. وذلك نتيجة لإمكاناته في مجموعة واسعة من تطبيقات العالم الحقيقي، بما في ذلك عمليات البحث والإنقاذ والاستكشاف ونقل الأجسام الكبيرة. حيث ثبت أن التحكم في التشكيل يمكن أن يكون أكثر كفاءة في إنجاز مثل هذه المهام المعقدة مقارنة مع إستخدام روبوت واحد، حيث يسمح بالتنفيذ المتوازي للمهام وزيادة قدرات النظام بشكل عام.

ومع ذلك، فإن التحكم في تشكيل الروبوتات المتنقلة ذات العجلات غير الشاملة يمكن أن يواجه العديد من التحديات. نذكر منها، القيود غير الشاملة التي تقيد حركة الروبوت، والتي تتطلب دراسة متأنية في مرحلة النمذجة وأثناء تصميم قوانين التحكم. فضلا عن وجود حالات عدم اليقين والاضطرابات في ديناميكيات الروبوت والتي تتطلب تصميم استراتيجيات تحكم قوية وقابلة للتكيف .

في هذه الأطروحة، تم دراسة مشكلة التحكم في تشكيل مجموعة من الربوتات من خلال اقتراح ثلاث طرق تحكم مختلفة. أولاً، نستكشف استراتيجية تشكيل القائد-المتابع من خلال تطوير وحدات تحكم بإستخدام وضع الانزلاق المتكامل الكسري الضبابي. يمكّن مخطط التحكم هذا الروبوتات التابعة من تتبع القائد بدقة وتحقيق نمط التشكيل المطلوب، في ظل وجود الاضطرابات والتشويشات الخارجية.

ثانيًا، تم تقديم وحدات تحكم موزعة و تكيفية لتحقيق التشكيل بإستعمال وضع الانزلاق االسريع الكسري . تهدف مدخلات التحكم هذه إلى تحقيق تقارب سريع و في زمن محدود للروبوت نحو الشكل المطلوب. حيث تم تطويرها بالإعتماد على نهج التوافق مما يجعل وحدات التحكم المقترحة مناسبة تماما لأنظمة الربوتات ذات الأعداد الكبيرة لأنه يتطلب اتصالات أقل بين الربوتات.

وأخيرا، تم تطوير متحكم بإستعمال وضع الانزلاق التنبئي المتقطع من أجل التحكم في تشكيل مجموعة من الروبوتات غير الشاملة. يمكن أن يؤدي توليف التحكم هذا إلى تشكيل النمط المطلوب بأداء مع معدل تقارب سريع وخالي من التشويش .

لإثبات فعالية وكفاءة وحدات التحكم المقترحة، تم إجراء دراسات مقارنة. تظهر النتائج المتحصل عليها على اداء جيد من حيث إنشاء و تتبع الروبوتات للتشكيل، كذلك المتانة ضد حالات عدم اليقين والاضطرابات الخارجية، مع قدرة الربوتات أيضا على تحقيق أنماط التكوين المعقدة.

# LIST OF ABBREVIATIONS

| | |
|---|---|
| **SOCA** | Second Order Consensus Algorithm |
| **SMC** | Sliding Mode Control |
| **DSM** | Discrete Sliding Mode |
| **ISM** | Integral Sliding Mode |
| **ITSM** | Integral Terminal Sliding Mode |
| **FISM** | Fuzzy Integral Sliding Mode |
| **FFOISM** | Fuzzy Fractional order Integral Sliding Mode |
| **FTMSC** | Fast Terminal Sliding Mode Control |
| **MPC** | Model Predictive Control |
| **DMPC** | Discrete Model Predictive Control |
| **DPSM** | Discrete Predictive Sliding Mode |
| **DSMC** | Distributed Sliding Mode Control |
| **ADFOFTSMC** | Adaptive Distributed Fractional Order Sliding Mode Control |

# TABLE OF CONTENTS

# LIST OF FIGURES

# LIST OF TABLES

# INTRODUCTION

In recent decades, cooperative control of multi robots systems have emerged as an exciting and rapidly growing field of research in robotics. A multi robots system is mainly consists of two or more robots that are able to collaborate and communicate to achieve a common objective. This concept is originally inspired by the collective behavior observed in nature, where various species exhibit a remarkable coordination and synchronization, allowing them to achieve complex tasks and survive in harsh environments.

One of the key aspects of cooperative control is the formation control of wheeled mobile robots. In formation control, the states of individual robots, such as position, velocity, and orientation, are regulated in a manner that collectively generates a specific geometric configuration. Instead of operating as individual entities, the robots in a formation maintain a structured and coordinated pattern, which enhances their overall performance and effectiveness. In recent years formation control has been used in numerous fields, including aerospace, agriculture, and military. Where it is used to perform different types of tasks such as exploration, environmental monitoring, search and rescue operation and large objects transportation ..etc.

One of the major advantages of formation control is that it can allows for a group of robots to perform complex tasks that would be difficult or impossible for a single robot to accomplish. For example, a team of robots can collaborate to transport large objects or cover a large area for surveillance purposes. Additionally, using formation control also improves the overall efficiency and reliability of the system, as the robots can share the workload and compensate for any failures or malfunctions of individual robots. Furthermore, formation control can provide significant advantages in military and surveillance applications, where the coordinated movements and communication are essential for mission success.

Despite its promising benefits, implementing formation control on nonholonomic mobile robots can be a challenging task. Nonholonomic robots have motion constraints

that limit their freedom of movement. Coordinating their actions while ensuring collision avoidance, formation maintenance, and achieving the desired formation shape becomes a complex optimization problem. In addition, the presence of uncertainties and external disturbances adds another layer of complexity to the formation control problem.

To address this challenges, we focus in this thesis on designing a new robust and adaptive control approaches for the formation control of nonholonomic wheeled mobile robots.

- **Motivation** : Wheeled mobile robots find application in a wide array of domains, yet using a single robot for acomplishing certain tasks can often limit its capabilities. On the contrary, using formation control of mobile robots offers a broader spectrum of possibilities and expand these limits due to the collaborative potential. However, the coordination of wheeled nonholonomic wheeled mobile robots into a formation is still progressing at a measured pace, impeding their widespread adoption and the realization of their full advantages. This motivated us to investigate this exciting field with the intention of accelerating its development.

- **Objectives of the thesis** : The primary objective of this dissertation is to offer novel robust and adaptive control approaches for a swarm of nonholonomic wheeled mobile robots, that enable them to navigate in an unknown environment while forming a specific formations and achieving a predefined tasks.

- **Contribution** : The contributions of this dissertation can be summarized as follow:

  Fuzzy fractional integral sliding mode control is implemented using the leader-follower formation strategy based on the dynamic model of the robots. This control scheme ensures that the follower robots can effectively track the leader robot and maintain the required formation shape, even when facing external disturbances and uncertainties in the robots dynamics. Furthermore, an adaptive distributed fractional fast terminal sliding mode control method, is designed to achieve rapid and finite-time convergence of the robots towards the desired formation. The distributed architecture of this method enhances scalability, fault tolerance, and minimizes inter-robot communication requirements. Moreover, a discrete predictive sliding mode controller is designed for formation control of nonholonomic robots. Such synthesis can achieve a well-formed and precise formation, characterized by a robust and practical chattering-free control inputs.

- **Organization of the manuscript** : This dissertation is organized into four chapters.

  In *Chapter 1*, an overview of formation control for nonholonomic wheeled mobile robots is presented. First, background and motivation about formation control is given. Then, we analyze the formation control issue from different aspects these include formation control problems, structures, and approaches. Moreover, a review is provided on recent control strategies employed in the literature for the formation control of nonholonomic wheeled mobile robots. Furthermore, essential notions such as graph theory, fractional calculus, and nonholonomic systems are explained.

  In *Chapter 2*, the leader follower formation control of multiple nonholonomic wheeled mobile robots is addressed. The kinematic and dynamic models of the robots are presented firstly. Then, a new robust control inputs for every follower robots in the formation are developed by combining three control techniques namely, integral sliding mode control ISM, fractional calculus FO, and fuzzy logic control. Moreover, the Lyapunov theory is used to prove the suggested control scheme's convergence and stability. Compared to the classical sliding mode controllers this proposed control laws can achieve a well formation maintenance and tracking, with a chattering free and robust control performances.

  *Chapter 3* presents the development of an adaptive distributed formation control for wheeled nonholonomic mobile robots according to the consensus-based approach. The communications between robots is represented using graph theory, so the relative heading angle and distance between the follower robots and the leader are no longer required. Fractional calculus FO is combined with fast terminal sliding mode control FTSMC to design a new distributed control inputs for each robot in order to accomplish the formation objective. To account for the presence of bounded disturbances and uncertainties, an adaptive mechanism is also proposed. Comparisons are made between the proposed distributed controller and two conventional control schemes namely, distributed sliding mode control DSMC and second order consensus algorithm SOCA to demonstrate the effectiveness of the suggested controller.

  *In the last chapter* we presents the design of a discrete predictive sliding mode controller for the formation control of nonholonomic wheeled mobile robots based on the leader follower strategy. The proposed controller addresses the challenges associated with nonholonomic constraints and the external disturbances

in the robots kinematics. The performance of the control method is evaluated through extensive simulations, and the results demonstrate its superiority over conventional discrete sliding mode control techniques. The findings indicate improved formation maintenance and tracking, with minimized control effort and reduced chattering phenomenon.

- **List of publications** :
  DAMANI, AY., BENSELAMA, ZA., HEJAR, R. "Formation control of non--holonomic wheeled mobile robots via fuzzy fractional-order integral sliding mode control." International Journal of Dynamics and Control. pp. 1-12, 2023. https://doi.org/10.1007/s40435-022-01109-x.

  DAMANI, AY., BENSELAMA, ZA., HEJAR, R. "Formation control of non--holonomic wheeled mobile robots using adaptive distributed fractional order fast terminal sliding mode control." Archive of Mechanical Engineering. pp. 567-587, 2023. https://doi.org/10.24425/ame.2023.148700.

  DAMANI, AY., BENSELAMA, ZA., HEJAR, R. "Discrete predictive sliding mode control of leader-follower formation control of nonholonomic mobile robots,". $2^{nd}$ Conference on Electrical Engineering (CEE'21). April 2021. Algiers, Algeria.

# CHAPTER 1

# An overview about formation control of nonholonomic wheeled mobile robots

## 1.1 Introduction

This chapter presents a comprehensive overview of the formation control of nonholonomic wheeled mobile robots. Initially, background and motivation about formation control are introduced. Then the formation control is analyzed based on different aspects such as, formation control problems, structures, and approaches. Additionally, a state of art about the different control strategies used for the formation control of nonholonomic wheeled mobile robots is provided. Finally, important concepts such as graph theory, fractional calculus and nonholonomic systems are defined.

## 1.2 Background and motivation

In recent decades, the domain of mobile wheeled robotics has received a lot of attention and shown incredible progress. This surge in interest is mainly due to the numerous advantages that mobile wheeled robots provide to both humans and industries. Wheeled mobile robotics, characterized by the use of wheeled platforms for autonomous or semi-autonomous mobility, has emerged as a transformative technology. Where its applications range from manufacturing and logistics to agriculture, healthcare, and beyond. The appeal of mobile wheeled robots lies in their capacity to execute tasks efficiently, consistently, and with a high degree of precision. Whether it's

automating repetitive industrial processes, exploring hazardous environments, or aiding in healthcare, these robots have proven to be invaluable assets.

However, it has become clear that some missions are extremely complicated and cannot be successfully excuted by a single mobile robot. These missions frequently need a level of coordination, cooperation, and adaptability that an individual robot struggle to perform. In response to the challenges that these complex missions pose, academics have turned to the natural world for inspiration. Nature is rich of evolved strategies for group coordination and collaboration, offers a blueprint for tackling tasks that are hard for individual agents. Observing how certain species execute intricate tasks in groups such as the coordinated movement of flocks of birds, schools of fishs, and ants and bee's colony (see Figure 1.1) researchers have sought to replicate these behaviors in the field of robotics.

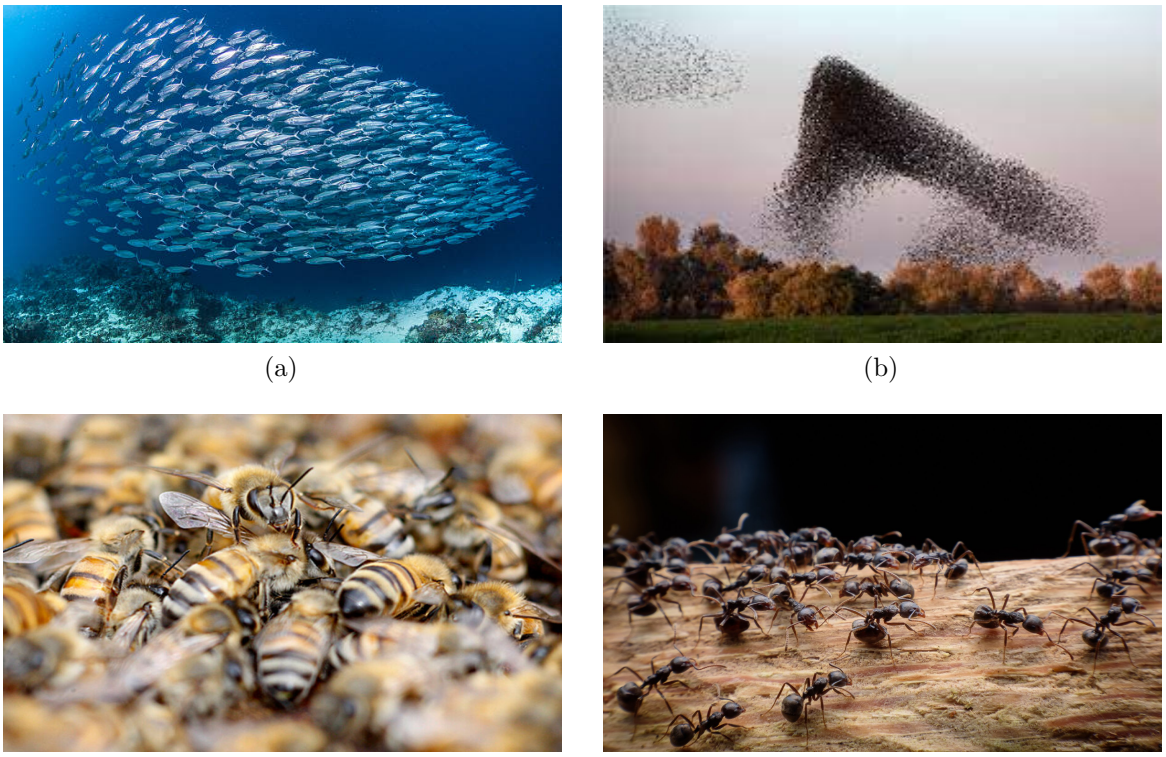

(a) (b)

(c) (d)

Figure. 1.1: Formations in biological systems, (a) fish schooling, (b) Birds flocking, (c) bee colony, (d) ant colony.

This initiative resulted in the invention of formation control, a concept in which numerous mobile robots collaborate in a coordinated manner, similar to animal behavior

seen in nature. Formation control shows great capabilities for performing hard tasks in unknown and hazardous environment. It enables robots to achieve a level of cooperation and adaptability that is critical in scenarios such as traffic flow improvement [1], environmental monitoring in remote and hostile terrains [2], object manipulation [3] and transportation [4], exploration [5], agriculture [6], search and rescue operations [7] and some military applications as depicted in Figure 1.2.

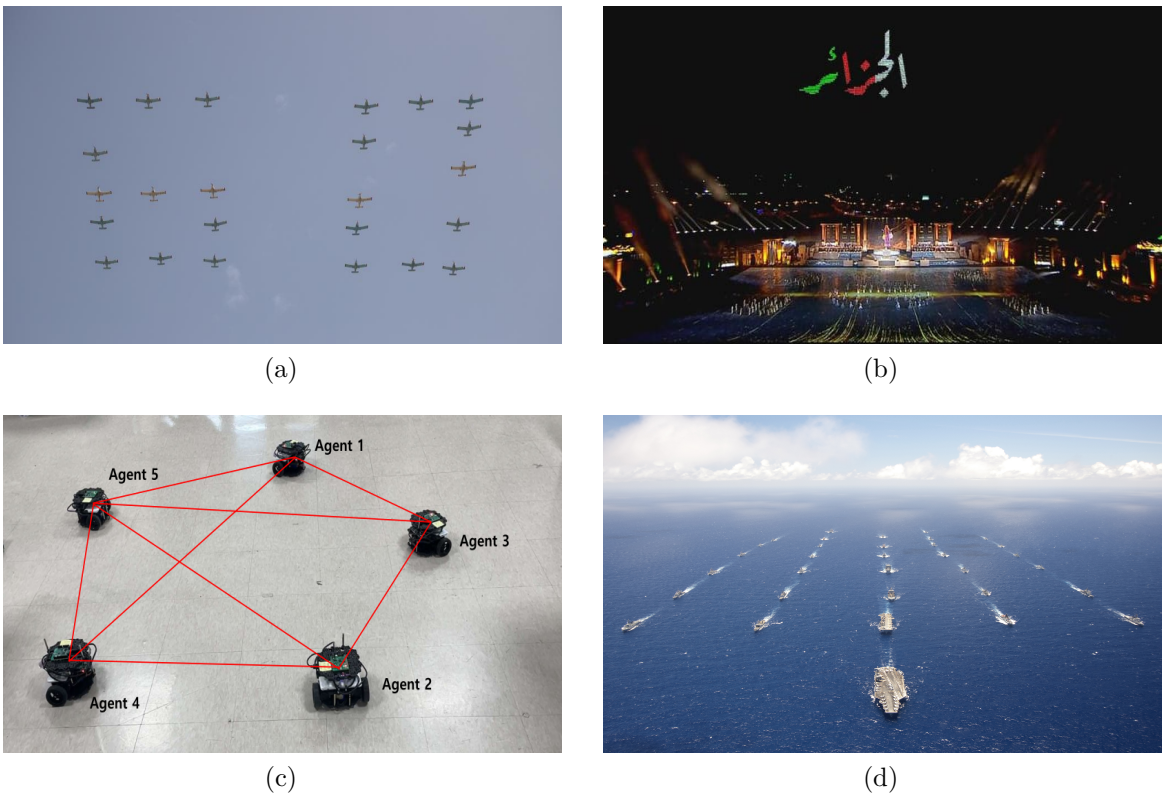


(a) (b) (c) (d)

Figure. 1.2: Formation control in real world applications, (a) Algerian fighter jets forming number 60 (in 60th anniversary celebration of Algeria's independence ), (b) drone swarm forming the word Algeria in Arabic (Arab Games, Algiers 2023), (c) formation of submarines, (d) group of wheeled robots forming a pentagon shape [8].

However, achieving formation control of nonholonomic wheeled mobile robots comes with its own challenges. The inherent nonholonomic constraints imposed by wheeled motion introduce complexities that demand innovative solutions. These challenges include issues related to path planning, trajectory tracking, collision avoidance, and maintaining the desired formation in the face of disturbances and uncertainties. Addressing these challenges is imperative to ensure the successful deployment of formation control strategies in real-world applications.

## 1.3 Overview of related work

Over the past few decades, significant progress has been made in the field of formation control of nonholonomic wheeled mobile robots. Researchers have adopted various analysis perspectives of formation control, including formation control problems, formation control structures, and formation control approaches. In the following sections we will provide an overview of some recent researches published on this field.

### 1.3.1 Formation control problems

In the context of formation control, there are two fundamental problems, namely formation producing and formation tracking. In formation producing (formation acquisition), the autonomous robots are required to produce a desired geometric shape and maintain it over time, without having to track any reference trajectory as shown in Figure 1.3. The focus in this problem is on achieving an optimal arrangement of robots to produce a desired shape, which may involve minimizing some criteria or satisfying certain characteristics.

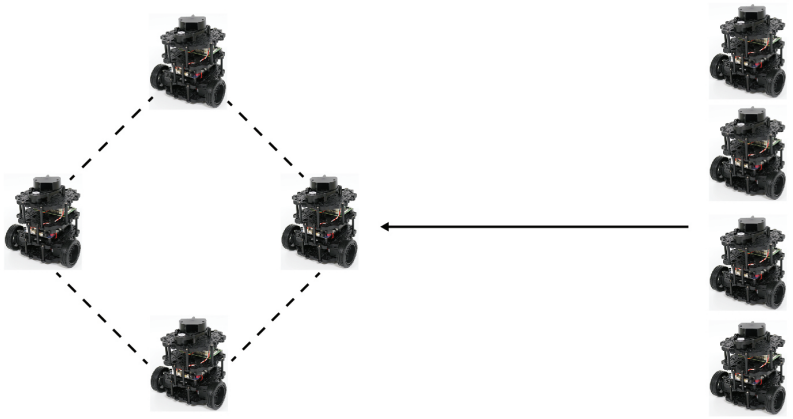

Figure. 1.3: Formation producing.

On the other hand, in formation tracking (Formation Maneuvering), the agents must achieve a desired geometric shape and track a reference trajectory produced by a leader while maintaining the formation as depicted in Figure 1.4. This problem involves not only optimizing the arrangement of robots but also coordinating their movements with respect to some reference trajectory. Both of these problems present unique challenges and require different control structures, approaches, and techniques to achieve.

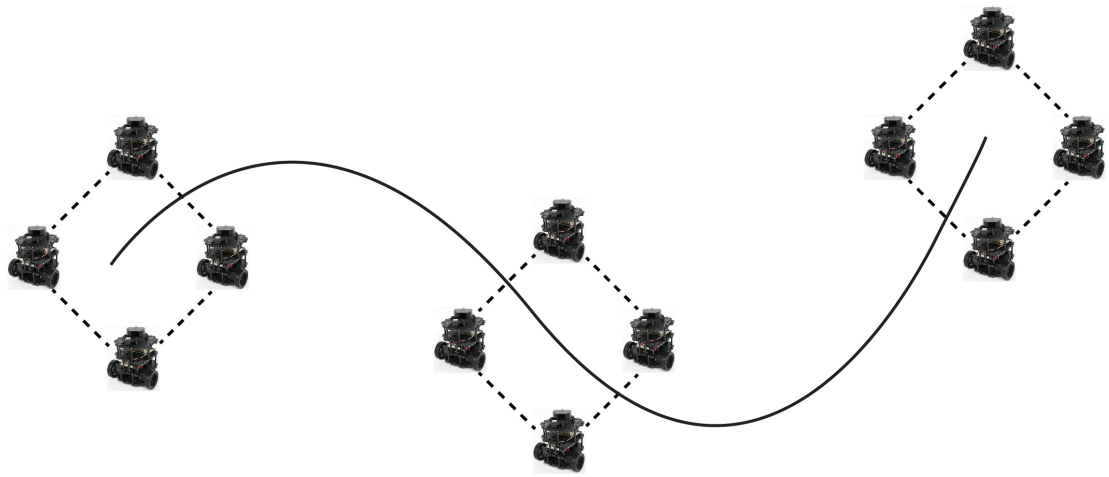

Figure. 1.4: Formation tracking.

### 1.3.2 Formation control structures

#### Centralized control structure

In centralized control structure a single control unit is employed to handle all the necessary information needed to achieve control objectives, (see Figure 1.5). This structure offers many advantages such as superior performance, optimal decisions, faster convergence and enhanced stability. However, there are also several challenges associated with centralized control systems. The system's reliance on one computational unit can make it vulnerable to potential failures or malfunctions, which can negatively impact overall performance. Additionally, the massive flow of information requires high computational power and time, leading to slower processing times and reduced responsiveness. Moreover, As the number of robots increases, the amount of data exchanged between the robots and the central controller can significantly increase, leading to scalability issues. Hence, despite its advantages, a centralized control system may not be suitable for applications that require high scalability and robustness.

#### Decentralized control structure

In a decentralized control structure, robots communicate only with their immediate neighbors in the formation, then the received information's is used to compute their control inputs (see Figure 1.6). This scheme has become increasingly popular in the

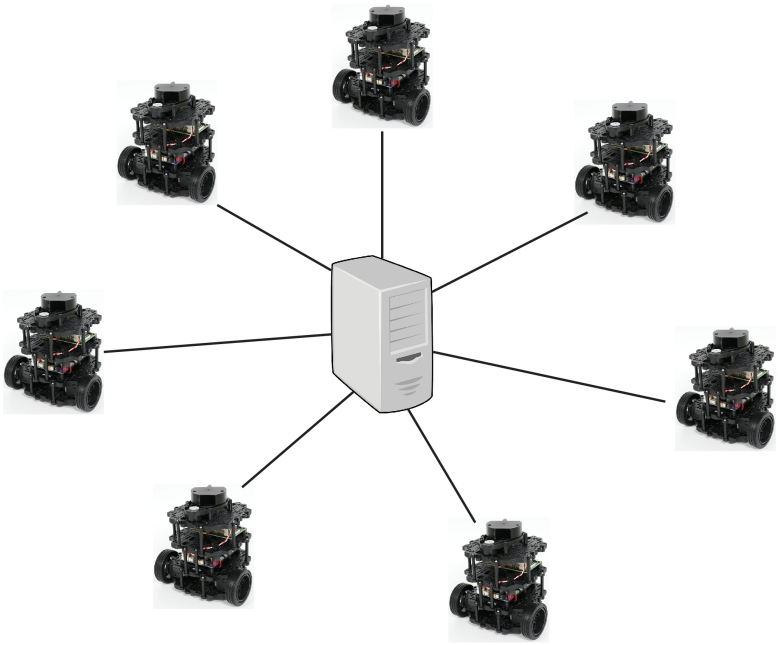

Figure. 1.5: Centralized control structure.

field of multi-robot systems (MRS) due to its many advantages over centralized control. Distributed control structure is particularly useful in mobile robot systems, where each robot has limited access to local information about its own state and the environment. By considering only local information, this approach can satisfy practical constraints such as limited communication among robots, the lack of robot sensing ability to obtain global information, and the need for scalability in robot formation. Additionally, distributed control is generally more cost-effective and efficient for larger systems than centralized control. However, it is important to note that distributed control may also lead to reduced stability and slower convergence.

### 1.3.3 Formation control strategies

In the literature, a variety of control approaches and strategies have been developed for multi-robot systems utilizing either centralized or decentralized structures, these control approaches are categorized based on different criteria. A common classification of formation control approaches is first introduced by [9] , where they characterized formation control approaches into three main categories: behavior-based, virtual structure and leader follower approach.

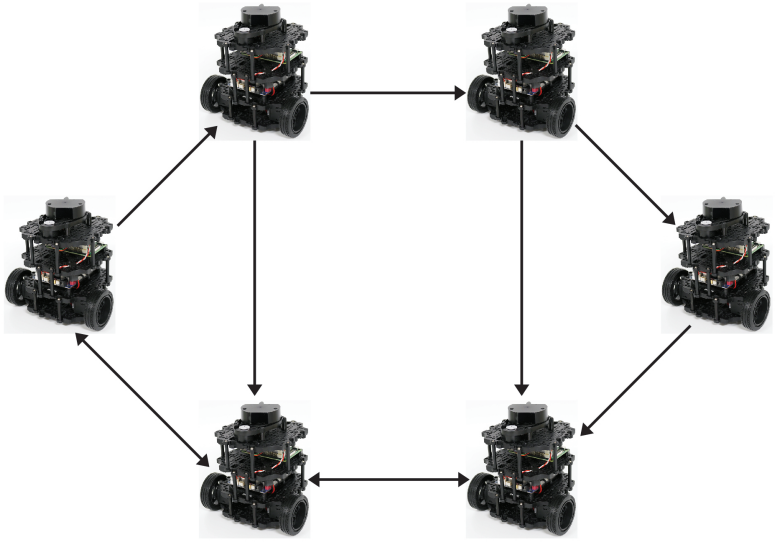

Figure. 1.6: Decentralized control structure.

In Behavior-based approach [10–16], the complex task of coordinating a group of robots into a specific formation is decomposed into simple individual behaviors or motion primitives. Where each robot can executes these behaviors independently, such as formation keeping, trajectory tracking, goal seeking, obstacle avoidance, and collision avoidance. The relative importance of each behavior is dynamically adjusted based on the current task and environment then the overall group behavior emerges from a weighted sum of these individual behaviors. An example of this approach is illustrated in Figure 1.7

This approach is firstly suggested by [17], the authors in [18] implement the behavior-based approach on a team of robots to achieve a formation, they combine a set of reactive behaviors with some navigational behaviors to allow for the robots to preserve the desired formation pattern, reach goals and avoid obstacles. In [19] a behavior based approach is used to solve two significant issues in formation control: (formation producing and formation maneuvering with obstacle avoidance), their proposed method involves using a classification-based search algorithm designed for large-scale robot formations, that can minimize the computational time and speed up the formation process. Authors in [20] propose a decentralized behavior-based formation control algorithm for a group of mobile robots that takes into account obstacle avoidance, their control algorithm depends only on the relative position between robots and obstacles without requiring information about the leader robot. This control method also allows

for the robots to avoid obstacles by using the concept of an escape angle.

Behavior-based approaches offer scalability and simplicity, making them a good choice for coordinating large groups of mobile robots. However, the effectiveness of this approach depends heavily on the design of the individual behaviors and the weighting of their importance. Careful consideration must be given to ensure that the individual behaviors work together cohesively to achieve the desired group behavior. Moreover, it might be challenging to ensure that the formation will converge to a desired configuration due to the complexity of its mathematical analysis.

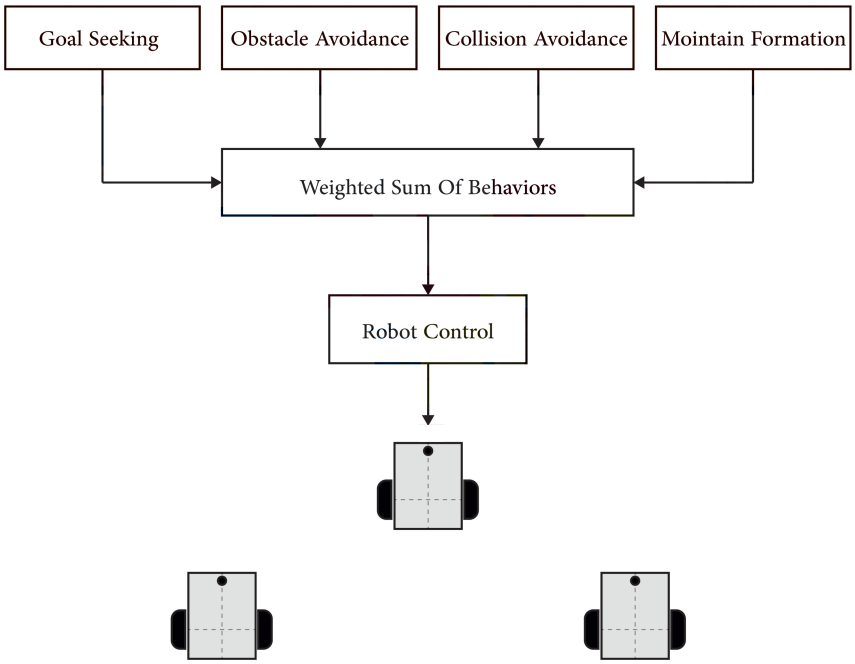


Figure. 1.7: behavior-based approach

In virtual structure approach [21–26], the desired formation is represented as a single rigid body, as shown in Figure 1.8. First the desired dynamics of the virtual structure are defined, than a set of control laws can be derived for each robot to achieve the formation objective.

To the best of our knowledge the concept of this strategy is firstly proposed by [27], authors in [28] combine virtual structure approach and consensus protocol to design new control laws for the formation control of nonholonomic wheeled mobile robots. The leader robot is considered as the origin of the rigid structure, then a coordinate

transformation method is used to obtain the relative coordinates of other robots, finally the formation tracking is achieved by using consensus control. In [29] the virtual structure strategy has been utilized for the formation control of wheeled mobile robots, by computing the relative position of each robot in the formation within the virtual structure, the formation control problem is converted into trajectory tracking problem, then the control laws for each robot are designed using the Backstepping techniques. The authors in [30] propose a formation control of team of nonholonomic mobile robots based on the virtual structure approach, a new path parameter has been utilized to generate the desired formation trajectories, where the potential function method has been employed to reproduce the formation reference trajectories in order to ensure that robots can avoid obstacles.

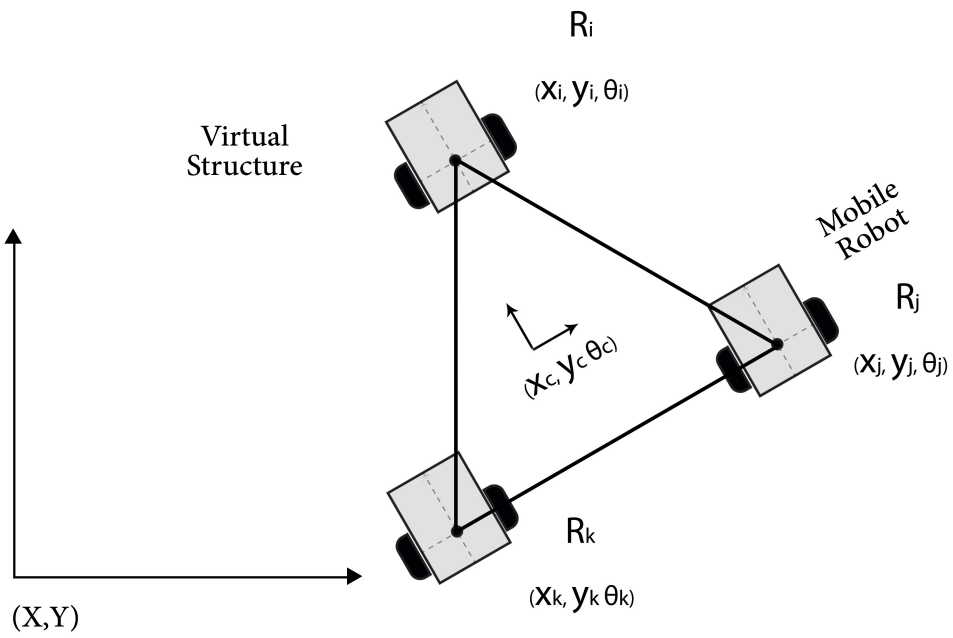


Figure. 1.8: virtual-structure approach

The main Advantage of this approach is that the formation can be easily maintained during maneuvers, with the virtual structure moving as a single entity in a predetermined direction and orientation. Nevertheless, this approach has its limitations. For instance, the formation shape cannot be frequently reconfigured, as this would require changing the virtual structure. Additionally, the controller is not distributed, which may pose challenges when solving certain formation application.

In leader-following approach [31–34], one of the robots is assigned with the leadership role and here the leader can be a (static leader, dynamic leader, or a virtual leader), while the other robots can be considered as followers and they should position themselves relatively to the leader robot by maintaining the desired bearing angle and separation distance.

This approach is the most popular approach among other strategies due to the simplicity of its design and implementation. However, its main drawbacks are the absence of direct feedback from followers to the leader and the formation may not tolerate well with the leader faults.

By using feedback linearization method two type of control algorithms has been proposed by [35] namely, Separation-bearing control and separation-separation control as shown on Figure 1.9. The Separation-bearing scheme is used for two robot formation where the follower robot $R_j$ need to position itself with separation distance $l_{ij}$ and bearing angle $\phi_{ij}$ with respect to its leader $R_i$. whereas the separation-separation control is used for three robot formation, the follower robot $R_k$ need to keep a desired separation distances $L_{ik}$ and $L_{jk}$ relative to its two leader robots $R_i$ and $R_j$. In [36] a leader follower formation control of group of nonholonomic wheeled mobile robots has been investigated, the authors use a combination of bio-inspired neuro-dynamics-based approach and backstepping control to solve the impractical jumps velocities of the follower robots. The Authors in [37] have proposed a new leader-follower formation control for a team of mobile robots, where the formation kinematic tracking model is designed based on the image space by using an onboard perspective cameras. Therefore, the formation tracking can be established without using the leader position or velocities. In [38], a distributed control algorithm for controlling the movement of nonholonomic mobile robots in a leader-follower formation has been suggested. By estimating the states of the leader robot in a decentralized manner and coordinating with other follower robots, the control laws for each follower robot was developed without requiring access to the complete state information of the leader. The authors in [39] discuss the leader-follower formation control of a group of nonholonomic mobile robots with uncertain dynamics, where communication among the robots is assumed to be restricted by a specific communication range. Despite this constraints their proposed control algorithm shows that robots can maintain formation and avoid collision with a prescribed transient and steady-state performance. In [40] ,a formation controller

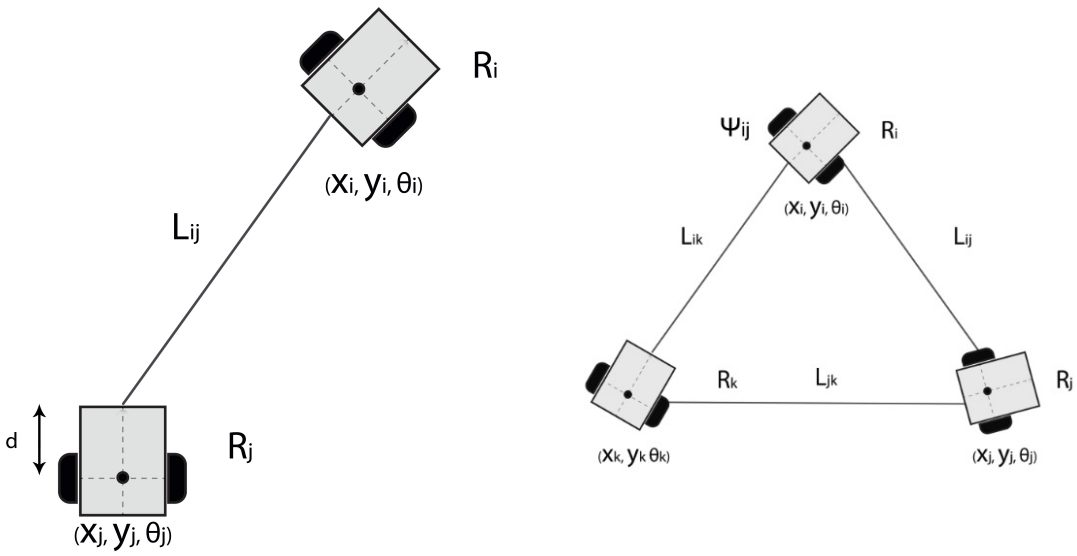


(a) (b)

Figure. 1.9: Leader follower approach, (a) Separation-bearing scheme, (b) Separation-separation scheme

for mobile robots based on the leader-following strategy have been proposed, where the leader's velocity is not directly measured but estimated using an adaptive control technique. The proposed controller does not require communication between robots and only relies on information from onboard sensors. The control laws are continuous and can be used without knowing the desired specification parameters.

Another interesting classification of formation control is introduced by [41], they distinguished the formation control into three approaches (distance-based, displacement-based and position-based control). This characterization is based on the sensing capability and interaction topologies between the agents.

In distance-based control [8, 42–46], the desired formation is achieved by actively control the distances between robots in order to achieve a particular formation that is defined by the desired inter-agent distances. This approach relies on the assumption that individual agents or robots have the ability to detect the relative positions of their neighboring robots in relation to their own local coordinate systems. However, it's important to note that the orientations of these local coordinate systems may not be perfectly aligned with each other.

In position-based control [47–51], agents have the ability to perceive their own positions in relation to a global coordinate system. By using this information, agents can adjust their positions in order to attain a specific formation that has been predetermined by desired locations with respect to a global coordinate system.

In Displacement-based control [52–57], robots control the displacements of their neighboring agents to achieve a predefined formation. This is achieved by define the desired displacements relative to a global frame, and assuming that each robot is capable of perceive the relative positions of its neighboring robots with respect to the global coordinate system. However, the agents must have knowledge of the orientation of the global frame, but do not need to have knowledge of their own positions or the coordinate system itself.

In summary, the control methods mentioned above have their own advantages and disadvantages. While position-based control is the most beneficial in terms of interaction topology, it requires a high level of knowledge and coordination within the system. On the other hand, distance-based control is the complete opposite in terms of these requirements. whereas, displacement-based control offers a balance between the two characteristics. Figure 1.10 illustrate the difference between these approaches in term of the robots sensing capability and interaction topology.

In addition to all control strategies listed above, there are also other techniques employed for formation control such as, consensus-based methods [58–62], model predictive control [63–67] and machine learning techniques [68–71].

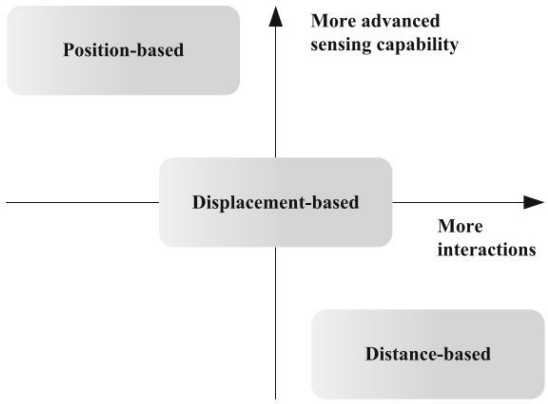


Figure. 1.10: Interaction topology vs sensing capability [41].

## 1.4 Preliminaries

In this section, some important preliminaries about algebraic graph theory, nonholonomic mobile robots and fractional calculus theories will be discussed.

### 1.4.1 Graph theory

Graph theory is a mathematical field that studies the properties of graphs. In graph theory, a graph is a mathematical structure that consists of a set of vertices (nodes), and a set of edges (links) that connect these nodes. The edges can represent any kind of relationship between the vertices, such as similarity, distance, or interaction. Graph theory provides a powerful toolset for modeling and analyzing complex systems that can be represented as networks or graphs, such as communication networks, social networks, and multi-agent systems. Graphs can be represented by using visual diagrams, where nodes are represented by points or circles, and edges are represented by lines or arrows connecting them (see Figure 1.11).

For a multi-robot system, the vertices of the graph can be used to represent the robots, while the edges can be used to represent communication link between each pair of robots. The corresponding graph of multi-robot system that consist of $N$ robot, can be denoted by $G = (V, E)$, where $V$ is a set of $N$ vertices $\{v_1, v_2, \ldots, v_N\}$, and $E \in V$ is the set of links between the vertices. Let $v_i$ and $v_j$ be two distinct nodes of $G$ , if information is being exchanged from $v_i$ to $v_j$ , then the edge $(v_i, v_j)$ is an element of the set $E$, and node $v_i$ is a neighbor of $v_j$ , and it is referred to as the parent node while $v_j$ is known as a child node. The set of neighbors of node $v_i$ , excluding itself, is denoted as $N_{v_i} = \{v_j \in V, (v_i, v_j) \in E\}$.

A graph is referred to as undirected graph, if there is an edge between two nodes $v_i$ and $v_j$, then there must also be an edge between nodes $v_j$ and $v_i$. If this condition is not met, then the graph is called a directed graph (digraph). In undirected graphs, the edges may not have arrows in their visual representation. Additionally, in a weighted graph, each edge $(v_i, v_j)$ has a weight $w_{ij}$ assigned to it. In the case of an undirected weighted graph, the weight of edge $(v_i, v_j)$ is equal to the weight of edge $(v_j, v_i)$.

**Definition 1.1.** In an undirected graph, a path is a sequence of vertices $\{v_1, v_2, \ldots, v_N\}$, such that each consecutive pair of vertices $\{v_i, v_{i+1}\}$ are connected by an edge. In other words, the path can be traversed in both directions along the edges.

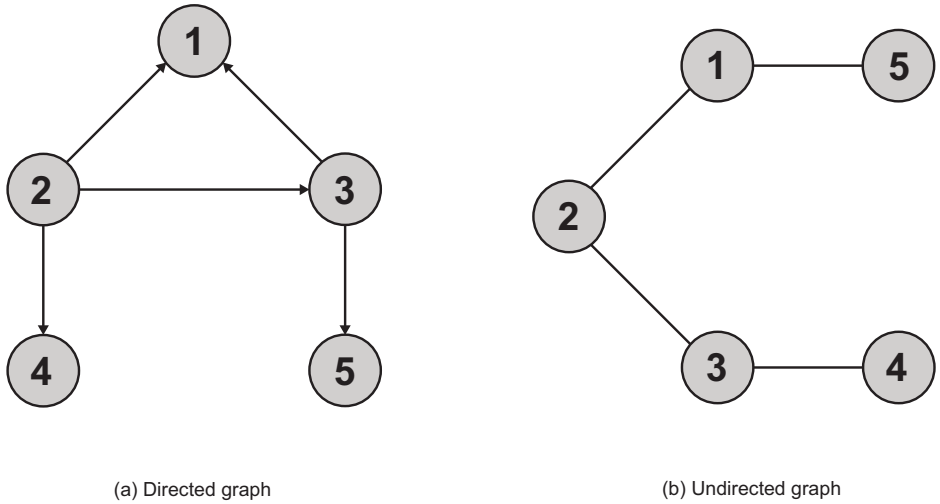


Figure. 1.11: Visual representation of graph, (a) directed graph, (a) undirected graph

In a directed graph, a path is a sequence of vertices $\{v_1, v_2, \ldots, v_N\}$, such that each consecutive pair of vertices $\{v_i, v_{i+1}\}$ are connected by a directed edge from $v_i$ to $v_{i+1}$. In other words, the path can only be traversed in the direction of the arrows.

**Definition 1.2.** a cycle in a graph is a closed path that begins and ends at the same vertex, and that does not repeat any other vertex in between, except for the starting vertex.

**Definition 1.3.** A directed graph is considered strongly connected when there is a directed path between every pair of nodes. On the other hand, an undirected graph is connected if there exists an undirected path between any two distinct nodes.

**Definition 1.4.** A tree in graph theory is a connected graph without cycles (acyclic graph). In directed graphs, a tree has a single root and a unique path from the root to every other vertex, while in undirected graphs, there is a unique path between any two vertices.

**Definition 1.5.** A spanning tree in graph theory is a subgraph that is a tree and includes all vertices of the graph. In directed graphs, it is a directed acyclic subgraph with a unique path from the root to every other vertex, while in undirected graphs, it is a connected, acyclic subgraph with a unique path between any two vertices.

### Adjacency matrix

An adjacency matrix is a square matrix used to represent a graph, where the rows and columns correspond to vertices, and the entries of the matrix indicate the presence or absence of edges between the vertices.

In a directed graph (digraph), the adjacency matrix $A$ is $n \times n$ binary matrix where the entry $A(i,j) = 1$ if there is a directed edge from vertex $v_i$ to vertex $v_j$, and 0 otherwise. The diagonal entries of the matrix are usually set to 0, since there are no self-loops in a digraph. Adjacency matrix of the digraph shown in Figure 1.11 can be given as :

$$A = \begin{bmatrix} 0 & 1 & 1 & 0 & 0 \\ 0 & 0 & 0 & 0 & 0 \\ 0 & 1 & 0 & 0 & 0 \\ 0 & 1 & 0 & 0 & 0 \\ 0 & 0 & 1 & 0 & 0 \end{bmatrix}$$

In an undirected graph, the adjacency matrix is a symmetric binary matrix where the entry $A(i,j)$ is 1 if there is an edge connecting vertex $v_i$ to vertex $v_j$, and 0 otherwise. The adjacency matrix of the undirected graph depicted in Figure 1.11 can be written as :

$$A = \begin{bmatrix} 0 & 1 & 0 & 0 & 1 \\ 1 & 0 & 1 & 0 & 0 \\ 0 & 1 & 0 & 1 & 0 \\ 0 & 0 & 1 & 0 & 0 \\ 1 & 0 & 0 & 0 & 0 \end{bmatrix}$$

**Degree Matrix**

The degree matrix of a graph is a diagonal matrix where the $i$-th diagonal entry is the degree of the $i$-th vertex in the graph. The degree of a vertex is defined as the number of edges incident to the vertex.

For an undirected graph with adjacency matrix $A$ the degree matrix is given by:

$$D = \text{diag}(\sum_{j=1}^{n} A_{ij}),$$

where diag(.) is the diagonal matrix.
The indegree matrix of a directed graph with adjacency matrix $A$ is given by:

$$D_{in} = \text{diag}(A^T \mathbf{1_n}),$$

where $\mathbf{1_n}$ is a vector of all ones. The degree matrix of the undirected graph depicted in Figure 1.11 can be written as :

$$D = \begin{bmatrix} 2 & 0 & 0 & 0 & 0 \\ 0 & 2 & 0 & 0 & 0 \\ 0 & 0 & 2 & 0 & 0 \\ 0 & 0 & 0 & 1 & 0 \\ 0 & 0 & 0 & 0 & 1 \end{bmatrix}$$

While the indegree matrix of the directed graph shown in Figure 1.11 can be written as :

$$D_{in} = \begin{bmatrix} 2 & 0 & 0 & 0 & 0 \\ 0 & 0 & 0 & 0 & 0 \\ 0 & 0 & 1 & 0 & 0 \\ 0 & 0 & 0 & 1 & 0 \\ 0 & 0 & 0 & 0 & 1 \end{bmatrix}$$

### Laplacian Matrix

A valuable tool for studying the dynamics and stability of multi-robot systems is the Laplacian matrix, it provides information about the graph's topology and connectivity. The Laplacian matrix can be defined as the difference between the degree matrix and the adjacency matrix of a graph.

The Laplacian matrix of an undirected graph with adjacency matrix $A$ is given by:

$$L = D - A,$$

where $D$ is the diagonal matrix of degrees. The Laplacian matrix of the undirected graph depicted in Figure 1.11 can be written as :

$$L = D - A = \begin{bmatrix} 2 & -1 & -1 & 0 & 0 \\ -1 & 2 & -1 & 0 & 0 \\ 0 & -1 & 2 & -1 & 0 \\ 0 & 0 & -1 & 1 & 0 \\ -1 & 0 & 0 & 0 & 1 \end{bmatrix}$$

For a directed graph with adjacency matrix $A$, the Laplacian matrix is can be defined as:

$$L = D_{\text{in}} - A,$$

where $D_{\text{in}}$ is the indegree matrix. The Laplacian matrix of the directed graph depicted in Figure 1.11 can be written as :

$$L = D_{\text{in}} - A = \begin{bmatrix} 2 & -1 & -1 & 0 & 0 \\ 0 & 0 & 0 & 0 & 0 \\ 0 & -1 & 1 & 0 & 0 \\ 0 & -1 & 0 & 1 & 0 \\ 0 & 0 & -1 & 0 & 1 \end{bmatrix}$$

**Lemma 1.1.** *The sum of each row in The Laplacian matrix $L$ is always zero $\sum_j L_{i,j} = 0$. Additionally, the eigenvalue 0 is associated with the eigenvector consisting of a vector of ones $L1_n = 0$, and all other non-zero eigenvalues of the Laplacian matrix are positive.*

**Lemma 1.2.** *If undirected graph is connected then 0 is a simple eigenvalue of the Laplacian matrix $L$ . Similarly, if a directed graph is strongly connected then 0 is a simple eigenvalue of $L$. This means that if the graph has at least one spanning tree, then 0 is a simple eigenvalue of $L$.*

### 1.4.2 Fractional calculus

Fractional calculus theory [72, 73] is a branch of mathematics that deals with generalizations of differentiation and integration to non-integer orders, known as fractional orders. In classical calculus, the derivatives and integrals are defined for integer orders only, while in fractional calculus, the orders can be any real number or even complex numbers.

The theory of fractional calculus has been developed since the 18th century, but it has gained significant attention in recent years due to its applications in many fields such as engineering, physics, economics, and control theory. In the following the three most used fractional calculus definitions in the literature (Riemann-Liouville, Caputo, and Grunwald-Letnikov), will be given.

#### Riemann-Liouville Definition

The Riemann-Liouville fractional integral of order $\alpha$ for a function $f(x)$ is given by:

$$I^{\alpha} f(x) = \frac{1}{\Gamma(\alpha)} \int_a^x (x-t)^{\alpha-1} f(t) dt \tag{1.1}$$

The Riemann-Liouville fractional derivative of order $\alpha$ for a function $f(x)$ is given by:

$$D^{\alpha} f(x) = \frac{1}{\Gamma(n-\alpha)} \frac{d^n}{dx^n} \int_a^x (x-t)^{n-\alpha-1} f(t) dt \tag{1.2}$$

where $n$ is an integer greater than $\alpha$ and $d^n/dx^n$ denotes the $n$-th derivative of $f(x)$, and $\Gamma(.)$ is the Euler Gamma function.

**The Caputo definition**

The Caputo fractional derivative of order $\alpha$ for a function $f(x)$ is given by:

$$^{C}D^{\alpha}f(x) = \frac{1}{\Gamma(n-\alpha)}\int_{a}^{x}(x-t)^{n-\alpha-1}\frac{d^n}{dt^n}f(t)dt \tag{1.3}$$

where $n$ is an integer greater than $\alpha$ and $d^n/dt^n$ denotes the $n$-th derivative of $f(t)$.

**Grunwald-Letnikov Definition**

The Grunwald-Letnikov fractional derivative of order $\alpha$ for a function $f(x)$ is given by:

$$\lim_{h\to 0}\frac{1}{h^{\alpha}}\sum_{k=0}^{\infty}(-1)^k\binom{\alpha}{k}f(x-kh) \tag{1.4}$$

where $\alpha$ is a positive real number and $\binom{\alpha}{k}$ denotes the binomial coefficient. The Grunwald-Letnikov definition is a discretized form of the fractional derivative that is useful for numerical calculations.

### 1.4.3 Nonholonomic wheeled mobile robots

In the field of formation control, nonholonomic wheeled mobile robots have been increasingly employed recently. This is primarily due to their wide area of applications and the difficulty of controlling their movements, making them a topic of interest in the research community. In the following, mathematical modeling of nonholonomic robots and some relevant concepts will be introduced.

**Holonomic and Nonholonomic systems**

Consider a mechanical system with $n$ generalized coordinates $q = [q_1, q_2, ..., q_n]$, where its dynamics are given by $\ddot{q} = f(q, \dot{q}, u)$ with $u$ is the external generalized input vector. The system is said to be holonomic if the constraints that govern its motion can be described as the time derivatives of functions of the generalized coordinates , that take the form $\phi(q, t) = 0$. Such constraints are referred to as holonomic or integrated constraints because it can be solved through integration. An example of holonomic

systems are the omnidirectional wheeled robots depicted in Figure 1.12.

In contrast, nonholonomic systems are those that have linear constraints with respect to their generalized coordinates $q$, formulated as $\phi(q,t)\dot{q}(t) = 0$, where $\dot{q}(t)$ is the vector of system velocities in the generalized coordinates. These constraints cannot be reduced or expressed as the derivative of a state function, making them non-integrable. As a result, such constraints are referred to as nonholonomic. The presence of nonholonomic constraints means that the generalized coordinates of the system are not independent from one another, making the equations of motion more complex to solve. Figure 1.13 shows an example of nonholonomic systems (differential drive robots).

(a) (b)

Figure. 1.12: Example of holonomic systems, (a) 3 mechanum wheeled robot, (b) 4 mechanum wheeled robot

(a) (b)

Figure. 1.13: Differential drive robots, (a) Pioneer 3DX model, (b) Turtlebot3 burger model.

### Mathematical model of nonholonomic wheeled mobile robot

A common type of nonholonomic systems is the differential drive robot (see Figure 1.14 ), it consists of two main wheels that are placed on a common axis and driven by two separated motors. Additionally, a one or more castor wheels are used to support the vehicle and prevent tilting [74]. This type of robots is usually subject to nonholonomic constraints (pure rolling and non slipping constraints). In other words, its motion is limited by the fact that its two wheels can only move in a straight line or turn about a fixed axis, and cannot move sideways.

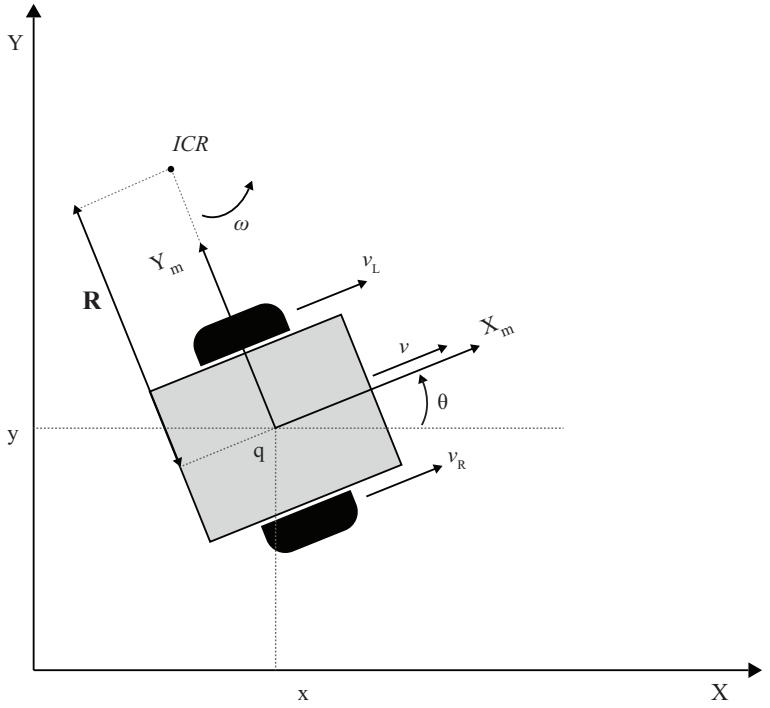


Figure. 1.14: Differential-drive mobile robot.

As illustrated in Figure 1.14, the (position/orientation) of the robot is denoted by $q = \begin{bmatrix} x & y & \theta \end{bmatrix}^T$ where $(x, y)$ represent its coordinates in the global frame $(OXY)$ and $\theta$ is the orientation angle. The rest of symbols shown in Figure 1.14 are defined as follow: $(v_R, v_L)$ are the linear velocities of the right and left wheels, respectively. $ICR$ is the instantaneous center of rotation, $R(t)$ is the instantaneous radius of the robot's driving trajectory (distance between the midpoint between the wheels and the ICR point). $L$ is the distance between the two wheels and $r$ represents the radius of the wheels. The angular and linear velocities of the robot are decribed by $\nu$ and $\omega$, respectively. At any given moment, the angular velocity $\omega(t)$ of the robot around the $ICR$ can be given as

$$\begin{cases} \omega(t) = \dfrac{v_L(t)}{R(t) - \frac{L}{2}} \\ \omega(t) = \dfrac{v_R(t)}{R(t) + \frac{L}{2}} \end{cases} \tag{1.5}$$

Using equation (1.5), $\omega(t)$ and $R(t)$ can be written as:

$$\begin{cases} \omega(t) = \dfrac{v_R(t) - v_L(t)}{L} \\ R(t) = \dfrac{L}{2} \dfrac{v_R(t) + v_L(t)}{v_R(t) - v_L(t)} \end{cases} \tag{1.6}$$

Then, the Linear velocity of the robot can be calculated as follow:

$$\nu(t) = R(t)\omega(t) = \frac{v_R(t) + v_L(t)}{2} \tag{1.7}$$

The kinematics of the robot based on the local coordinates can be given as:

$$\dot{q}_m = \begin{bmatrix} \dot{x}_m \\ \dot{y}_m \\ \dot{\theta}_m \end{bmatrix} = \begin{bmatrix} r/2 & r/2 \\ 0 & 0 \\ r/L & -r/L \end{bmatrix} \begin{bmatrix} \omega_R \\ \omega_L \end{bmatrix} \tag{1.8}$$

By defining the rotation matrix $R(\theta)$ as:

$$R(\theta) = \begin{bmatrix} cos(\theta) & sin(\theta) & 0 \\ -sin(\theta) & cos(\theta) & 0 \\ 0 & 0 & 1 \end{bmatrix}$$

The kinematic model of the differential drive is obtained as follow:

$$\dot{q} = \begin{bmatrix} \dot{x} \\ \dot{y} \\ \dot{\theta} \end{bmatrix} = R(\theta)\dot{q}_m = \begin{bmatrix} \cos\theta & 0 \\ \sin\theta & 0 \\ 0 & 1 \end{bmatrix} \begin{bmatrix} \nu \\ \omega \end{bmatrix} \tag{1.9}$$

From the kinematic model in equation (1.9), we obtain:

$$\nu = \dot{x}cos\theta + \dot{y}sin\theta \tag{1.10}$$

Then the rolling constraints for each wheel of the robot, which indicates that any motion along the direction of the wheels plane should be purely rotational, can be represented by using equations (1.7) and (1.10) as follow:

$$\begin{cases} \nu_R = r\omega_R = \dot{x}cos\theta + \dot{y}sin\theta \\ \nu_L = r\omega_L = \dot{x}cos\theta + \dot{y}sin\theta \end{cases} \tag{1.11}$$

On the other hand, the non slipping constraint can be expressed as:

$$-\dot{x}sin\theta + \dot{y}cos\theta = 0 \tag{1.12}$$

Equation (1.12) means that, the robot motion perpendicular to the wheels plane must equal to zero.

The nonholonomic constraint in (1.12) can be written as:

$$\phi(q,t)\dot{q}(t) = 0 \tag{1.13}$$

Where $\phi(q,t) = \begin{bmatrix} -sin\theta(t) & cos\theta(t) & 0 \end{bmatrix}^T$ and $\dot{q}(t) = \begin{bmatrix} \dot{x}(t) & \dot{y}(t) & \dot{\theta}(t) \end{bmatrix}^T$.

## 1.5 Conclusion

In this chapter, we have presented a detailed analysis of formation control of multi-robot systems, highlighting the challenges and problems that arise in this field, as well as the control structures and methods that can be utilized to achieve formation control for wheeled mobile robots with nonholonomic constraints. Additionally, we have provided a brief explanation of graph theory, fractional calculus theory and other concepts which will be relevant to the subsequent chapters.

# CHAPTER 2

# Formation control of nonholonomic wheeled mobile robots via fuzzy fractional order integral sliding mode control

## 2.1 Introduction

This chapter presents a robust formation control scheme for a team of nonholonomic wheeled mobile robots. First the formation kinematic controller is introduced according to the leader-following strategy, then by employing the dynamic model of the robots, a combination of fractional calculus theories and integral sliding mode control is adopted to provide a robust dynamic control laws for every follower robots to track the leader and accomplish the required formation pattern even in the presence of external disturbances and model uncertainties. Furthermore, the chattering phenomenon is mitigated using a fuzzy logic control. Then by using the Lyapunov theory, the proposed control scheme's convergence and stability are demonstrated. Finally, a comparative study is conducted to evaluate the performance of the suggested control strategy.

As discussed in chapter 1, the leader-follower approach has been widely utilized in the literature due to its ease implementation and the simplicity of its design, various control techniques has been employed to achieve the formation control of wheeled nonholonomic robots according to this strategy, to name a few Backstepping algorithms [36, 75] , Sliding mode control [75–78], Model predictive control [79, 80] , and Feedback

Linearization methods. [81].

Its well known, that the sliding mode control has a higher reliability and robustness against system unmodeled dynamics, uncertainties and disturbances amongst the pre-mentioned control schemes, which motivated researchers to implement several sliding mode controllers to the formation control of multi-robots. For example, in [75] a fuzzy sliding mode control FSMC is mixed with a Backstepping algorithm for the formation control of wheeled mobile robots subjected to kinematic model uncertainties. The authors in [76] , used integral sliding mode control ISMC to solve the issue of mismatched model uncertainties in the leader-follower formation control of nonholonomic mobile robots, in [78] a combination between Lyaponuv-based control and a sliding mode control SMC are utilized for the leader follower formation control, based on an augmented angle strategy. The authors in [82] propose an adaptive formation control of noholonomic robots using fast terminal sliding mode control FTSMC, where they used a fuzzy logic control FLC to deal with chattering phenomenon. In [77] integral terminal sliding mode control ITSMC is proposed to control a swarm of nonholonomic mobile robots using the leader follower approach, where the absence of leader velocity measurement is considered as a parametric uncertainty.

Recently, fractional calculus has been implemented in control theory for controlling some dynamic systems [83–85]. The concepts of FO integral and derivatives can be utilized in combination with other conventional control techniques such as PID [86] and sliding mode control SMC [87], which can introduce an additional layer of adaptability to the control system parameters, resulting in enhanced performance and desirable outcomes.

In this chapter, the aforementioned control techniques, namely, ISM control and FO calculus are mixed together with a fuzzy logic control FLC in-order to develop a new robust control laws for the formation control of nonholonomic mobile robots. Such synthesis can incorporates the following key features. The ISM control scheme can assure a high precision and accuracy tracking with a fast convergence rate and robustness against system unknown disturbances, parameters variation and uncertainties. The fractional order integral in the control law operate as adjustable control gains, where the optimal control performances is obtained by tuning the FO's appropriately. While the fuzzy logic is used to suppress the chattering behavior caused by the sliding mode switching control action. A comparative studies have been carried out to

investigate the effectiveness of the FFOISM controller. Based on the obtained results, the suggested control technique outperforms other sliding mode control methods in terms of robustness, chattering elimination, tracking accuracy and convergence.

## 2.2 Nonholonomic mobile robot model

### 2.2.1 Kinematic model

A basic type of nonholonomic mobile robots is the differential drive robot depicted in Figure 2.1. In the global frame $(O, X, Y)$ , the posture of the robot $i$ is given by $q_i = \begin{bmatrix} x_i & y_i & \theta_i \end{bmatrix}^T$ where $(x_i, y_i)$ represent the coordinates and $\theta_i$ denotes the orientation of the robot.

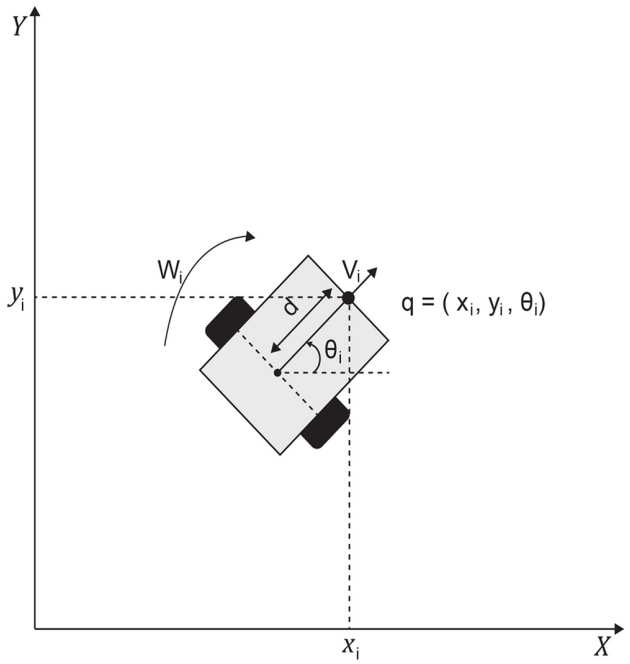


Figure. 2.1: Nonholonomic mobile robot.

Under the non-slipping and pure rolling conditions, the nonholonomic constraints of a robot $i$ can be given as :

$$\dot{y}_i \cos\theta_i - \dot{x}_i \sin\theta_i - d\dot{\theta}_i = 0 \tag{2.1}$$

Where $d$ denotes the distance between the robot rear-axle and its front-end. The kinematic model of the mobile robot $i$ is given as follow :

$$\dot{q}_i = \begin{bmatrix} \dot{x}_i \\ \dot{y}_i \\ \dot{\theta}_i \end{bmatrix} = \begin{bmatrix} \cos\theta_i & -d\sin\theta_i \\ \sin\theta_i & d\cos\theta_i \\ 0 & 1 \end{bmatrix} \begin{bmatrix} \nu_i \\ \omega_i \end{bmatrix} = J_i(q_i)U_i \tag{2.2}$$

Where $\omega_i, \nu_i$ represents the robot angular and linear velocities, respectively. $J_i(q_i) \in R^{3\times2}$ is the matrix of velocity transformation and $U_i \in R^{2\times1}$ is the vector of velocity input.

### 2.2.2 Dynamical model

The dynamical model of nonholonomic mobile robot can be expressed based on the Euler-Lagrange equation as follow:

$$M_j(q_j)\ddot{q}_j + V_{mj}(q_j,\dot{q}_j)\dot{q}_j + G_j(q_j) + F_j(q_j) + B_j(q_j)\tau_{dj} = B_j(q_j)\tau_j - A_j^T(q_j)\lambda_j \tag{2.3}$$

Where $M_j(q_j) \in R^{3\times3}$ is the matrix of inertia , $V_{mj}(q_j,\dot{q}_j) \in R^{3\times3}$ is the matrix of centripetal and Coriolis forces, $G_j(q_j) \in R^{3\times1}$ is the gravity vector , $F_j(q_j) \in R^{3\times1}$ is the vector of surface friction, $\tau_{dj} \in R^{2\times1}$ denotes the external disturbance , $B_j(q_j) \in R^{3\times2}$ is the matrix of input transformation , $\tau_j \in R^{2\times1}$ is the control input vector , $A_j^T(q_j) \in R^{3\times1}$ is the vector of nonholonomic constraint and $\lambda_j$ denotes the Lagrange multiplier. The pre-mention matrices and vectors are defined as follows :

$$M_j(q_j) = \begin{bmatrix} m & 0 & md\sin\theta_j \\ 0 & m & -md\cos\theta_j \\ md\sin\theta_j & -md\cos\theta_j & I \end{bmatrix}$$

$$V_{mj}(q_j,\dot{q}_j) \begin{bmatrix} 0 & 0 & md\dot{\theta}_j\cos\theta_j \\ 0 & 0 & md\dot{\theta}_j\sin\theta_j \\ 0 & 0 & 0 \end{bmatrix}$$

$$B_j(q_j) = \frac{1}{r}\begin{bmatrix} \cos\theta_j & \cos\theta_j \\ \sin\theta_j & \sin\theta_j \\ R & -R \end{bmatrix}$$

$$\tau_j = \begin{bmatrix} \tau_{lj} \\ \tau_{rj} \end{bmatrix}, \ \tau_{dj} = \begin{bmatrix} \tau_{dlj} \\ \tau_{drj} \end{bmatrix}$$

$$\lambda_j = -m(\dot{x}_j \cos\theta_j + \dot{y}_j \sin\theta_j)\dot{\theta}_j, \ A_j^T(q_j) = \begin{bmatrix} -\sin\theta_j & \cos\theta_j & -d \end{bmatrix}^T$$

Where $2R$ denotes the robot width, $m$ is the mass of the robot, $r$ is the robot wheel radius and $I$ is the moment of inertia. Equation (2.3) can be re-written in more suitable form for the purpose of control by substituting equation (2.2) and its derivative in equation (2.3) then by multiplying both sides with $J_j^T(q_j)$ which yields the following :

$$\bar{M}_j(q_j)\dot{U} + \bar{V}_{mj}(q_j, \dot{q}_j)U + \bar{F}_j(\dot{q}_j) + \bar{\tau}_{dj} = \bar{B}_j(q_j)\tau_j \tag{2.4}$$

Where $\bar{M}_j = J_j^T M_j J_j \in R^{2\times 2}$, $\bar{F}_j = J_j^T F_j \in R^{2\times 1}$, $\bar{B}_j = J_j^T B_j$, $\bar{\tau}_{dj} = \bar{B}_j \tau_{dj}$ and $\bar{V}_{mj} = J_j^T(M_j \dot{J}_j + V_{mj} J_j) \in R^{2\times 2}$

Neglecting the surface friction and assuming all system parameters are known, external disturbances and model uncertainties are zero then equation (2.4) can be reformulated as follow :

$$\dot{U}_j(t) = H\tau_j(t) \tag{2.5}$$

Where $H = \bar{M}_j^{-1}(q_j)\bar{B}_j(q_j)$ , $\bar{M}_j = \begin{bmatrix} m & 0 \\ 0 & I - md^2 \end{bmatrix}$, $\bar{V}_{mj} = 0$ and $\bar{B}_j = \frac{1}{r}\begin{bmatrix} 1 & 1 \\ R & -R \end{bmatrix}$

## 2.3 Leader follower based formation and kinematic controller design

### 2.3.1 Leader follower based formation model

Consider the leader follower formation structure presented in Figure 2.2, where the posture of the leader robot is denoted by $q_i = \begin{bmatrix} x_i & y_i & \theta_i \end{bmatrix}^T$ and the follower robot posture is represented by $q_j = \begin{bmatrix} x_j & y_j & \theta_j \end{bmatrix}^T$ , while $q_j^d = \begin{bmatrix} x_d & y_d & \theta_d \end{bmatrix}^T$ describe the desired posture of the follower robot.

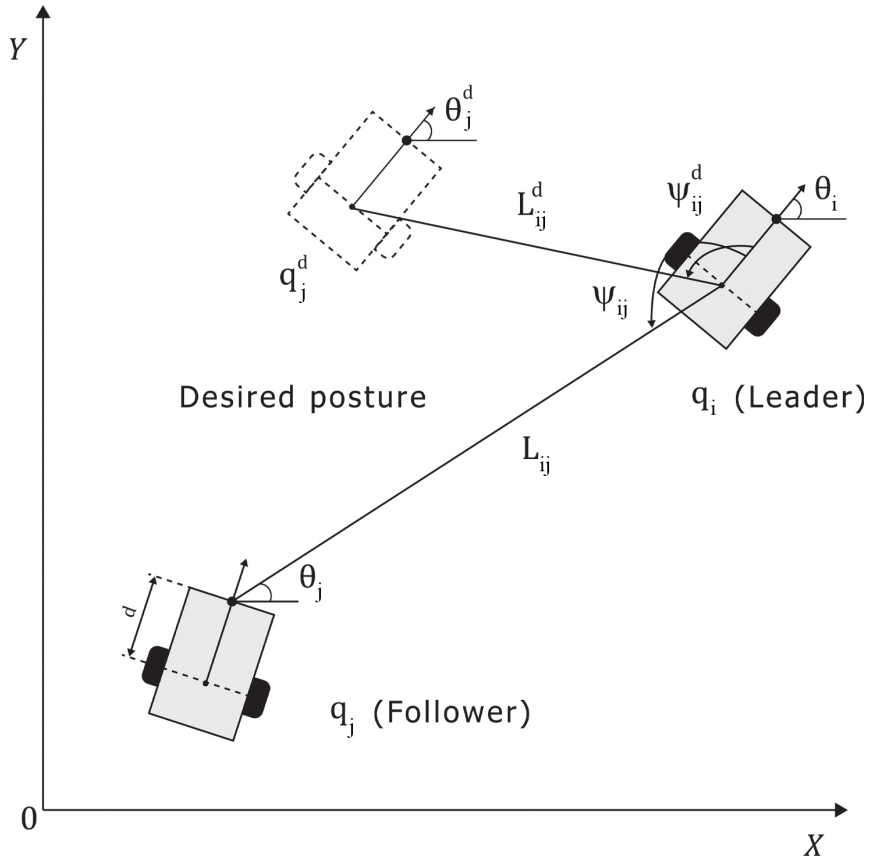


Figure. 2.2: The structure of leader follower formation.

The actual bearing angle and separation distance between the follower robot and it's leader are given as $\psi_{ij}$ and $L_{ij}$, whereas $L^d_{ij}$, $\psi^d_{ij}$ are the desirable separation and orientation angle respectively.

As shown in Figure 2.2, the desired posture $q^d_j$ can be obtained using geometric relation between robots as follows :

$$q^d_j = \begin{bmatrix} x^d_j \\ y^d_j \\ \theta^d_j \end{bmatrix} = \begin{bmatrix} x_i - d\cos\theta_i + L^d_{ij}\cos\left(\psi^d_{ij} + \theta^d_i\right) \\ y_i - d\sin\theta_i + L^d_{ij}\sin\left(\psi^d_{ij} + \theta^d_i\right) \\ \theta_j \end{bmatrix} \tag{2.6}$$

The follower robot posture is given by :

$$q_j = \begin{bmatrix} x_j \\ y_j \\ \theta_j \end{bmatrix} = \begin{bmatrix} x_i - d\cos\theta_i + L_{ij}\cos\left(\psi_{ij} + \theta_i\right) \\ y_i - d\sin\theta_i + L_{ij}\sin\left(\psi_{ij} + \theta_i\right) \\ \theta_j \end{bmatrix} \tag{2.7}$$

The relative distance $L_{ij}$ and bearing angle $\psi_{ij}$ can be given as :

$$\begin{cases} L_{ij} = \sqrt{L_{ijx}^2 + L_{ijy}^2} \\ \psi_{ij} = \arctan(\dfrac{L_{ijy}}{L_{ijx}}) - \theta_i + \pi \end{cases} \tag{2.8}$$

Where :

$$\begin{cases} L_{ijx} = x_i - x_j - d\cos\theta_i \\ L_{ijy} = y_i - y_j - d\sin\theta_i \end{cases} \tag{2.9}$$

Once the desired and actual posture of the follower robots are obtained , the tracking error of the formation (for each follower robot) can be given as follow :

$$\begin{aligned} e_j &= \begin{bmatrix} x_{e_j} \\ y_{e_j} \\ \theta_{e_j} \end{bmatrix} \\ &= \begin{bmatrix} \cos\theta_j & \sin\theta_j & 0 \\ -\sin\theta_j & \cos\theta_j & 0 \\ 0 & 0 & 1 \end{bmatrix} \begin{bmatrix} x_j^d - x_j \\ y_j^d - y_j \\ \theta_j^d - \theta_j \end{bmatrix} \\ &= \begin{bmatrix} L_{ij}^d \cos\left(\psi_{ij}^d + \theta_{ij}\right) - L_{ij}\cos\left(\psi_{ij} + \theta_{ij}\right) \\ L_{ij}^d \sin\left(\psi_{ij}^d + \theta_{ij}\right) - L_{ij}\sin\left(\psi_{ij} + \theta_{ij}\right) \\ \theta_j^d - \theta_j \end{bmatrix} \end{aligned} \tag{2.10}$$

Where $\theta_{ij} = \theta_i - \theta_j$, taking the derivative of equation (2.10) yields the following leader follower formation error dynamics:

$$\begin{aligned} \dot{e}_j &= \begin{bmatrix} \dot{x}_{e_j} \\ \dot{y}_{e_j} \\ \dot{\theta}_{e_j} \end{bmatrix} \\ &= \begin{bmatrix} \nu_i\cos\theta_{ij} + \omega_j y_{e_j} - \nu_j - L_{ij}^d\sin(\psi_{ij}^d + \theta_{ij}) \\ \nu_i\sin\theta_{ij} + \omega_j x_{e_j} - \omega_j + L_{ij}^d\cos(\psi_{ij}^d + \theta_{ij}) \\ \omega_j^d - \omega_j \end{bmatrix} \end{aligned} \tag{2.11}$$

Where $\omega_j, \nu_j$ are the follower robots angular and linear velocities, respectively.

Refereeing to [36], the robots orientations will be unequal during the formation, hence the desired bearing angle cannot be chosen as $\theta_j^d = \theta_i$ , instead its chosen such that its derivative becomes :

$$\dot{\theta}_j^d = (\nu_i \sin\theta_{ij} + L_{ij}^d \omega_i \cos(\psi_{ij}^d + \theta_{ij}) + 2K_2 y_{e_j})/d \tag{2.12}$$

Hence, the tracking error dynamics becomes [36] :

$$\begin{aligned} \dot{e}_j &= \begin{bmatrix} \dot{x}_{e_j} \\ \dot{y}_{e_j} \\ \dot{\theta}_{e_j} \end{bmatrix} \\ &= \begin{bmatrix} \nu_i \cos\theta_{ij} + \omega_j y_{e_j} - \nu_j - L_{ij}^d \sin(\psi_{ij}^d + \theta_{ij}) \\ \nu_i \sin\theta_{ij} + \omega_j x_{e_j} - \omega_j + L_{ij}^d \cos(\psi_{ij}^d + \theta_{ij}) \\ \dot{\theta}_j^d - \omega_j \end{bmatrix} \end{aligned} \tag{2.13}$$

### 2.3.2 Formation kinematic controller design

The formation objective is to ensure that every follower robot in the formation is keeping the desired bearing angle and separation distance relative to the leader robot, which implies that the following must satisfies :

$$\begin{cases} \lim_{t\to\infty}(L_{ij}^d - L_{ij}) = 0 \\ \lim_{t\to\infty}(\psi_{ij}^d - \psi_{ij}) = 0 \end{cases} \tag{2.14}$$

To achieve this control objective, the Backstepping Algorithm is selected to design the following kinematic controller, for each follower robot in the formation [36]:

$$\begin{cases} \omega_j = (\nu_i \sin\theta_{ij} + L_{ij}^d \omega_i \cos(\psi_{ij}^d + \theta_{ij}))/d \\ \quad + (k_2 y_{e_j} + k_3 \theta_{e_j})/d \\ \nu_j = k_1 x_{e_j} + \nu_i \cos\theta_{ij} - L_{ij}^d \omega_i sin(\psi_{ij}^d + \theta_{ij}) \end{cases} \tag{2.15}$$

Where $k_1, k_2, k_3$ are positive real numbers.

## 2.4 Formation dynamic controller design

### 2.4.1 Concepts on fractional calculus

As it mentioned in Chapter 1, fractional calculus theory can be viewed as an extension of classical calculus. It generalize the traditional concepts of derivatives and integrals to include fractional or non-integer orders, in fractional calculus the derivative operator is denoted by $D^{\alpha} = d^{\alpha}/dt$ where $\alpha$ is a real number.

**Definition 2.1.** Using Riemann-Liouville (RL) definition, the $\alpha$-order fractional derivative of function $f(t)$ over time can be expressed as follow [88]:

$$\begin{aligned} D^{\alpha} f(t) &= \frac{d^{\alpha} f(t)}{dt^{\alpha}} \\ &= \frac{1}{\Gamma(n-\alpha)} \left(\frac{d^n}{dt^n}\right) \int_0^t \frac{f(\tau)}{(t-\tau)^{\alpha+1-n}} d\tau \end{aligned} \tag{2.16}$$

Where $(n-1 < \alpha < n)$ and $\Gamma(.)$ represent the Gamma function defined in (2.17).

$$\Gamma(\alpha) = \int_0^{\infty} e^{-t} t^{\alpha-1} dt \tag{2.17}$$

**propriety 2.1.** *The n-th order derivative* $(d^n/dt^n)$ *of* $f(t)$ *can be written by using the fractional derivative operator* $D^{\alpha}$ *as follow :*

$$D^{\alpha+n} f(t) = \frac{d^n}{dt^n} \left(D^{\alpha} f(t)\right) = D^{\alpha} \left(\frac{d^n f(t)}{dt^n}\right) \tag{2.18}$$

#### 2.4.1.1 Sliding mode control

The procedure of designing a sliding mode controller consist of two main steps : It starts by choosing an appropriate sliding surface to design the equivalent control input $\tau_{eq}(t)$, which keeps the states of the system on the sliding manifold, and the second step is to push the system states to slide along the sliding manifold toward the origin by using the switching control law $\tau_{sw}(t)$ . Hence the complete sliding mode controller can be written as the sum of both control actions as :

$$\tau_j(t) = \tau_{eq_j}(t) + \tau_{sw_j}(t) \tag{2.19}$$

### 2.4.2 Design of the FO integral sliding mode controller

In this subsection , the FO calculus methods are used alongside with the sliding mode control to derive dynamic control laws $\tau_j(t)$, to deal with the system dynamic behaviors and to ensure that the followers actual velocities converge to the auxiliary velocities produced by the formation Backstepping controller defined in equation (2.15) . First the difference between the actual follower robots velocities $U_j = \begin{bmatrix}\nu_j & \omega_j\end{bmatrix}^T$ and the auxiliaries velocities $U_{c_j} = \begin{bmatrix}\nu_{c_j} & \omega_{c_j}\end{bmatrix}^T$ is considered as the velocity tracking error, and it's given as follow :

$$e_{c_j}(t) = \begin{bmatrix} e_{cj_1}(t) \\ e_{cj_2}(t) \end{bmatrix} = \begin{bmatrix} \nu_j(t) - \nu_{c_j}(t) \\ \omega_j(t) - \omega_{c_j}(t) \end{bmatrix} \tag{2.20}$$

Then the sliding surface function is chosen as :

$$S_j(t) = e_{c_j}(t) + \lambda \int e_{c_j}(\tau) d\tau \tag{2.21}$$

Based on definition 2.1 and by using propriety 2.1, equation (2.21) can be reformulated as :

$$S_j(t) = e_{c_j}(t) + \lambda \mathcal{D}^{-\alpha}\{e_{c_j}(t)\} \tag{2.22}$$

Taking the time derivatives of equation (2.22) gives the following :

$$\dot{S}_j(t) = \dot{e}_{c_j}(t) + \lambda \mathcal{D}^{1-\alpha}\{e_{c_j}(t)\} \tag{2.23}$$

The equivalent control law $\tau_{eq_j}(t)$ that forces all states trajectories to lie on the sliding surface can be obtained by setting $\dot{S}_j(t) = 0$ :

$$\begin{aligned} \dot{S}_j(t) &= \dot{e}_{c_j} + \lambda \mathcal{D}^{1-\alpha}\{e_{c_j}(t)\} \\ &= \dot{U}_j(t) - \dot{U}_{c_j}(t) + \lambda \mathcal{D}^{1-\alpha}\{e_{c_j}(t)\} = 0 \end{aligned} \tag{2.24}$$

Then substituting (2.5) into (2.24) yields :

$$\dot{S}_j(t) = H\tau_j(t) - \dot{U}_{c_j}(t) + \lambda \mathcal{D}^{1-\alpha}\{e_{c_j}(t)\} = 0 \tag{2.25}$$

Solving equation (2.25) gives the following equivalent control law $\tau_{eq_j}(t)$ :

$$\tau_{eq_j}(t) = -H^{-1}\Big[-\dot{U}_{c_j}(t) + \lambda \mathcal{D}^{1-\alpha}\{e_{c_j}(t)\}\Big] \tag{2.26}$$

Then, the following switching control law is introduced:

$$\tau_{sw_j}(t) = -H^{-1}\Big[Ksgn(S_j(t))\Big] \tag{2.27}$$

Where $sgn(.)$ represent the Signum function, $K = \begin{bmatrix} k_1 & 0 \\ 0 & k_2 \end{bmatrix}$ and $k_i$ are positive real numbers. Therefore, the complete control law is given as :

$$\begin{aligned} \tau_j(t) &= \tau_{eq_j}(t) + \tau_{sw_j}(t) \\ &= -H^{-1}\Big[-\dot{U}_{c_j}(t) + \lambda \mathcal{D}^{1-\alpha}\{e_{c_j}(t)\} + Ksgn(S_j(t))\Big] \end{aligned} \tag{2.28}$$

By considering the existence of parameters uncertainties and external disturbances in real world application, equation (2.5) is rewritten as [79]:

$$\dot{U}_j(t) = \bar{H}\tau_j(t) + \zeta(t) \tag{2.29}$$

Where $\bar{H}$ represent the nominal part of the system matrix $H$. $\zeta(t)$ is the vector which contain the model uncertainties denoted by $\Delta H$, and the system external disturbances $\tau_d$, which can be written as follow :

$$\zeta(t) = \Delta H\tau_j(t) + \tau_{d_j}(t) \tag{2.30}$$

Assuming that $\zeta(t)$ is bounded and satisfy the following condition $|\zeta(t)| \leq \delta$, where $\delta$ is a positive number.

Then, the FOISM controller described by equation (2.28) is redefined as follow :

$$\begin{aligned} \tau_j(t) &= \tau_{eq_j}(t) + \tau_{sw_j}(t) \\ &= -\bar{H}^{-1}\Big[-\dot{U}_{c_j}(t) + \lambda \mathcal{D}^{1-\alpha}\{e_{c_j}(t)\} + Ksgn(S_j(t))\Big] \end{aligned} \tag{2.31}$$

### 2.4.3 Stability analysis

**Theorem 2.1.** *Using the kinematic controller (2.15) and the FOISM control law in (2.31), the tracking errors of the formation described in equation (2.10) and the velocity tracking error defined in (2.20) will converge to zero asymptotically.*

*Proof.* Consider the Lyapunov function candidate defined in equation (2.32):

$$\mathfrak{V}(t) = \mathfrak{V}_1(t) + \mathfrak{V}_2(t) \tag{2.32}$$

Where $\mathfrak{V}_1(t)$ is chosen as :

$$\mathfrak{V}_1(t) = \frac{1}{2}(x_{e_j}^2 + y_{e_j}^2) + \frac{dk_3\theta_{e_j}^2}{2k_2} \tag{2.33}$$

And $\mathfrak{V}_2(t)$ is selected as :

$$\mathfrak{V}_2(t) = \frac{1}{2}S(t)^T S(t) \tag{2.34}$$

It's clear that $\mathfrak{V}(t) \geq 0$, substituting equations (2.13) and (2.15) in the time derivative of $\mathfrak{V}_1(t)$ results the following [36]:

$$\begin{aligned} \dot{\mathfrak{V}}_1(t) &= -k_1 x_{e_j}^2 - k_2 y_{e_j}^2 - k_3\theta_{e_j} y_{e_j} \\ &\quad - k_3^2\theta_{e_j}^2/k_2 + k_3\theta_{e_j} y_{e_j} \\ &= -k_1 x_{e_j}^2 - k_2 y_{e_j}^2 - k_3\theta_{e_j}^2 \leq 0 \end{aligned} \tag{2.35}$$

The existence of nonlinear sliding surface is given by the following sufficient condition :

$$\frac{1}{2}\frac{d}{dt}S(t)^T S(t) < -\eta|S(t)| \tag{2.36}$$

Taking the derivative of $\mathfrak{V}_2(t)$ along the time yields:

$$\begin{aligned} \dot{\mathfrak{V}}_2(t) &= S(t)^T \dot{S}(t) \\ &= S(t)^T \left[\dot{U}_j(t) - \dot{U}_{c_j}(t) + \lambda \mathcal{D}^{1-\alpha}\{e_{c_j}(t)\}\right] \end{aligned} \tag{2.37}$$

Using equation (2.36) and Substituting (2.29) and (2.31) into (2.37) results the following :

$$\begin{aligned} \dot{\mathfrak{V}}_2(t) &= S(t)^T \left[\zeta(t) - K sgn(S_j(t))\right] \\ &= S(t)\zeta(t) - K|S(t)| \\ &\leq |S(t)|\delta - K|S(t)| < -\eta|S(t)| < 0 \end{aligned} \tag{2.38}$$

By selecting the switching controller gain $K$ as follows :

$$K > \delta + \eta \tag{2.39}$$

Then $\mathfrak{V}_2(t) < 0$ , hence $\mathfrak{V}(t)$ is stable in the sense of Lyapunov and the formation kinematic tracking errors $e$ and dynamic tracking error $e_c$ will asymptotically converge to zero, and this ends the proof of Theorem 2.1. □

### 2.4.4 Design of fuzzy FO integral sliding mode controller

Its well known that the sliding mode control methods can assure a robust and higher control precision with a rapid convergence rate. However, the switching control action can leads to chattering behavior around the neighborhood of the sliding manifold, therefore, a Fuzzy Logic Controller FLC is utilized to dynamically adjust the switching gain K to suppress the chattering behavior.

The following steps are involved into the design procedure of the FFOISM control : First the sliding surfaces $S_j$ is selected as the fuzzy inference system FIS input variable and it consist of seven fuzzy sets denoted by [**NB**] Negative Big, [**NM**] Negative Medium, [**NS**] Negative Small, [**PS**] Positive Small, [**PM**] Positive Medium, [**PB**] Positive Big and [**ZO**] Zero, while the gain $K$ of the switching controller is chosen as the fuzzy inference system FIS output variable and it contain four fuzzy sets, labeled as follow : [**S**] Small, [**M**] Medium, [**B**] Big and [**Z**] Zero. Figure 2.3 shows the triangular type of the output and input membership functions.

In the next step, the fuzzy rule base is developed, where the $i$th fuzzy rule is given as follow:

$$\text{Rule(i)} :: \quad \text{IF} \quad \text{S}_j^u \quad \text{is} \quad \text{A}_\text{j}^i \quad \text{THEN} \quad \text{K}_f^u \quad \text{is} \quad \text{B}_\text{j}^i$$

$B_j^i$ and $A_j^i$ denotes the set labels of the fuzzy output and input variables respectively . The rule base used for the FFOISM controller is shown in Table 2.1. Finally, the method of center average defuzzifcation is used to convert the fuzzy variable $\text{K}_f^u$ into it's crisp output value $K_f$.

Table 2.1: FLC rule base.

| $S_j$ | NB | NM | NS | ZO | PS | PM | PB |
|---|---|---|---|---|---|---|---|
| $K_f$ | B | M | S | Z | S | M | B |

The complete architecture of the proposed control scheme is explained in the diagram shown in Figure 2.4.

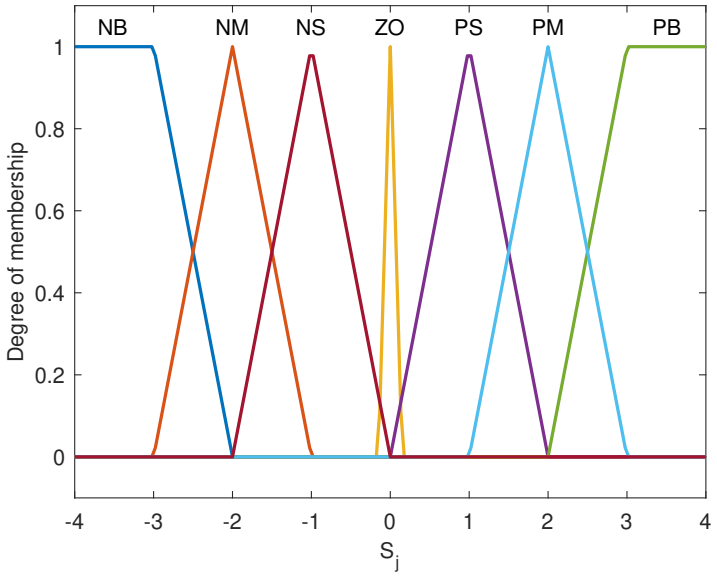


(a)

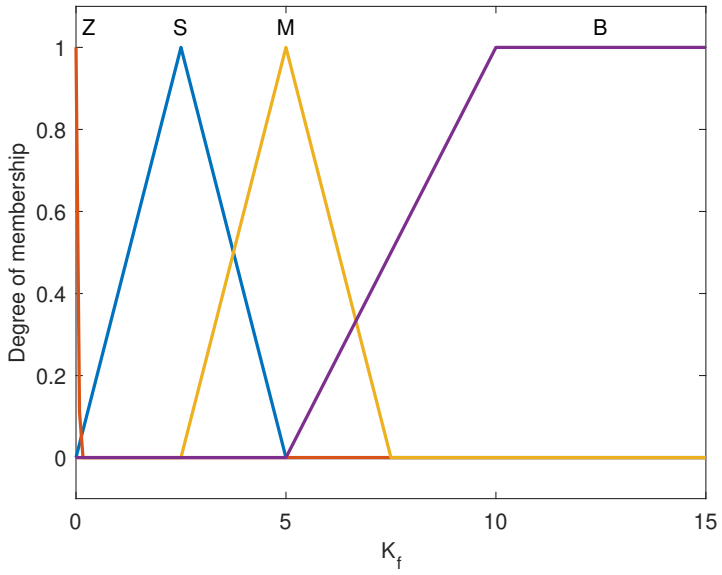


(b)

Figure. 2.3: The fuzzy logic controller Membership functions, (a) the input $S_j$ membership function, (b) the output $K_f$ membership function.

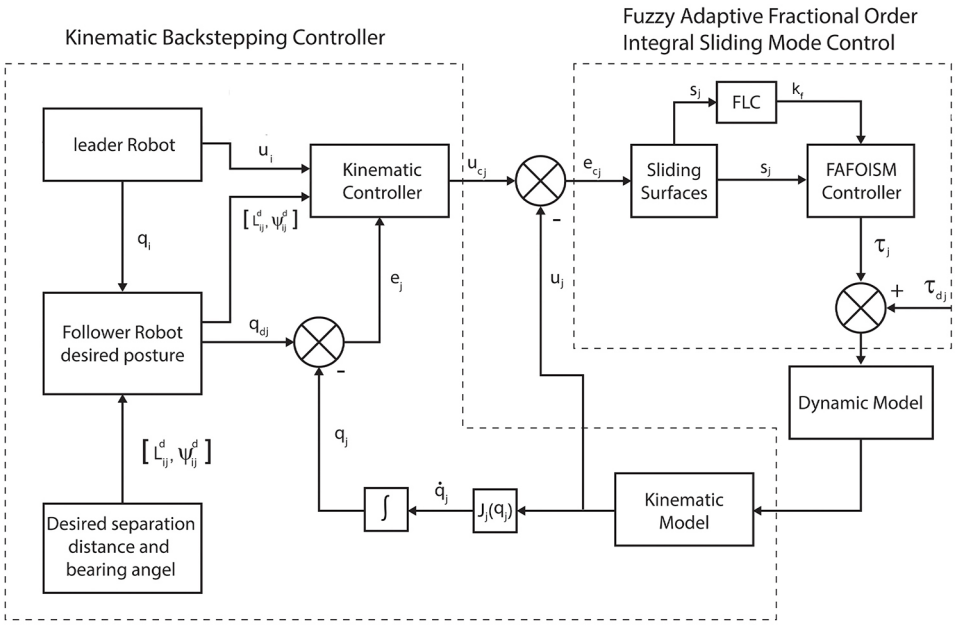


Figure. 2.4: Complete architecture of the FFOISM controller for follower robot $R_j$.

## 2.5 Simulation results

Simulation examples of leader follower formation control using MATLAB are presented in this section. In all examples the parameters of each mobile robot are chosen as $m = 4Kg$, $I = 3.7Kgm^2$, $R = 0.15m$ and $r = 0.03m$. The external disturbances for each follower robots in the formation are selected as :

$$\tau_d = \begin{bmatrix} 0.1\cos(2t) \\ 0.1\sin(2t) \end{bmatrix} \tag{2.40}$$

And the parametric uncertainties were achieved by the following :

$$\Delta H = \begin{bmatrix} 0.2\sin(t) & 0.1\cos(t) \\ 0.2\sin(t) & 0.3\cos(t) \end{bmatrix} \tag{2.41}$$

For both control laws given by (2.15) and (2.31), the following parameters are used: $k_1 = 10, k_2 = 2, k_3 = 5, d = 0.1, \lambda = 5 * 10^{-2}, \alpha = 0.2$.

### 2.5.1 Triangular-like formation on a sinusoidal trajectory

In this simulation a 3 mobile robots are supposed to achieve a triangular like formation. One of the robot is assigned with leader role in the formation and is tracking a sinusoidal trajectory given by :

$$\begin{cases} x_r = -6 + 2t \\ y_r = 2\sin(t) \end{cases} \tag{2.42}$$

To achieve the desired formation pattern both follower robots must keep a desired separation distance $L_d = 1m$ relative to the leader, a desired bearing angle $\phi_d = 4\pi/3$ for the first follower and $\phi_d = 2\pi/3$ for the second follower.

The leader robot initial posture is chosen as $q_l = \begin{bmatrix} -6.0 & 0.0 & \pi/4 \end{bmatrix}^T$. The initial posture of the first follower robot is selected as $q_1 = \begin{bmatrix} 6.0 & -1.0 & \pi/4 \end{bmatrix}^T$, and the second follower robot initial posture is chosen as $q_2 = \begin{bmatrix} 6.0 & 1.0 & \pi/4 \end{bmatrix}^T$ .

The formation trajectories are presented in Figure 2.5. The dynamic control laws $\tau_j$ are depicted in Figure 2.7, while the tracking errors for both followers are illustrated in Figure 2.6, and the velocities of the followers are shown in Figure 2.8.

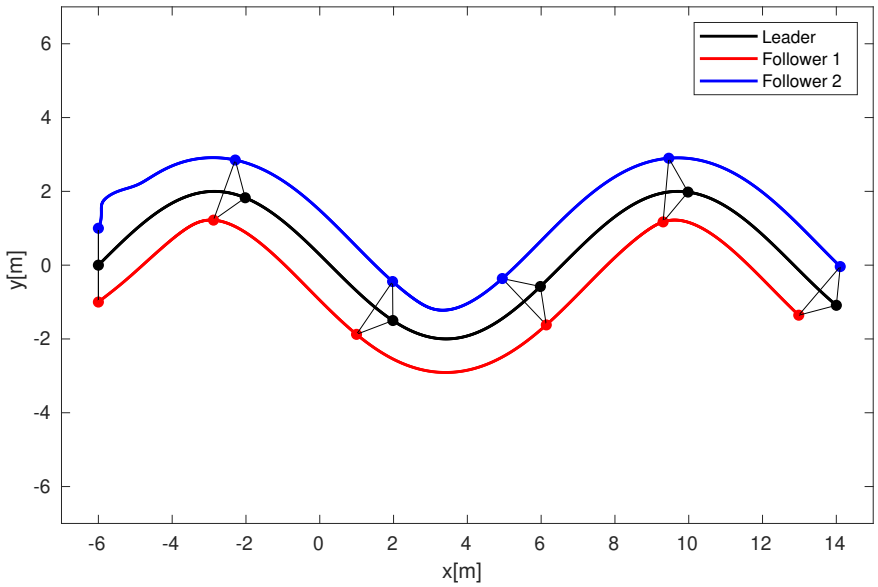


Figure. 2.5: Triangular-like leader follower formation control on a Sinusoidal Trajectory .

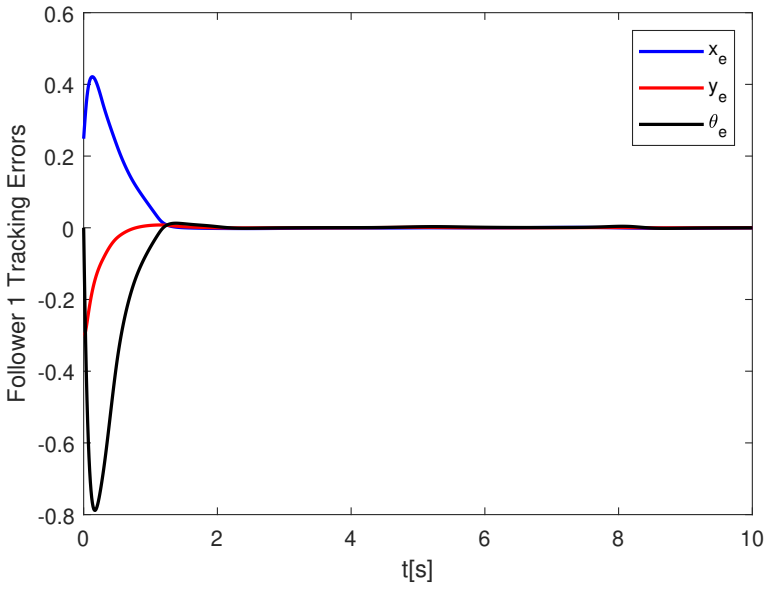


(a)

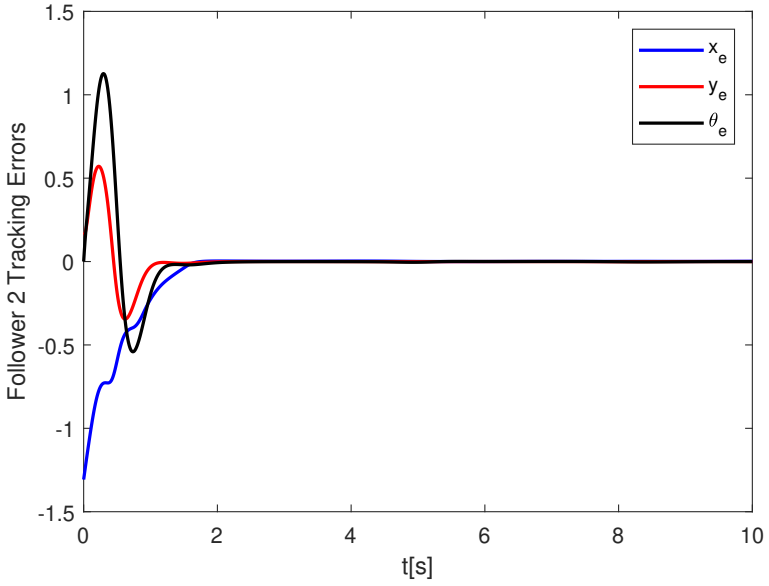


(b)

Figure. 2.6: Formation tracking errors, (a) follower 1 tracking errors, (b) follower 2 tracking errors

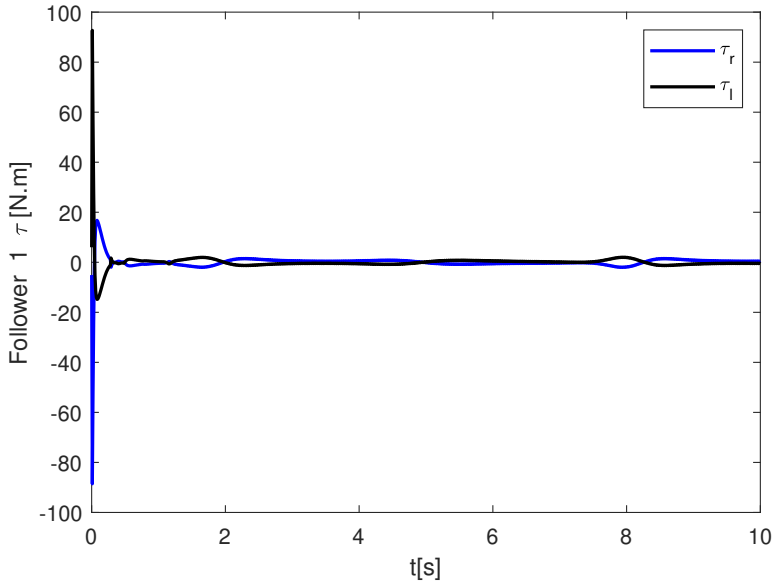


(a)

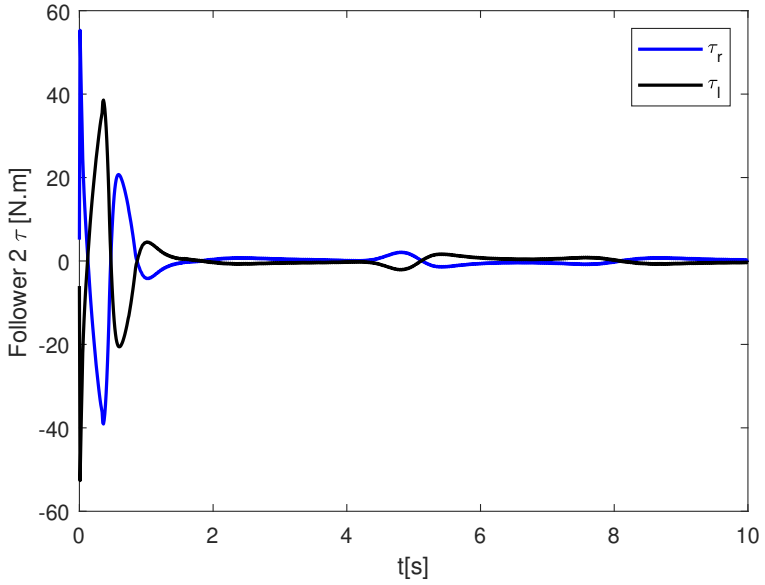


(b)

Figure. 2.7: The control torques of follower robots, (a) follower 1 left and right wheels torques, (b) follower 2 left and right wheels torques

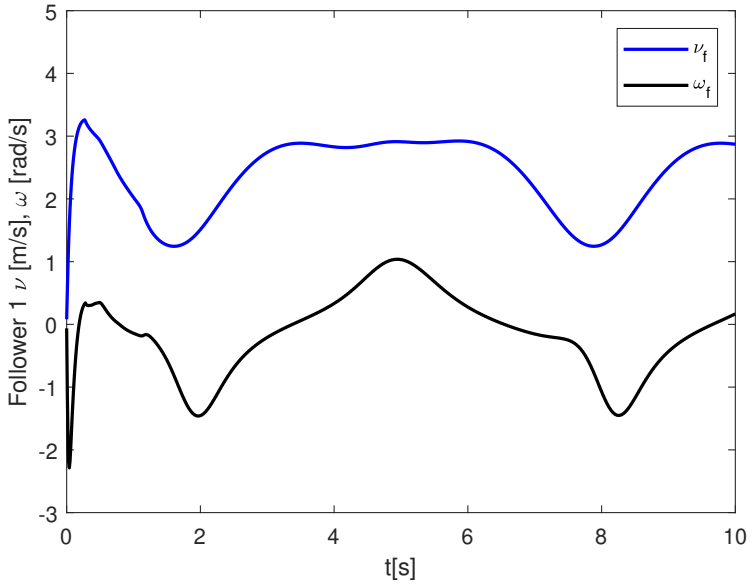


(a)

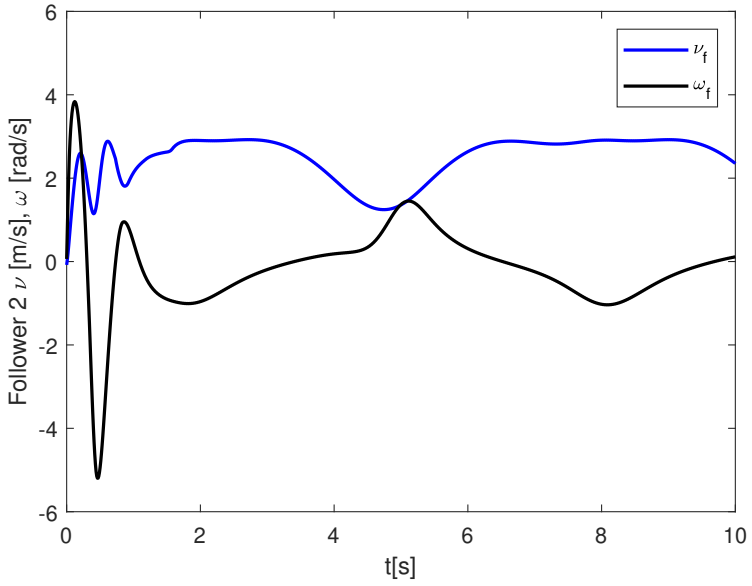


(b)

Figure. 2.8: The velocities of follower robots, (a) follower 1 linear and angular velocities, (b) follower 2 linear and angular velocities

### 2.5.2 Comparative study and results discussion

To examine the performance of the proposed control method, a comparative study is presented in this subsection. The FFOISM control scheme is compared to another three control methods, namely : (**I**) Integral Sliding Mode ISM proposed in [89], with a constant switching gain $K$ $[\tau_{sw_j}(t) = ksgn(S_j(t))]$ , (**II**) Integral Sliding Mode ISMC where the *Signum* function in the switching control is replaced with a continuous tangent hyperbolic function *tanh* $[\tau_{sw_j(t)} = ktanh(S_j(t))]$, and with (**III**) Fuzzy Integral Sliding Mode FISM where the order of the integral in the sliding surface is chosen as an integer $\alpha = 1$.

For simplicity a 2-robot formation is considered in this simulation, where the leader robot is moving on a circular like trajectory with a constant velocities $\nu = 1m$ and $\omega = 1rad/s$ . The desired separation and heading angle are selected as $L_d = 2m$, $\phi_d = 4\pi/3$, respectively . The initial leader robot posture is $q_l = \begin{bmatrix} 1 & 0 & \pi/2 \end{bmatrix}^T$, and the follower robot initial posture is chosen as $q_1 = \begin{bmatrix} 2.5 & -0.75 & \pi/2 \end{bmatrix}^T$.

In-addition, the formation tracking performances of the follower robot controlled by the FFOISM are compared with the other control methods using two different performance indexes. Table 2.2 shows the obtained comparison results, while the tracking error indexes were achieved using equation (2.43), where $t$ denotes the simulation time :

$$IAE = \int_0^t |e|dt, \quad ITAE = \int_0^t t|e|dt \tag{2.43}$$

Comparison between the formation trajectories is illustrated in Figure 2.9. In Figure 2.13 a comparison between the dynamic control laws $\tau_j$ using the FFOISM controller and the other control methods is presented. Figure 2.14 shows a comparison between the velocities of the follower robot, while a comparison between the formation tracking errors is depicted in Figure 2.10, Figure 2.11 and Figure 2.12, respectively.

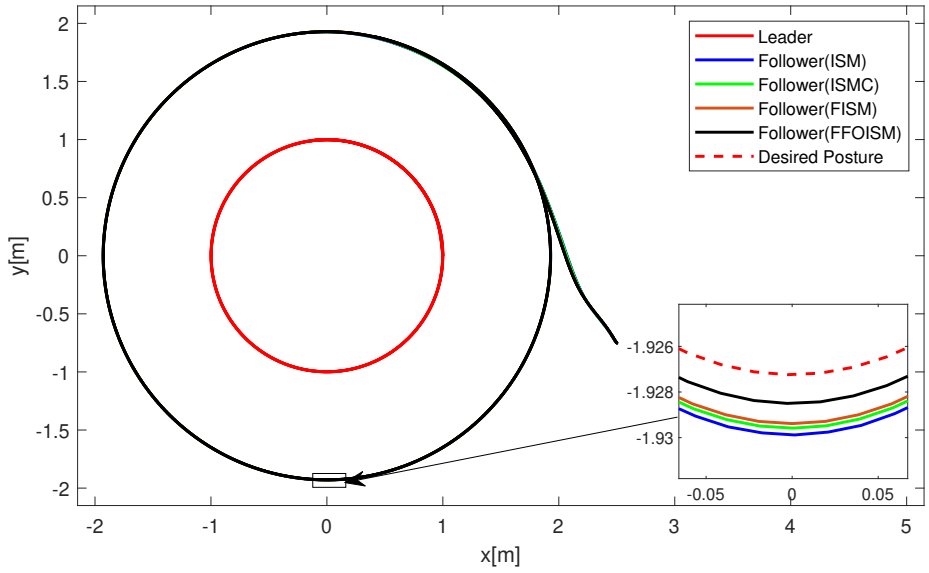


Figure. 2.9: Leader follower formation control on a Circular Trajectory.

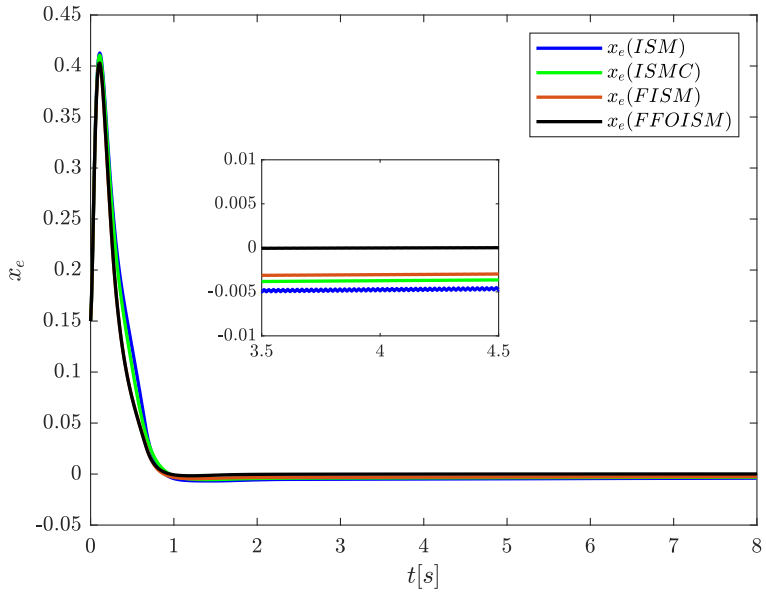


Figure. 2.10: Comparison between the follower robot formation tracking error on the x-axis.

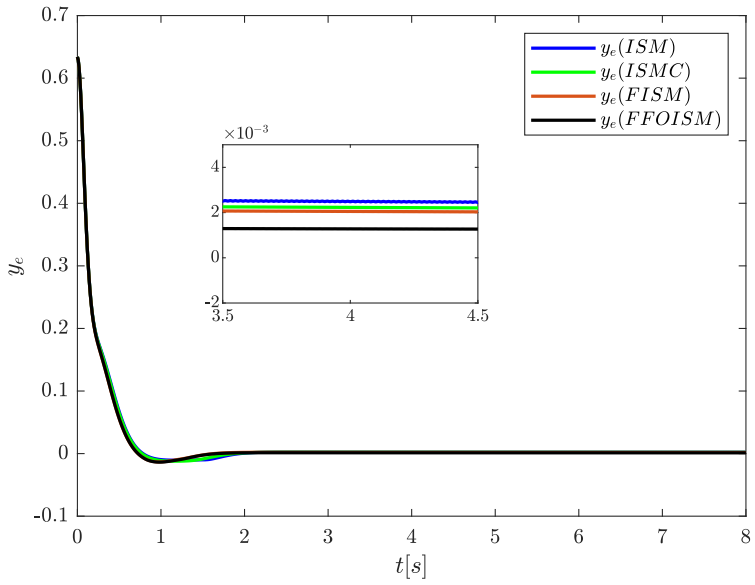


Figure. 2.11: Comparison between the follower robot formation tracking error on the y-axis.

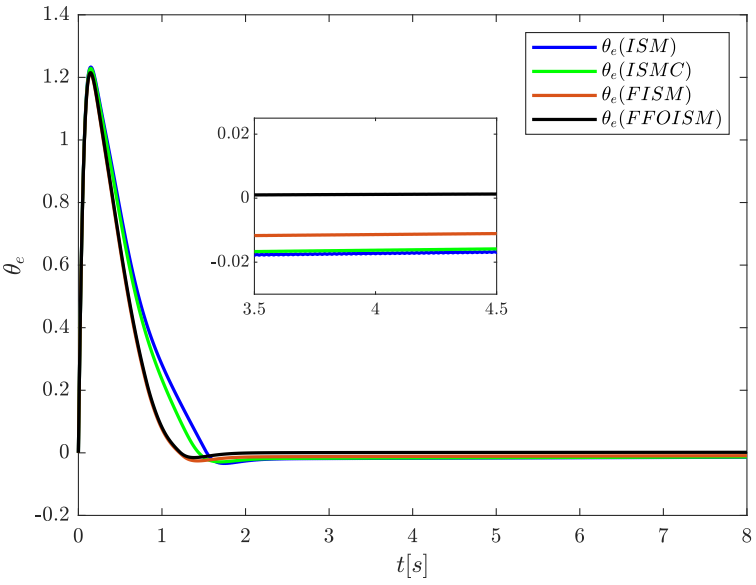


Figure. 2.12: Comparison between the follower robot formation heading angle error.

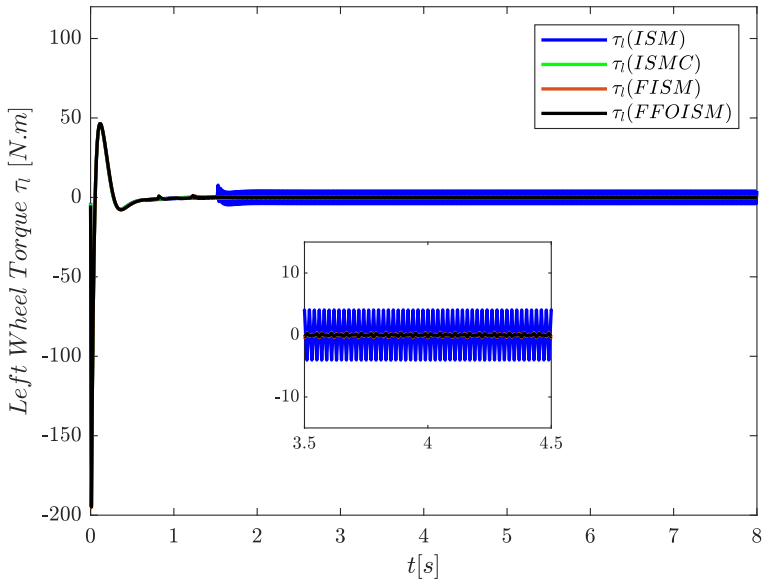


(a)

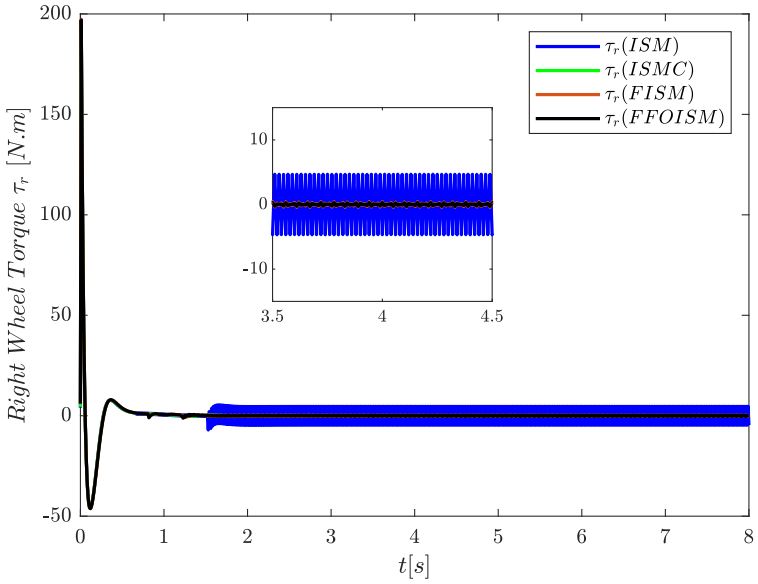


(b)

Figure. 2.13: Comparison between left and right wheels torques, (a) left wheel torque, (b) right wheel torque.

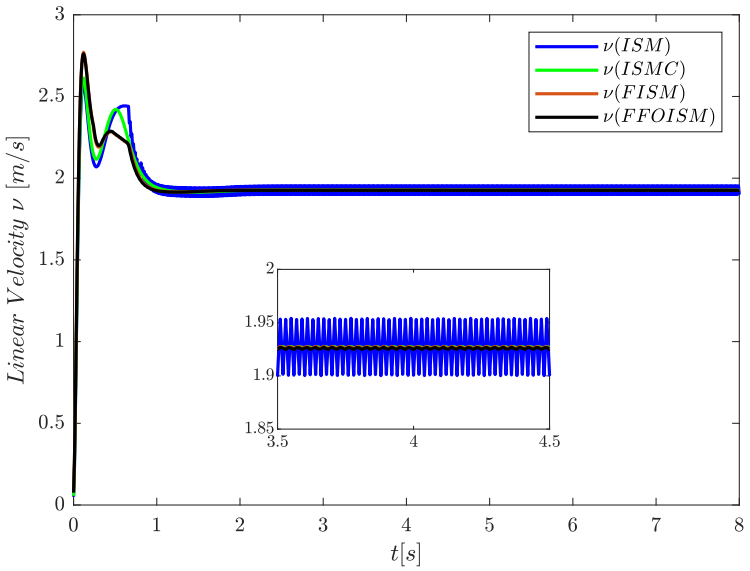


(a)

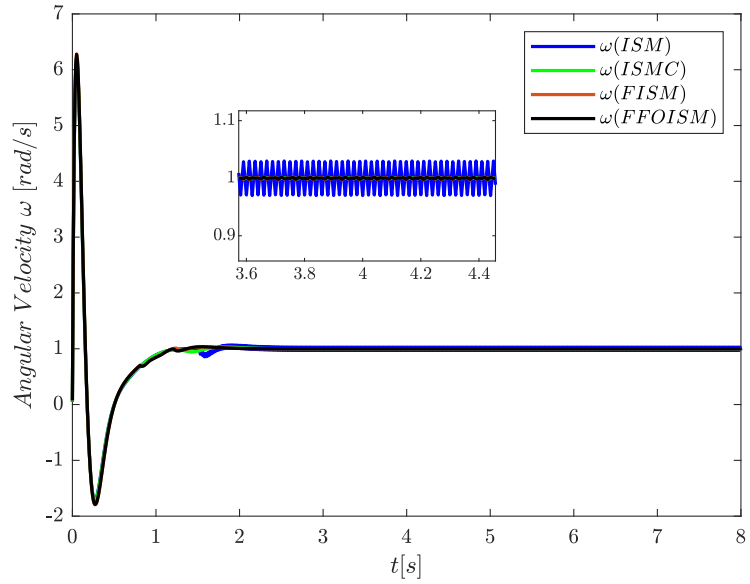


(b)

Figure. 2.14: Comparison between the velocities commands, (a) linear velocity, (b) angular velocity.

Table 2.2: Comparison between the kinematic tracking errors.

| | IAE | | | ITAE | | |
|---|---|---|---|---|---|---|
| tracking errors | $x_e$ | $y_e$ | $\theta_e$ | $x_e$ | $y_e$ | $\theta_e$ |
| ISM [89] | 0.1818 | 0.1515 | 0.9218 | 0.1806 | 0.1069 | 0.8869 |
| ISMC | 0.1676 | 0.1490 | 0.8662 | 0.1468 | 0.0987 | 0.8094 |
| FISM | 0.1459 | 0.1425 | 0.7090 | 0.1193 | 0.0895 | 0.5649 |
| FFOISM | 0.1261 | 0.1384 | 0.6495 | 0.0322 | 0.0677 | 0.2825 |

The simulations results in Figure 2.5 shows the well achievement of the leader follower formation control , and as illustrated in Figure 2.6 the formation tracking errors for both follower robots converge to zero over time, under the existence of model uncertainty and system external disturbances using the FFOISM control method.

In the comparative study section, it is obvious that the formation control is well established using all control strategies but from the zoomed view in Figure 2.9, one can conclude that FFOISM control has a better accuracy rate then the other methods. Meanwhile, the comparison between the dynamic control inputs shown in Figure 2.13 and the velocities commands illustrated in Figure 2.14, it is clear that the ISM control method can lead to the chattering phenomenon.

Moreover, From the magnified views of the formation tracking errors in Figure 2.10, Figure 2.11 and Figure 2.12, it can be seen that changing the *sgn* function with *tanh* function in the switching control law $\tau_{sw}$ can solve the chattering problem. However, it can reduce the tracking performances compared to FISM and FFOISM where the switching gain $k_f$ is dynamically adjusted using FLC techniques, on the other hand the comparison results obtained in Table 2.2 indicate that the FFOISM control method have the lowest error tracking values $\mathbf{IAE} = (0.1261, 0.1384, 0.6495)$ and $\mathbf{ITAE} = (0.0322, 0.0677, 0.2825)$ among other used control methods.

Therefore, according to the above comparison outcomes. It has been demonstrated that the proposed FFOISM controller can lead to a better control performances among other three methods, in terms of robustness against system uncertainties and disturbances, tracking accuracy, and convergence rate .

## 2.6 Conclusion

Formation control of nonholonomic wheeled mobile robots according to the leader follower strategy has been discussed in this chapter. The concepts of fractional order calculus are used together with the sliding mode control method to design a robust dynamic control inputs for each follower robots in the formation, to follow the leader robot and preserve the required formation pattern under the existence of unknown disturbances and model uncertainties. In addition, the chattering elimination is achieved with the aid of a fuzzy logic controller. The simulation results and the comparison outcomes clarified that the suggested control scheme provide a better control performances compared to other used sliding mode controllers.

# CHAPTER 3

# Adaptive distributed fractional order fast terminal sliding mode formation control of nonholonomic wheeled mobile robots

## 3.1 Introduction

In this chapter, an adaptive distributed formation controller for wheeled nonholonomic mobile robots is developed. The dynamical model of the robots is first derived by employing the Euler-Lagrange equation while taking into consideration the presence of disturbances and uncertainties in practical applications. Then, by incorporating fractional calculus in conjunction with fast terminal sliding mode control and consensus protocol, a robust distributed formation controller is designed to assure a fast and finite-time convergence of the robots towards the required formation pattern. Additionally, an adaptive mechanism is integrated to effectively counteract the effects of disturbances and uncertain dynamics. Moreover, the suggested control scheme's stability is theoretically proven through the Lyapunov theorem. Finally, simulation outcomes are provided to demonstrate the enhanced performance and efficiency of the suggested control technique.

Consensus theory has been widely employed to design distributed formation control algorithms for multi-robot systems. Where the primary objective of using consensus protocol is to synchronize the motion of robots to reach a common position or velocity in order to establish a certain geometric shape. Different control strategies have been

used alongside with consensus protocol to address the formation control problem, these include Model predictive control [90], Backstepping techniques [91, 92], Sliding mode control [93–95] and other control schemes [96–98].

Sliding mode control outperforms the previously mentioned control schemes when it comes to dealing with system parameters variation, uncertainties and external disturbances. This superior performance has led to its widespread adoption in the control of multi-robot systems. The authors in [99] combine sliding mode control with fuzzy logic techniques to design an adaptive decentralized formation controller for team of mobile robots under directed topologies with uncertain dynamics. In [100] consensus-based approach has been utilized in conjunction with sliding mode control to design a distributed controller for the formation of a team of unicycles. Authors in [101] investigate the formation control of multi nonholonomic wheeled robots. They develop a finite-time observer utilizing integral sliding mode method to estimate the robots velocities, then a dynamic output feedback controller has been used to drive all robots towards the predefined formation geometric configuration.

Motivated by the above discussion, an adaptive distributed fractional fast terminal sliding mode controller for multi-robots formation is suggested in this chapter. Unlike Chapter 2, graph theory and consensus-based techniques are used in this chapter to model the communication topology between the robots. Therefore, the control scheme design does not necessitate prior knowledge of the required bearing angle and separation distance for each robot in relation to its leader. Instead, the follower robot can get information only from its neighboring robots. The implementation of the fast terminal sliding mode control FTSMC method allow the robots to achieve both rapid and finite-time convergence towards the desired pattern despite the existence of uncertain dynamics and disturbances. The inclusion of the FO derivatives into the FTSMC controller offers more freedom for control parameter selection, fine-tuning of the fractional orders leads to a desirable control performances. Additionally, an adaptive learning rule is used to estimate the bounded uncertainties and disturbances in the system. The performances of the suggested control method is evaluated through simulation results. The comparison outcomes demonstrate the superiority of the ADFOFTSMC in terms of robustness, rapidity and accuracy.

## 3.2 preliminaries

### 3.2.1 Algebraic graph theory

In this chapter, a multi mobile robot system consist of n robot with only one leader is addressed, the followers are denoted by indices $(1,2,...,n-1)$, while the leader robot is labeled with index $n$, and the exchange of information between the followers and the leader robot is considered to be unidirectional. In other words, the followers cannot send information's to the leader robot.

let $\bar{\mathcal{G}} = (\bar{\mathcal{V}}, \bar{\mathcal{E}})$ be a sub-graph of digraph $\mathcal{G}$, then the adjacency matrix of $\bar{\mathcal{G}}$ can be written as :

$$\bar{\mathcal{A}} = \begin{bmatrix} \bar{a}_{11} & \bar{a}_{12} & \dots & \bar{a}_{1(n-1)} \\ \bar{a}_{21} & \bar{a}_{22} & \dots & \bar{a}_{2(n-1)} \\ \vdots & \vdots & \ddots & \vdots \\ \bar{a}_{(n-1)1} & \bar{a}_{(n-1)2} & \dots & \bar{a}_{(n-1)(n-1)} \end{bmatrix}$$

The sub-graph $\bar{\mathcal{G}}$ Laplacian matrix is written as follow:

$$\bar{\mathcal{L}} = \bar{\mathcal{D}} - \bar{\mathcal{A}}$$

With in-degree matrix $\bar{\mathcal{D}} = diag(\sum_{j=1}^{n-1} \bar{a}_{ij})$. The connection between the leader and followers is represented by a diagonal matrix $\bar{\mathcal{B}}$, where $\bar{\mathcal{B}} = \text{diag}\left\{\bar{b}_1, \bar{b}_2, \dots, \bar{b}_{n-1}\right\}$ and $\bar{b}_i = \bar{a}_{in}, i = 1,2,\dots,n-1$.

**Lemma 3.1.** *Let $\mathcal{G} = (\mathcal{V}, \mathcal{E})$ be a digraph, then the corresponding right eigenvector of the Laplacian matrix $\mathcal{L}$ associated with the eigenvalue 0 is the vector $\mathbf{1}_n$, only if the digraph $\mathcal{G}$ has a spanning tree, this mean that $\mathcal{L}\mathbf{1}_n = 0$.*

**Lemma 3.2.** *$\bar{\mathcal{L}}\mathbf{1}_{n-1} = 0$, if the sub-graph $\bar{\mathcal{G}}$ has a spanning tree [102], $(\bar{\mathcal{L}} + \bar{\mathcal{B}})$ is non-singular matrix and* $\text{Rank}(\bar{\mathcal{L}} + \bar{\mathcal{B}}) = n - 1$ .

### 3.2.2 Nonholonomic robot dynamic model

Consider the differential drive wheeled mobile robot illustrated in Figure 2.1, the generalized coordinates of the robot head is denoted by $q_i = \begin{bmatrix} x_i & y_i & \theta_i \end{bmatrix}^T$ where $\theta_i$ is the heading angle, $y_i$ and $x_i$ are the robot head Cartesian coordinates. This type of robots is subjected to nonholonmic constraints described by equation (2.1). The

distance between the head of the robot and its center of mass is denoted by $d$.
By using the nonholonomic constraint (2.1), the robot kinematic equation can be expressed as follow:

$$\dot{q}_i = \begin{bmatrix} \dot{x}_i \\ \dot{y}_i \\ \dot{\theta}_i \end{bmatrix} = \begin{bmatrix} \cos\theta_i & -d\sin\theta_i \\ \sin\theta_i & d\cos\theta_i \\ 0 & 1 \end{bmatrix} \begin{bmatrix} \nu_i \\ \omega_i \end{bmatrix} = \mathcal{J}(q_i)\mathcal{U}_i \tag{3.1}$$

Where $\nu_i$ denotes the robot linear velocity and $\omega_i$ is the angular velocity.

In this Chapter, the Euler-Lagrange equation is utilized to formulate the dynamic model of the $i$-th robot in the multi-robot system as follow:

$$M(q_i)\ddot{q}_i + V_m(q_i,\dot{q}_i)\dot{q}_i + \Delta_i = B(q_i)\tau_i \tag{3.2}$$

The matrices $M_i(q_i), V_{mi}(q_i,\dot{q}_i)$ and $B_i(q_i)$ in equation (3.2) are given as follow:

$$\tau_i = \begin{bmatrix} \tau_{l_i} \\ \tau_{r_i} \end{bmatrix}, \ \Delta_i = \begin{bmatrix} \Delta_{x_i} & \Delta_{y_i} & \Delta_{\theta_i} \end{bmatrix}^T$$

$$V_m(q_i,\dot{q}_i) = \begin{bmatrix} 0 & 0 & md\dot{\theta}_i\cos\theta_i \\ 0 & 0 & md\dot{\theta}_i\sin\theta_i \\ 0 & 0 & 0 \end{bmatrix}$$

$$B(q_i) = \frac{1}{r}\begin{bmatrix} \cos\theta_i & \cos\theta_i \\ \sin\theta_i & \sin\theta_i \\ R & -R \end{bmatrix}$$

$$M(q_i) = \begin{bmatrix} m & 0 & md\sin\theta_i \\ 0 & m & -md\cos\theta_i \\ md\sin\theta_i & -md\cos\theta_i & I \end{bmatrix}$$

Where $\Delta_i$ is a vector consist of disturbances and uncertain dynamics, $\tau_i$ is the vector of control inputs, $I$ denotes the total moment of inertia, $r$ is the robot wheel radius, $m$ represent the robot mass and $2R$ denotes the robot width.

By substituting the kinematic equation (3.1) into equation (3.2), the following robot dynamics are obtained:

$$\bar{M}(q_i)\dot{\mathcal{U}}_i + \bar{V}_m(q_i,\dot{q}_i)\mathcal{U}_i + \mathcal{J}^T(q_i)\Delta_i = \bar{B}(q_i)\tau_i \tag{3.3}$$

Where:

$$\bar{M}(q_i) = \mathcal{J}^T(q_i)M(q_i)\mathcal{J}(q_i),$$

$$\bar{V}m(q_i,\dot{q}_i) = 0,\ \bar{B}(q_i) = \mathcal{J}^T(q_i)B(q_i)$$

Under the assumption that $M(q_i)$ is invertible subject to $I - md^2 \neq 0$. Then equation (3.3) can be reformulated as follow:

$$\dot{\mathcal{U}}_i = \bar{M}^{-1}(q_i)\bar{B}(q_i)\tau_i - \bar{M}^{-1}(q_i)\mathcal{J}^T(q_i)\Delta_i \tag{3.4}$$

The kinematic equation (3.1) can be re-written as:

$$\begin{bmatrix}\dot{x}_i\\ \dot{y}_i\end{bmatrix} = \begin{bmatrix}\cos\theta_i & -d\sin\theta_i\\ \sin\theta_i & d\cos\theta_i\end{bmatrix}\begin{bmatrix}\nu_i\\ \omega_i\end{bmatrix} = \mathcal{H}(\theta_i)\begin{bmatrix}\nu_i\\ \omega_i\end{bmatrix} \tag{3.5}$$

Taking time derivative of (3.5), yield the following:

$$\begin{bmatrix}\ddot{x}_{hi}\\ \ddot{y}_{hi}\end{bmatrix} = \mathcal{H}_i(\theta_i)\left[\bar{M}^{-1}(q_i)\bar{B}(q_i)\tau_i - \bar{M}^{-1}(q_i)\mathcal{J}^T(q_i)\Delta_i\right] + \begin{bmatrix}\sigma_{1_i}\\ \sigma_{2_i}\end{bmatrix} \tag{3.6}$$

Where

$$\begin{bmatrix}\sigma_{1_i}\\ \sigma_{2_i}\end{bmatrix} = \begin{bmatrix}-\nu_i\omega_i\sin(\theta_i) - d\omega_i^2\cos(\theta_i)\\ \nu_i\omega_i\cos(\theta_i) - d\omega_i^2\sin(\theta_i)\end{bmatrix} \tag{3.7}$$

By defining $\tau_i$ as follow:

$$\begin{bmatrix}\tau_{l_i}\\ \tau_{r_i}\end{bmatrix} = (\mathcal{H}_i(\theta_i)\bar{M}^{-1}(q_i)\bar{B}(q_i))^{-1}\begin{bmatrix}u_{x_i} - \sigma_{1_i}\\ u_{y_i} - \sigma_{2_i}\end{bmatrix} \tag{3.8}$$

Substituting equation (3.8) in (3.6), results the following simplified equivalent model of the $i$-th robot:

$$\begin{bmatrix}\dot{x}_i\\ \dot{y}_i\end{bmatrix} = \begin{bmatrix}v_{x_i}\\ v_{y_i}\end{bmatrix}$$
$$\begin{bmatrix}\dot{v}_{x_i}\\ \dot{v}_{y_i}\end{bmatrix} = \begin{bmatrix}u_{x_i}\\ u_{y_i}\end{bmatrix} + \begin{bmatrix}\delta_{x_i}\\ \delta_{y_i}\end{bmatrix} \tag{3.9}$$

where $(v_{xi}, v_{yi})$ are the x-axis and y-axis robot velocities, respectively. $(u_{xi}, u_{yi})$ are the system control inputs and $(\delta_{xi}, \delta_{yi})$ denotes the bounded uncertainties described by:

$$\begin{bmatrix} \delta_{xi} \\ \delta_{yi} \end{bmatrix} = -\mathcal{H}_i(\theta_i)\bar{M}^{-1}(q_i)\mathcal{J}^T(q_i)\Delta_i \tag{3.10}$$

**Assumption 3.1.** *The parametric uncertainties described in (3.10) are assumed to be bounded, which mean there exist a positive constants such that* $|\delta_{xi}| < \Delta_x$ *and* $|\delta_{yi}| < \Delta_y$.

## 3.3 Formation controller synthesis

In this section, the synthesis of an adaptive distributed formation controller is presented. The main objective is to drive the robots to form a desired pattern while achieving velocity consensus by exchanging information with local neighboring robots.

### 3.3.1 Formation error dynamics

Let $z_i = [x_i \ y_i]^T$ , $v_i = [v_{x_i} \ v_{y_i}]^T$ and $\delta_i = [\delta_{x_i} \ \delta_{y_i}]^T$. Then, the follower robots augmented state vector can be described as:

$$\begin{aligned} \dot{z} &= v \\ \dot{v} &= u + \delta \end{aligned} \tag{3.11}$$

With $z = \begin{bmatrix} z_1^T & z_2^T & \dots & z_{n-1}^T \end{bmatrix}$, $v = \begin{bmatrix} v_1^T & v_2^T & \dots & v_{n-1}^T \end{bmatrix}$ and $\delta = \begin{bmatrix} \delta_1^T & \delta_2^T & \dots & \delta_{n-1}^T \end{bmatrix}$.

By defining the formation desired pattern positions as $f_i = [f_{ij}^x \ f_{ij}^y]^T$, then, the tracking error vector of the formation can described by:

$$e = ((\bar{\mathcal{L}} + \bar{\mathcal{B}}) \otimes I_2)(z - f) - (\bar{\mathcal{B}} 1_{n-1} \otimes I_2) z_n \tag{3.12}$$

Where $I_2 \in R^{2\times 2}$ is the identity matrix, $\otimes$ is the Knocker product, $f = \begin{bmatrix} f_1^T & f_2^T & \dots & f_{n-1}^T \end{bmatrix}$, $e_i = [e_{x_i} \ e_{y_i}]^T$ and $e = \begin{bmatrix} e_1^T & e_2^T & \dots & e_{n-1}^T \end{bmatrix}$.

Taking the derivative of (3.12) yield the following tracking error dynamics:

$$\dot{e} = ((\bar{\mathcal{L}} + \bar{\mathcal{B}}) \otimes I_2) v - (\bar{\mathcal{B}} 1_{n-1} \otimes I_2) v_n \tag{3.13}$$

Hence, the second derivative of equation (3.12) becomes:

$$\begin{aligned}\ddot{e} &= ((\bar{\mathcal{L}}+\bar{\mathcal{B}})\otimes I_2)u + ((\bar{\mathcal{L}}+\bar{\mathcal{B}})\otimes I_2)\delta \\ &\quad -(\bar{\mathcal{B}}1_{n-1}\otimes I_2)u_n\end{aligned} \tag{3.14}$$

### 3.3.2 Fractional order fast terminal sliding mode controller design

Sliding mode control is composed of two control actions, the switching control $u_{sw}(t)$ and the equivalent control $u_{eq}(t)$. Consequently, the total control scheme can be expressed as follow:

$$u(t) = u_{eq}(t) + u_{sw}(t) \tag{3.15}$$

With $u_{eq} = \begin{bmatrix} u_{1,eq}^T & u_{2,eq}^T & \dots & u_{(n-1),eq}^T \end{bmatrix}$, $u_{sw} = \begin{bmatrix} u_{1,sw}^T & u_{2,sw}^T & \dots & u_{(n-1),sw}^T \end{bmatrix}$, where $u_{i,eq} = [u_{xi,eq} \; u_{yi,eq}]^T$ and $u_{i,sw} = [u_{xi,sw} \; u_{yi,sw}]^T$

In this chapter, the sliding manifold is defined as follow:

$$S = \dot{e} + \alpha_1 e + \alpha_2 e^{\beta_1/\beta_2} \tag{3.16}$$

Where $\alpha_1 > 0, \alpha_2 > 0$, $\beta_1, \beta_2$ are positive odd integers, with $\beta_1 < \beta_2 < 2\beta_1$, and $S = \begin{bmatrix} S_1^T & S_2^T & \dots & S_{(n-1)}^T \end{bmatrix}$ is the vector of sliding surfaces, in which $S_i = [S_{x_i} \; S_{y_i}]^T$.

**Lemma 3.3.** *The time interval required for any initial state $e \neq 0$ to reach the equilibrium state $e = 0$ along the sliding surface defined in (3.16), can be calculated as:*

$$t_f = \frac{\beta_2}{\alpha_1(\beta_2 - \beta_1)} \ln \frac{\alpha_1 (e_0)^{(1-\frac{\beta_1}{\beta_2})} + \alpha_2}{\alpha_2} \tag{3.17}$$

By using Definition 2.1 and Propriety 2.1, equation (3.16) can be re-written as:

$$S = D^{\alpha} e + \alpha_1 e + \alpha_2 e^{\beta_1/\beta_2} \tag{3.18}$$

The sliding surface $S$ first derivative can be given as:

$$\begin{aligned}\dot{S} &= D^{\alpha+1} e + \alpha_1 \dot{e} + \alpha_2 (\beta_1/\beta_2) \dot{e} e^{(\beta_1/\beta_2)-1} \\ \dot{S} &= ((\bar{\mathcal{L}}+\bar{\mathcal{B}})\otimes I_2)u + ((\bar{\mathcal{L}}+\bar{\mathcal{B}})\otimes I_2)\delta - (\bar{\mathcal{B}}1_{n-1}\otimes I_2)u_n \\ &\quad + \alpha_1 \dot{e} + \alpha_2 (\beta_1/\beta_2) \dot{e} e^{(\beta_1/\beta_2)-1}\end{aligned} \tag{3.19}$$

In the absence of system uncertainties the derivative of $S$ becomes:

$$\begin{aligned}\dot{S} = ((\bar{\mathcal{L}}+\bar{\mathcal{B}})\otimes I_2)u - (\bar{\mathcal{B}}1_{n-1}\otimes I_2)u_n \\ + \alpha_1\dot{e} + \alpha_2(\beta_1/\beta_2)\dot{e}e^{(\beta_1/\beta_2)-1}\end{aligned} \tag{3.20}$$

Hence, the equivalent control law can be derived by solving $\dot{S}=0$:

$$u_{eq} = -((\bar{\mathcal{L}}+\bar{\mathcal{B}})^{-1}\left[-(\bar{\mathcal{B}}1_{n-1}\otimes I_2)u_n + \alpha_1\dot{e} + \alpha_2(\beta_1/\beta_2)\dot{e}e^{(\beta_1/\beta_2)-1}\right] \tag{3.21}$$

And the switching control action is defined as follow:

$$u_{sw} = -(\bar{\mathcal{L}}+\bar{\mathcal{B}})^{-1}\left[\mathcal{K}\,\mathrm{sign}\,(S)\right] \tag{3.22}$$

Where sign(.) is the Signum function and $\mathcal{K}$ is a positive gain.

### 3.3.3 Design of adaptive fractional order fast terminal sliding mode controller

In practical scenarios, the measurement of accurate values of uncertainties and disturbances can be challenging. Therefore, an adaptive mechanism is designed to estimate the upper bounds of this factors.

First, let $\hat{\Delta} = \left[\hat{\Delta}_1^T\ \hat{\Delta}_2^T\ \dots\ \hat{\Delta}_{(n-1)}^T\right]$ be the vector of estimated uncertainties bounds with $\hat{\Delta}_i = [\hat{\Delta}_{x_i}\ \hat{\Delta}_{y_i}]^T$.

Then the error of estimation can be defined as:

$$\tilde{\Delta} = \Delta - \hat{\Delta} \tag{3.23}$$

Where $\tilde{\Delta} = \left[\tilde{\Delta}_1^T\ \tilde{\Delta}_2^T\ \dots\ \tilde{\Delta}_{(n-1)}^T\right]$, $\Delta = \left[\Delta_1^T\ \Delta_2^T\ \dots\ \Delta_{(n-1)}^T\right]$ with $\tilde{\Delta}_i = [\tilde{\Delta}_{x_i}\ \tilde{\Delta}_{y_i}]^T$ and $\Delta_i = [\Delta_{x_i}\ \Delta_{y_i}]^T$ .

Consider the following adaptive rule:

$$\dot{\hat{\Delta}} = 2\gamma((\bar{\mathcal{L}}+\bar{\mathcal{B}})\otimes I_2)|S| \tag{3.24}$$

Where $\gamma = [\gamma_1\ \gamma_2 \dots \gamma_{n-1}]$ and $\gamma_i > 0$

Therefore, the final formation controller can be expressed as follow:

$$u = u_{eq} - \hat{\Delta}\,\mathrm{sign}(S) \tag{3.25}$$

**Theorem 3.1.** *Assuming that the digraph $\mathcal{G}$ associated with the multi-robots system described in (3.11) have a spanning tree. The formation objective can be accomplished and the tracking errors described in (3.12) will asymptotically reach the origin in finite-time, by utilizing the proposed controller (3.25) with the adaptive algorithm (3.24).*

*Proof.* Let $\mathfrak{V}$ be a candidate Lyapunov function:

$$\mathfrak{V} = \frac{1}{2}S^T S + \frac{1}{2\gamma}\tilde{\Delta}^T\tilde{\Delta} \tag{3.26}$$

Then the Lyapunov function $\mathfrak{V}$, first derivative is given as follow:

$$\begin{aligned}\dot{\mathfrak{V}} &= S^T\dot{S} + \frac{1}{\gamma}\tilde{\Delta}^T\dot{\tilde{\Delta}} \\ &= S^T\dot{S} - \frac{1}{\gamma}\tilde{\Delta}^T\dot{\hat{\Delta}}\end{aligned} \tag{3.27}$$

Substituting equation (3.19) into (3.27) lead to:

$$\begin{aligned}\dot{\mathfrak{V}} = S^T\Big[&((\bar{\mathcal{L}}+\bar{\mathcal{B}})\otimes I_2)u + ((\bar{\mathcal{L}}+\bar{\mathcal{B}})\otimes I_2)\delta - (\bar{\mathcal{B}}1_{n-1}\otimes I_2)u_n \\ &+\alpha_1\dot{e} + \alpha_2(\beta_1/\beta_2)\dot{e}e^{(\beta_1/\beta_2)-1}\Big] - \frac{1}{2\gamma}\tilde{\Delta}^T\dot{\hat{\Delta}}\end{aligned} \tag{3.28}$$

Substituting the control law (3.25) into equality (3.28) yield the following:

$$\dot{\mathfrak{V}} = S^T\Big[((\bar{\mathcal{L}}+\bar{\mathcal{B}})\otimes I_2)\delta - ((\bar{\mathcal{L}}+\bar{\mathcal{B}})\otimes I_2)\hat{\Delta}\,\mathrm{sign}(S)\Big] - \frac{1}{2\gamma}\tilde{\Delta}^T\dot{\hat{\Delta}} \tag{3.29}$$

Using Assumption 3.1 and the adaptive rule in equation (3.24), gives the following:

$$\begin{aligned}\dot{\mathfrak{V}} &= S^T\Big[((\bar{\mathcal{L}}+\bar{\mathcal{B}})\otimes I_2)(\delta - \hat{\Delta}\,\mathrm{sign}(S))\Big] - \tilde{\Delta}^T((\bar{\mathcal{L}}+\bar{\mathcal{B}})\otimes I_2)|S| \\ &\leq ((\bar{\mathcal{L}}+\bar{\mathcal{B}})\otimes I_2)(|S|\otimes I_2)(\Delta - \hat{\Delta} - \tilde{\Delta}) = 0\end{aligned} \tag{3.30}$$

Based on equation (3.30), it can concluded be that the tracking errors of the formation will asymptotically reach 0 in finite-time, and Theorem 3.1 proof is completed. □

According to Theorem 3.1 the formation of multi-robots system (3.11) can be established by using the control scheme (3.25). Therefore equation (3.12) can be described as follow:

$$((\bar{\mathcal{L}}+\bar{\mathcal{B}})\otimes I_2)(z-f)=(\bar{\mathcal{B}}1_{n-1}\otimes I_2)z_n \tag{3.31}$$

Using Lemma 3.2 and assuming that $\mathcal{G}$ has a directed spanning tree then, the following can be obtained:

$$\begin{aligned}((\bar{\mathcal{L}}+\bar{\mathcal{B}})\otimes I_2)(z-f)&=(\bar{\mathcal{B}}1_{n-1}\otimes I_2)z_n\\((\bar{\mathcal{L}}+\bar{\mathcal{B}})\otimes I_2)(z-f)&=((\bar{\mathcal{L}}+\bar{\mathcal{B}})\otimes I_2)(1_{n-1}\otimes I_2)z_n\\(z-f)&=(1_{n-1}\otimes I_2)z_n\end{aligned} \tag{3.32}$$

From equation (3.32), one can conclude that positions consensus can be established when the tracking errors of the formation converges to zero.

## 3.4 Simulation Results

Numerical simulation based on MATLAB environment are presented in this section, a multi-robot system consist of six nonholonomic wheeled mobile robots is considered in this simulation example. The parameters of each robot are selected as in [103]: $d=0.04m$, $R=.0265m$, $r=0.02m$, $m=.032Kg$ and $I=1.7^{-4}Kg.m^2$.

A communication graph $\mathcal{G}$ with a directed topology is used for modeling the connection between robots, the representation of $\mathcal{G}$ is depicted in Figure 3.1, where the node labeled with number 6 represent the leader robot and the reset of vertices (1-5) are the followers. The matrices $\mathcal{L},\mathcal{A}$ and $\mathcal{B}$ associated with $\mathcal{G}$ are given as follow:

$$\mathcal{L}=\begin{bmatrix}1&0&0&0&0&-1\\-1&1&0&0&0&0\\-1&0&1&0&0&0\\0&-1&0&2&-1&0\\0&0&-1&0&1&0\\0&0&0&0&0&0\end{bmatrix}$$

$$\mathcal{A} = \begin{bmatrix} 0 & 0 & 0 & 0 & 0 & 1 \\ 1 & 0 & 0 & 0 & 0 & 0 \\ 1 & 0 & 0 & 0 & 0 & 0 \\ 0 & 1 & 0 & 0 & 1 & 0 \\ 0 & 0 & 1 & 0 & 0 & 0 \\ 0 & 0 & 0 & 0 & 0 & 0 \end{bmatrix}, \quad \mathcal{B} = \begin{bmatrix} 1 & 0 & 0 & 0 & 0 & 0 \\ 0 & 0 & 0 & 0 & 0 & 0 \\ 0 & 0 & 0 & 0 & 0 & 0 \\ 0 & 0 & 0 & 0 & 0 & 0 \\ 0 & 0 & 0 & 0 & 0 & 0 \\ 0 & 0 & 0 & 0 & 0 & 0 \end{bmatrix}$$

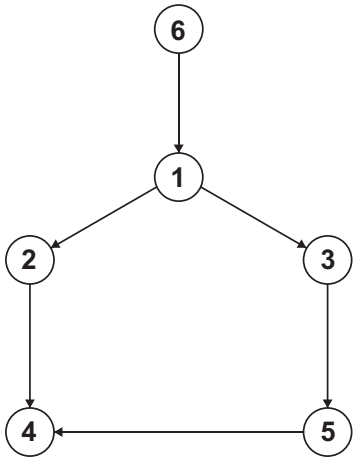


Figure. 3.1: Formation communication graph.

A comparative study is carried out to examine the efficacy of suggested ADFOFTSMC method, where it compared to the second order consensus algorithm SOCA proposed in [104], and the distributed sliding mode control DSMC in [103].

The suggested controller design parameters are chosen as follow: $\alpha_1 = \frac{1}{2}$, $\alpha_2 = 1$, $\beta_1 = 7$, $\beta_2 = 9$, $\alpha = 0.78$ and $\gamma = 10$. the uncertainties terms $\Delta_i$ in equation (3.2) are supposed be uniformly randomly distributed between $-.025$ and $.025$.

In order to establish a Hexagon-like formation the robots desired postures are defined as: $f_{x_i} = [-0.125\ -0.375\ -0.5\ -0.375\ -0.125]$ and $f_{y_i} = [0.2165\ 0.2165\ 0\ -0.2165\ -0.2165]$, Figure 3.2 shows the desired formation shape. The leader robot is assumed to move in sinusoidal motion with $v_{x_i} = .25m/s$, $v_{y_i} = .05 * \cos(.25\pi t)m/s$ and the robots initial positions are selected as follow: $x_i = [0.10\ -0.25\ -0.50\ -0.4\ -0.1\ 0.25]$ and $y_i = [0.4\ 0.5\ 0.45\ -0.3\ -0.5\ 0]$.

Table 3.1: Formation tracking performances .

| $E(t)$ | SOCA [104] | DSMC [103] | ADFOFTSMC |
|---|---|---|---|
| RMSE | $384.50 \times 10^{-3}$ | $372.40 \times 10^{-3}$ | $280.30 \times 10^{-3}$ |
| ISE | $2.2175 \times 10^{3}$ | $2.0801 \times 10^{3}$ | $1.1783 \times 10^{3}$ |
| ITSE | $1.6769 \times 10^{3}$ | $1.6120 \times 10^{3}$ | $0.3996 \times 10^{3}$ |
| ITAE | $6.3164 \times 10^{3}$ | $5.8919 \times 10^{3}$ | $1.2690 \times 10^{3}$ |
| IAE | $2.7677 \times 10^{3}$ | $2.6831 \times 10^{3}$ | $1.2682 \times 10^{3}$ |

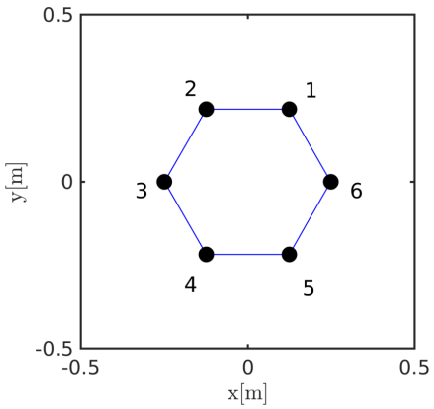


Figure. 3.2: Desired formation pattern.

Furthermore, the formation tracking performances are analyzed using the following error indexes $RMSE = \sqrt{\frac{1}{T}\int_0^T E(t)^2 dt}$, $ISE = \int_0^T E(t)^2 dt$, $ITSE = \int_0^T tE(t)^2 dt$, $ITAE = \int_0^T t|E(t)|dt$, $IAE = \int_0^T |E(t)|dt$, where $T$ is the simulation time and $E(t)$ is defined in (3.33), Table 3.1 shows the tracking performance results.

$$E(t) = \sum_{i=1}^{5} |e_{x_i}(t)| + \sum_{i=1}^{5} |e_{y_i}(t)| \tag{3.33}$$

The simulation results for the second order consensus algorithm are illustrated in Figure 3.3, Figure 3.4 and Figure 3.5, where Figure 3.3 presents the formation desired pattern at several moments, Figure 3.4 depicts the formation tracking errors $(e_{x_i}, e_{y_i})$ and the robots control inputs $(\tau_{l_i}, \tau_{r_i})$ are presented in Figure 3.5. While the obtained results of the DSMC are presented in Figure 3.6, Figure 3.7 and Figure 3.8, respectively. Finally, the proposed ADFOFTSMC results are depicted in Figure 3.9, Figure 3.10 and Figure 3.11.

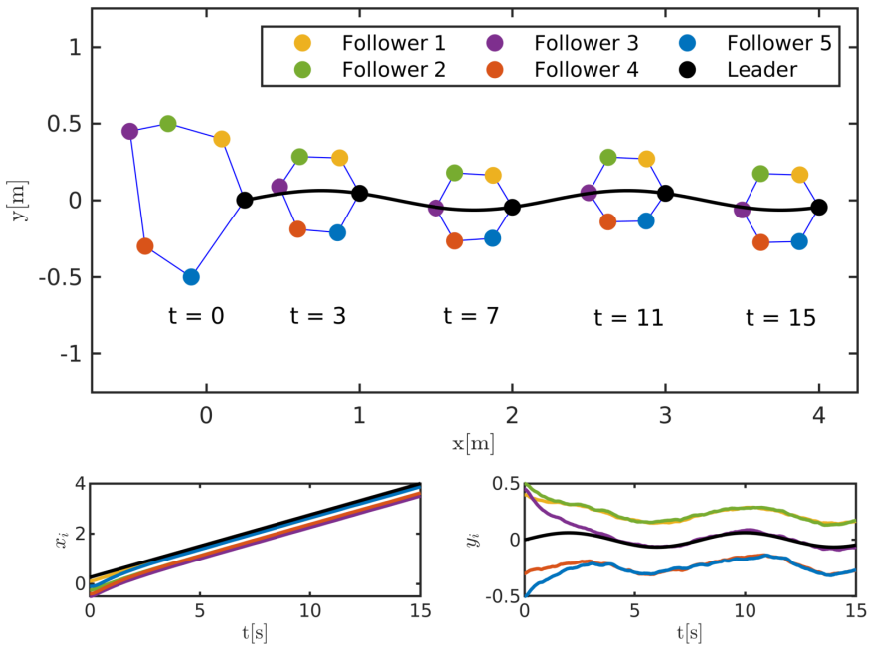


Figure. 3.3: Desired formation pattern at several moment with the leader trajectory (black line), based on SOCA [104].

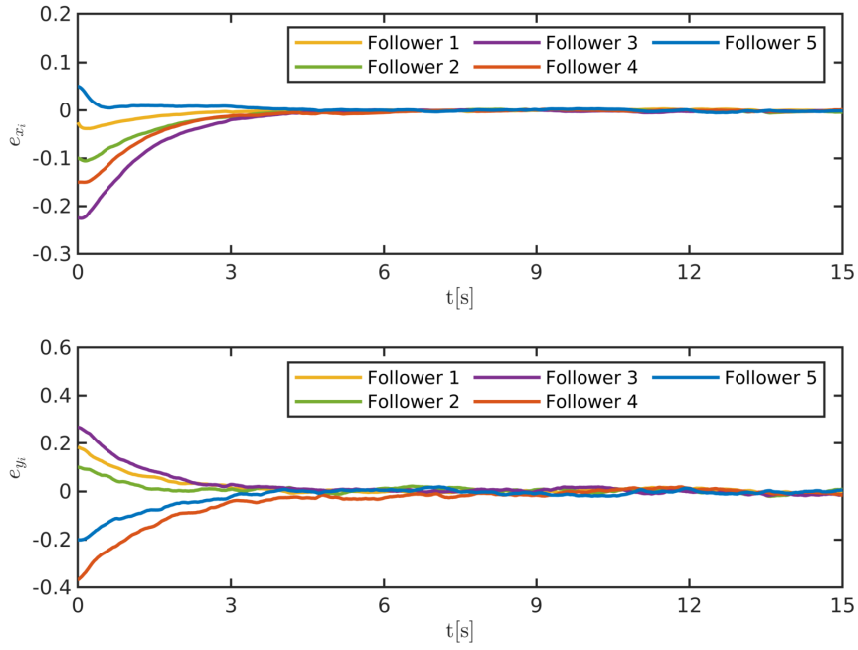


Figure. 3.4: Followers tracking errors, based on SOCA [104].

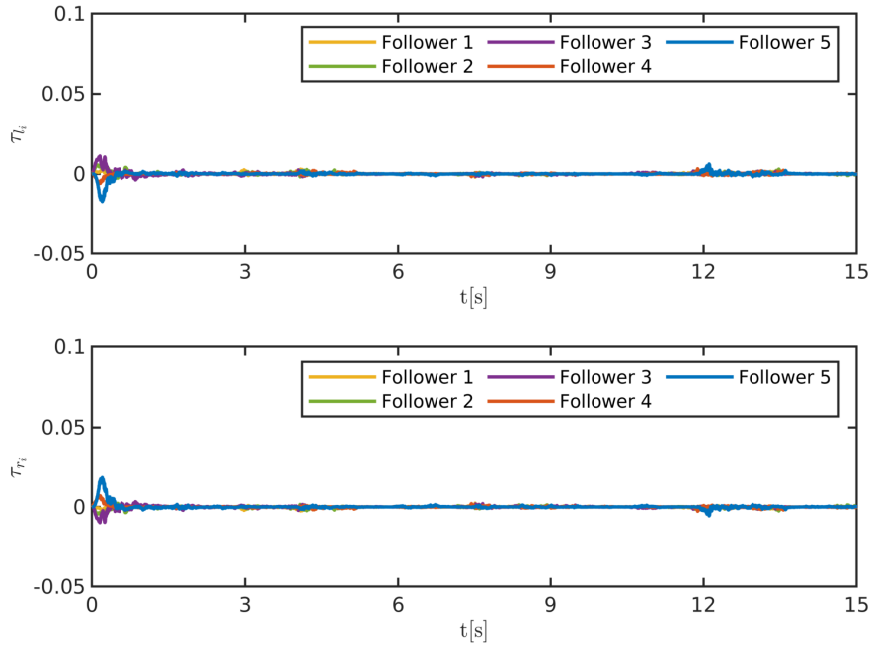


Figure. 3.5: Followers control inputs, based on SOCA [104].

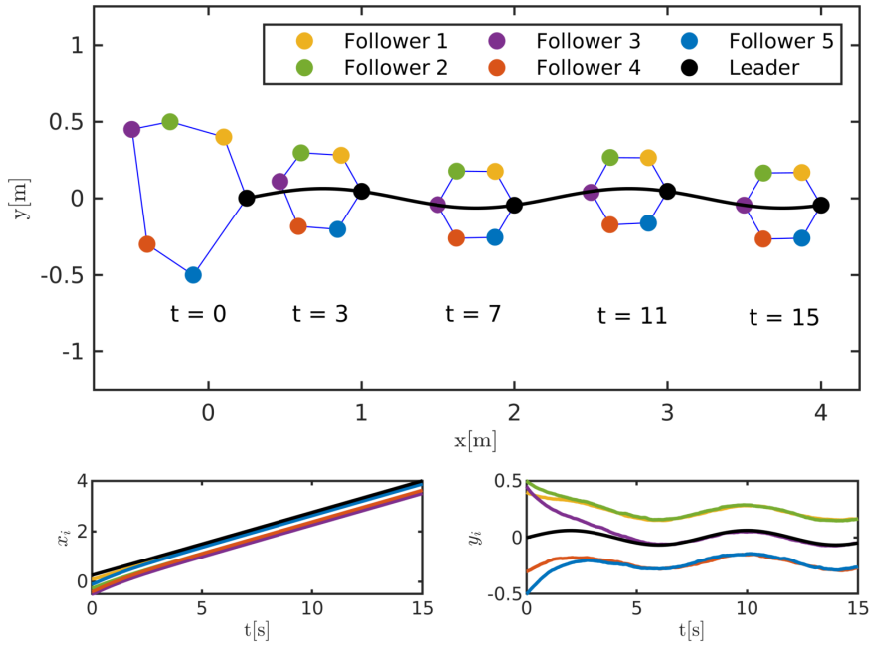


Figure. 3.6: Desired formation pattern at several moment with the leader trajectory (black line), based on DSMC [103].

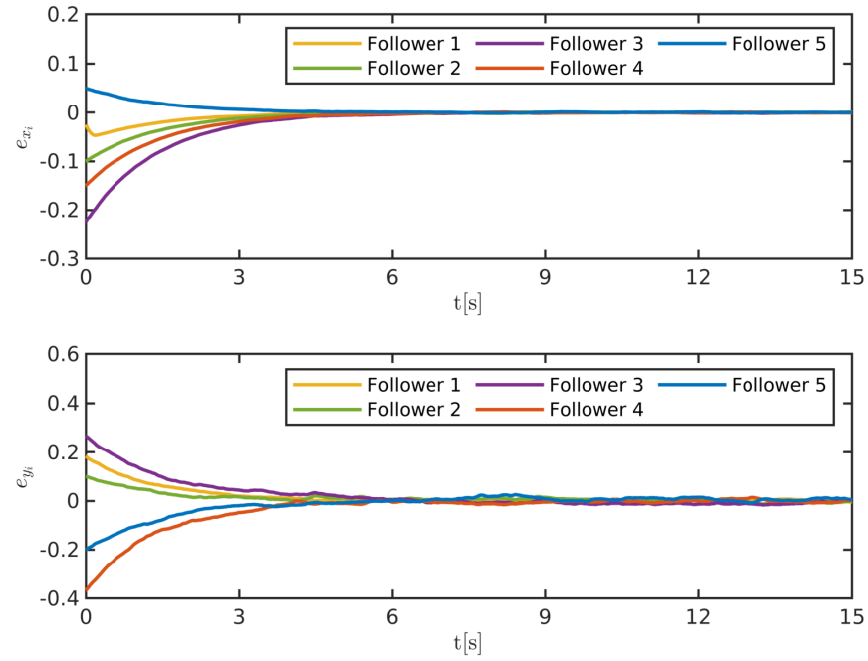


Figure. 3.7: Followers tracking errors, based on DSMC [103].

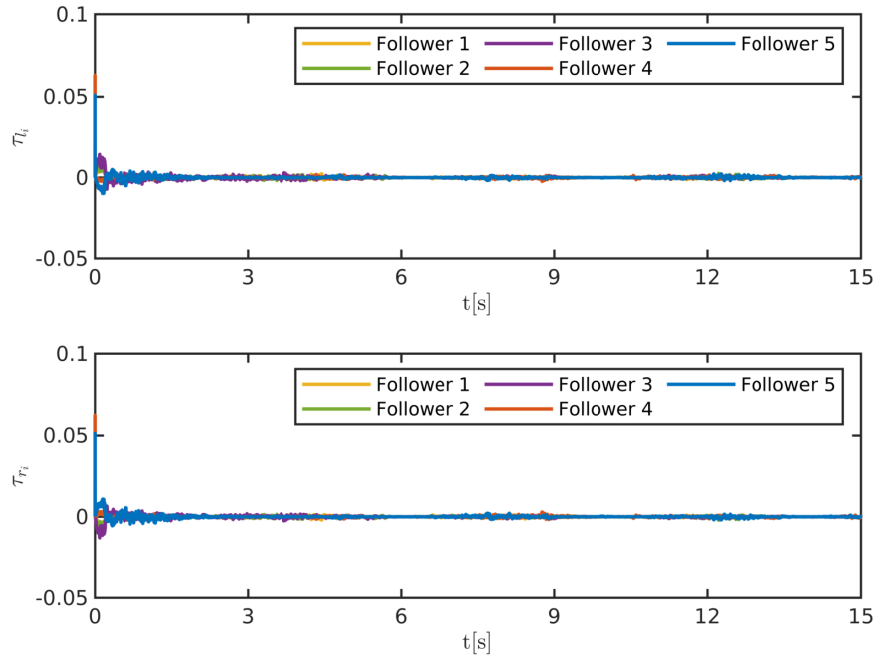


Figure. 3.8: Followers control inputs, based on DSMC [103].

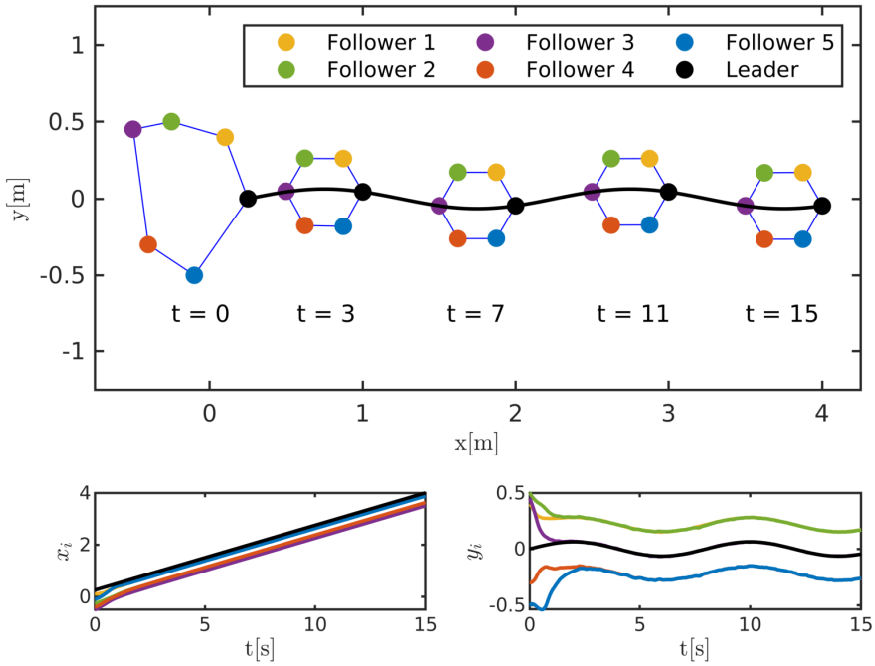


Figure. 3.9: Desired formation pattern at several moment with the leader trajectory (black line), based on ADFOFTMSC.

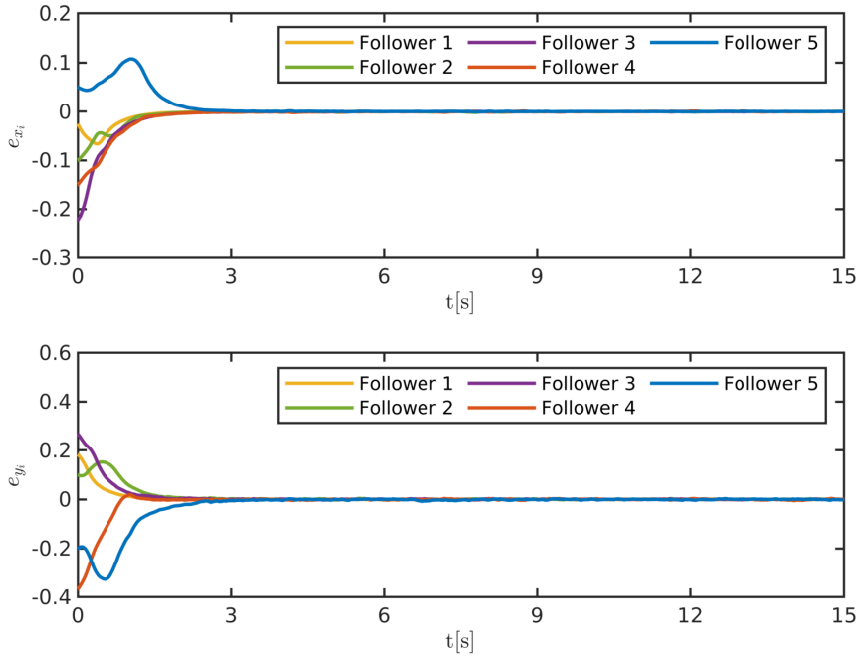


Figure. 3.10: Followers tracking errors, based on ADFOFTMSC.

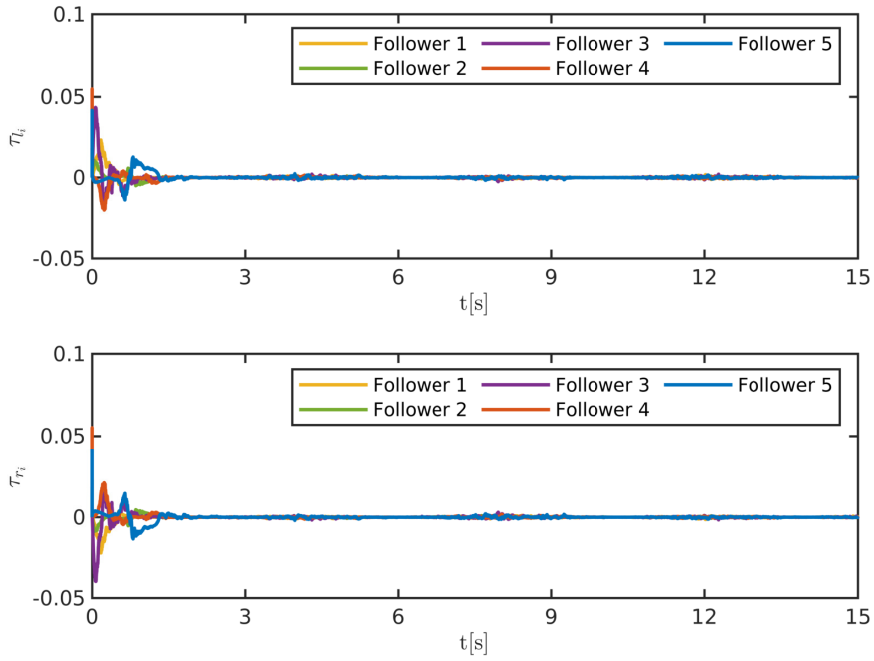


Figure. 3.11: Followers control inputs, based on ADFOFTMSC.

The simulation results presented in Figure 3.3, Figure 3.6 and Figure 3.9 demonstrate the successful achievement of the formation using all control strategies. Nevertheless, it is evident that the utilization of the proposed ADFOFTMSC leads to a faster convergence rate of the robots towards the desired formation pattern. Meanwhile, the evaluation of the tracking errors of the robots, depicted in Figure 3.4, Figure 3.7 and Figure 3.10, clearly demonstrates that the SOCA and DSMC methods exhibit inferior performance in terms of disturbances and uncertainties rejection when compared to the proposed control method. Additionally, the ADFOFTMSC control technique has the minimal error tracking values when compared to SOCA and DSMC methods, as shown by the comparison between the tracking error indices shown in Table 3.1.

The aforementioned comparison results, illustrate that the ADFOFTMSC method surpasses the other used control techniques in terms of control performances. The proposed controller can ensure superior robustness against system uncertainties and disturbances and achieves higher tracking accuracy with a faster convergence rate, which lead to an accurate and efficient formation control of robots.

## 3.5 Conclusion

An adaptive distributed formation controller for wheeled nonholonomic mobile robots is developed in this chapter. The dynamic model of the robots is formulated using the Euler-Lagrange equation, with considering the existence of bounded uncertainties and disturbances in practical scenarios. Through the integration of fractional calculus with fast terminal sliding mode control and consensus algorithm, a robust distributed formation controller has been designed to drive the followers robots to establish the predefined formation geometric shape while tracking their leader. Furthermore, an adaptive mechanism is devised to effectively mitigate the impact of uncertainties and disturbances. The suggested control scheme stability has been analyzed utilizing the Lyapunov theorem. The efficiency of the suggested control technique has been investigated through conducting a comparative study. The outcomes highlight the superior performance of the suggested controller in terms of formation accuracy, robustness and convergence.

# CHAPTER 4

# Discrete predictive sliding mode control of leader-follower formation of nonholonomic mobile robots

## 4.1 Introduction

In this chapter we investigate the leader-follower based formation control of wheeled nonholonomic mobile robots. First, the formation control problem is converted into a trajectory tracking problem. Then by using a linear formation tracking error dynamics a discrete sliding mode DSM controller is designed for the follower robots to follow their leader and to establish the required spacial geometric configuration. Moreover, a discrete model predictive control DMPC is also integrated with the DSM control to minimize the control effort and to surpass the chattering phenomena. Finally, we present simulation results that assess the performance of the suggested control schemes.

In the literature, Researchers have employed various control techniques to establish formation control of wheeled nonholonomic mobile robots using the leader-following strategy. These include graph theory approaches [105], consensus algorithms [106, 107], SMC sliding mode control [108], MPC model predictive control [109, 110], PID control [111] and RL reinforcement learning [112].

Among this control schemes, sliding mode control (SMC) approaches have been widely adopted in formation control of mobile robots. primarily due to its appealing attributes, such as finite-time convergence and resilience against perturbations and

uncertainties. However, the chattering phenomenon resulting from the reaching law, and its corresponding high control effort, stands as its primary limitation, which have inspired substantial research to address these issue. For example, authors in [113] addressed the formation control of nonholonomic mobile robots. a globally finite-time stable sliding mode controller has been designed. Then, a continuous reaching law has been derived to mitigate the chattering caused by control limitations and computation time delays. In [114] a second order sliding mode controller has been developed , based on the relative motion states and without the leader velocity measurement, to stabilize the robots towards the required time-varying formation and to avoid the the chattering phenomena. The authors in [115] design a sliding mode formation controller for differential drive robots. They used a novel approach inspired by immune regulation mechanisms, coupled with fuzzy boundary layer method. To reduce the chattering and to compensate uncertainty without requiring prior knowledge of its boundaries. In [116] a tracking control method for multiple robots has been presented. A sliding mode controller has been introduced to asymptotically stabilize the robots into the required formation. To address the velocity jump issue, authors incorporates a novel sliding mode approach based on the neural dynamic model.

On the other hand, employing model predictive control MPC for the formation control of nonholonomic mobile robots can effectively account for physical limits of the robots, making it capable for yielding an optimal formation tracking and maintenance. The authors in [117] used a virtual robot as a leader, then an MPC method is applied to the followers to accomplish the leader-follower formation objective based on two models. Novel terminal state regions and controllers are developed to assure the stability of the controller. In [118] a multi-robot systems was controlled using a cooperative CCEA coevolutionary algorithm based MPC approach. To predict the future states, they utilized the past state values of the robots, rather than their current values. And the asymptotic stability has been guaranteed, by tuning the sampling period and choosing suitable constraints of the states and inputs. The authors in [119] suggested an MPC controller for a leader follower formation based on the separation-bearing-orientation scheme. the particle swarm algorithm is employed for solving the optimization problem, where the global solution is considered as the control input.

The key contribution of this chapter lies in the development of a controller that combines discrete model predictive control MPC and discrete sliding mode control to achieve a robust and accurate formation control of nonholonomic wheeled mobile robots.

The integration of MPC allows for optimal formation producing and tracking with constrained states and inputs, while the sliding mode control ensures robustness against kinematic perturbations subjected to the robots model in practice. By leveraging the strengths of both control techniques, the proposed method aims to improve the overall formation control performances. To evaluate the effectiveness of suggested control method, simulation examples are conducted. Where a comparison is made between the performance of the proposed method and conventional discrete sliding mode control technique. The results clearly demonstrate the superior performance of the proposed method.

## 4.2 Problem Formulation

### 4.2.1 Nonholonomic mobile robot kinematic model

Consider the differential-drive wheeled mobile robot shown in Figure 1.14. Let $q = [x\ y\ \theta]^T$ be the robot center of mass posture, where $(x, y)$ denotes the position of the robot in the global Cartesian frame $(OXY)$ and $\theta$ is the orientation angle.

This robot satisfy the following pure rolling and non-slipping nonholonomic constraints given by:

$$\dot{y}\cos\theta - \dot{x}\sin\theta = 0 \tag{4.1}$$

By using the nonholonomic constraints in (4.1), the kinematic model of the robot can be described as follow:

$$\dot{q} = \begin{bmatrix} \cos\theta & 0 \\ \sin\theta & 0 \\ 0 & 1 \end{bmatrix} \begin{bmatrix} \nu \\ \omega \end{bmatrix} = J(q)u \tag{4.2}$$

Where $\omega$ is the robot angular velocity and $\nu$ is the robot linear velocity.

In practice, the robot model is subjected to kinematic uncertainty and input disturbances. Hence, a more realistic model of the robot can be expressed as follow [120]:

$$\dot{q} = J(q)(u + \Delta) \tag{4.3}$$

Where $\Delta = [\delta_\nu \ \delta_\omega]^T$ denotes the unknown input disturbances, and its assumed to be upper bounded by [120]:

$$|\Delta| \leq \gamma$$

where $\gamma$ is a positive constant.

### 4.2.2 Leader follower formation model

Figure 4.1 show the basic architecture of the leader-follower formation approach. Where the posture of the leader robot $R_l$ is $q_l = [x_l \ y_l \ \theta_l]^T$ and the posture of the follower robot $R_f$ is given by $q_f = \left[x_f \ y_f \ \theta_f\right]^T$ and the desired posture for the follower robot is given by $q_d = [x_d \ y_d \ \theta_d]^T$.

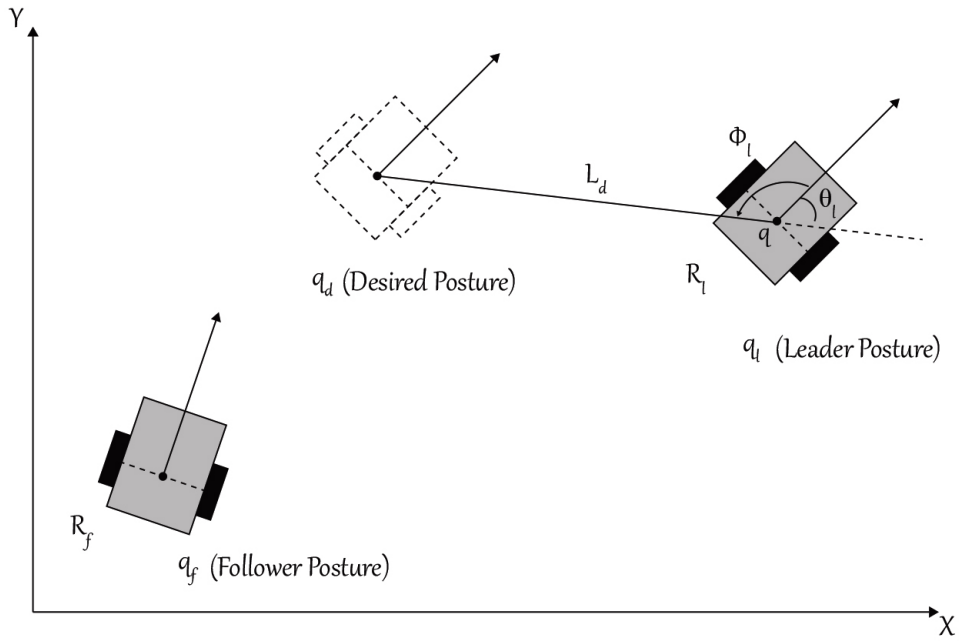


Figure. 4.1: Leader-Follower Formation Structure.

The leader-follower approach can be seen as a trajectory tracking problem where the follower robot must track the trajectories generated by the leader robot in-order to preserve the required separation distance $L_d$ and heading angle $\Phi_d$, and to form the

predefined formation shape. Hence the desired posture $q_d$ can be given as [121]:

$$q_d = \begin{bmatrix} x_d \\ y_d \\ \theta_d \end{bmatrix} = \begin{bmatrix} x_l + L_d \cos(\Phi_d + \theta_l) \\ y_l + L_d \sin(\Phi_d + \theta_l) \\ \text{atan2}(\dot{y}_d, \dot{x}_d + \kappa\pi) \end{bmatrix} \tag{4.4}$$

Where $k = 0, 1$ is the driving direction ( 0 for the forward motion and 1 for reverse) and $atan2$ is the four-quadrant inverse tangent function. To accomplish the formation objective, the follower robot need to follow the reference trajectory consist of the set of the desired postures $q_d$, which implies that the following must satisfy:

$$\lim_{t \to \infty} \left( q_d - q_f \right) = 0 \tag{4.5}$$

### 4.2.3 Leader follower formation error dynamics

Since the leader-follower formation is converted to a trajectory tracking problem, the tracking error model of the formation can be written as:

$$e = \begin{bmatrix} x_e \\ y_e \\ \theta_e \end{bmatrix} = \begin{bmatrix} \cos\theta & \sin\theta & 0 \\ -\sin\theta & \cos\theta & 0 \\ 0 & 0 & 1 \end{bmatrix} \begin{bmatrix} x_d - x_f \\ y_d - y_f \\ \theta_d - \theta_f \end{bmatrix} \tag{4.6}$$

The tracking error dynamics of the formation can be obtained by taking the time derivative of (4.6) and by using equations (4.3) and (4.1) as follow [122]:

$$\dot{e} = \begin{bmatrix} \dot{x}_e \\ \dot{y}_e \\ \dot{\theta}_e \end{bmatrix} = \begin{bmatrix} \cos\theta_f & 0 \\ \sin\theta_f & 0 \\ 0 & 1 \end{bmatrix} \begin{bmatrix} v_d \\ \omega_d \end{bmatrix} + \begin{bmatrix} -1 & y_e \\ 0 & -x_e \\ 0 & -1 \end{bmatrix} \begin{bmatrix} u + \Delta \end{bmatrix} \tag{4.7}$$

Where $v_d$ and $\omega_d$ are the linear and angular feedforward control input defined as:

$$\begin{cases} v_d = \pm\sqrt{\dot{x}_d^2 + \dot{y}_d^2} \\ \omega_d = \frac{\dot{x}_d \ddot{y}_d - \dot{y}_d \ddot{x}_d}{\dot{x}_d^2 + \dot{y}_d^2} \end{cases} \tag{4.8}$$

Where $(+)$ for the forward motion and $(-)$ for backward motion . By neglecting the input disturbance $\Delta = \begin{bmatrix} \delta_{\nu_f} & \delta_{\omega_f} \end{bmatrix}^T$, then defining the control input vector of the follower robot $u$ as the sum of the feedforward and feedback control action:

$$u = u_d + u_c \tag{4.9}$$

Where $u_d = \begin{bmatrix} v_d \cos\theta_e & \omega_d \end{bmatrix}^T$ is the feedforward control vector and $u_c = \begin{bmatrix} u_{c1} & u_{c2} \end{bmatrix}^T$ is the feedback vector input.
Assuming $\Delta = 0$ and substituting (4.9) into equation (4.7), gives the following tracking error dynamics :

$$\begin{aligned} \dot{x}_e &= \omega_d y_e - u_{c1} + u_{c2} y_e \\ \dot{y}_e &= v_d \sin\theta_e - \omega_d x_e - u_{c2} x_e \\ \dot{\theta}_e &= -u_{c2} \end{aligned} \tag{4.10}$$

Using (4.9) and linearizing (4.10) around ($x_e = y_e = \theta_e = 0$ and $u_{c1} = u_{c2} = 0$ ) results the following linear model [123] :

$$\dot{e} = \begin{bmatrix} 0 & \omega_d & 0 \\ -\omega_d & 0 & v_d \\ 0 & 0 & 0 \end{bmatrix} e + \begin{bmatrix} -1 & 0 \\ 0 & 0 \\ 0 & -1 \end{bmatrix} u_c \tag{4.11}$$

Which can be written in a state-space form as:

$$\dot{e}(t) = A_c(t)e(t) + B_c u_c(t) \tag{4.12}$$

## 4.3 Discrete predictive sliding mode control

### 4.3.1 Discrete sliding mode control design

The linearized model of the tracking error dynamics (4.12) can be written in discrete form as :

$$e(k+1) = A(k)e(k) + Bu_c(k) \tag{4.13}$$

Where:

$$A = I + A_c(t)T_s, B = B_c T_s$$

And $A \in \mathbb{R}^{n\times n}$, $n$: number of states variable, $B \in \mathbb{R}^{n\times m}$ m : number of input variable and $T_s$ : is the sampling time.

Consider the discrete-time system (4.13), then the following sliding mode function is defined:

$$S(k) = Ce(k) \tag{4.14}$$

Where $C \in \mathbb{R}^{m\times n}$ Is the gain matrix. For a discrete-time system (4.13), a quasi-sliding mode reaching law is given as in [124]:

$$S(k+1) - S(k) = -q_s T_s S(k) - \varepsilon T_s \operatorname{sign}(S(k)) \tag{4.15}$$

With : $\varepsilon > 0$, $\mathrm{q_s} > 0$ and $1 - \mathrm{q_s} T_s > 0$. The control law for the discrete-time system (4.13) can be derived by comparing (4.15) with (4.16) :

$$\begin{aligned} S(k+1) - S(k) &= Ce(k+1) + Ce(k) \\ &= CA(k)e(k) + CBu_c(k) - Ce(k) \end{aligned} \tag{4.16}$$

Then, solving for $u_c(k)$ gives the following control input:

$$\begin{aligned} u_c(k) = -(CB)^{-1}[&CA(k)e(k) - Ce(k) \\ &+ q_s T_s S(k) + \varepsilon T_s \operatorname{sign}(S(k))] \end{aligned} \tag{4.17}$$

### 4.3.2 Discrete predictive sliding mode control design

The main idea of predictive sliding mode control is to find a control law $u_c(k)$ that drive the predictive sliding function vector $S_p(k+1)$ to a reference sliding function vector $S_r(k+1)$, by minimizing a quadratic cost function $J_{DMPC}(u_c(k), N_p, N_c)$.

Consider the discrete sliding mode problem for the system (4.13), taking the reaching law (4.15) as a reference sliding surface results the following :

$$\begin{cases} S_r(k+\mathrm{p}) = (1 - \mathrm{q_s} T_s) S_r(k+p-1) \\ \qquad\qquad - \varepsilon T_s \operatorname{sign}(S_r(k+p-1)) \\ S_r(k) = S(k) \end{cases} \tag{4.18}$$

The value of the sliding function vector (4.14) at time instant $p$ can be obtained as:

$$\begin{aligned} S(k+p) = C \prod_{j=1}^{p-1} A(k+j)e(k) + \sum_{i=1}^{p} \left( C \prod_{j=1}^{p-1} A(k+j) \right) \\ \times BU_c(k+i-1) + CBU_c(k+p-1) \end{aligned} \tag{4.19}$$

By defining the predictive sliding function $S_p$ as follow:

$$S_p(k+1) = [S(k+1), S(k+2), \ldots, S(k+N_p)]^T \tag{4.20}$$

Where $N_p$ is the prediction horizon, then $S_p(k+1)$ can be described as:

$$S_p(k+1) = F(k)e(k) + H(k)U_c(k) \tag{4.21}$$

Where:

$$F(k) = [CA(k), CA(k+1)A(k), \ldots, C\tilde{A}(k,0)]^T$$

$$H(k) = \begin{bmatrix} CB & 0 & \cdots & 0 \\ CA(k+1)B & CB & \cdots & \vdots \\ \vdots & \vdots & \ddots & \vdots \\ C\tilde{A}(k,1) & C\tilde{A}(k,2)B(k+1) & \cdots & CB \end{bmatrix}$$

And:

$$C\tilde{A}(k,\mathrm{i}) = C\prod_{j=\mathrm{i}}^{p-1} A(k+j)$$
$$U_c(k) = [u_c(k), u_c(k+1), \ldots, u_c(k+p)]^T$$

Then, we introduce the following cost function:

$$\begin{aligned} J_{DPSM} = &\sum_{j=1}^{N_p} q_j \left(S_p(k+1) - S_r(k+j)\right)^2 \\ &+ \sum_{i=1}^{N_c} r_i \left(U_c(k) - U_{eq}(k)\right)^2 \end{aligned} \tag{4.22}$$

Where $U_{eq}(k)$ is the discrete sliding mode equivalent control given by:

$$U_{eq}(k) = (CB)^{-1}[CA(k)e(k)] \tag{4.23}$$

The cost function in (4.22) can be described in quadratic form as:

$$\begin{aligned} J_{DPSM}\left(U_c(k), N_p, N_c\right) = &\left\|\left(S_p(k+1) - S_r(k+1)\right)\right\|_Q^2 \\ &+ \left\|\left(U_c(k) - U_{eq}(k)\right)\right\|_R^2 \end{aligned} \tag{4.24}$$

Hence, the optimal control law input $U_c(k)$ can be obtained by $\frac{dJ_{DPSM}}{dU_c} = 0$ as:

$$U_c(k) = -\left(H^T Q H + R\right)^{-1}\left[H^T(Fe(k)\ - S_r(k+1)) - RU_{eq}\right] \tag{4.25}$$

Where $Q$ and $R$ are weighting matrices given as:

$$Q = \begin{bmatrix} q_1 & 0 & \dots & 0 \\ 0 & q_2 & \dots & 0 \\ \vdots & \vdots & \ddots & \vdots \\ 0 & 0 & \dots & q_{N_p} \end{bmatrix}$$

$$R = \begin{bmatrix} r_1 & 0 & \dots & 0 \\ 0 & r_2 & \dots & 0 \\ \vdots & \vdots & \ddots & \vdots \\ 0 & 0 & \dots & r_{N_c} \end{bmatrix}$$

## 4.4 Simulation results

In this section, Two simulation examples are presented, a leader-follower formation control of two nonolonomic wheeled mobile robots is considered, where the first robot is assigned as a leader and the second robot is acting as follower.

The control parameters for the DSM and PDSM methods were determined by trial and error as follow : $q_s = \text{diag}[3,0,0,6], \varepsilon = 0.001 \times I_{2\times 2}, N_p = 4, N_c = 3, R = 10^{-3} \times I_{2\times 2}, Q = \text{diag}[5,0,0,5]$ and the gain matrix $C$ is chosen as follow:

$$C = \begin{bmatrix} 1.0 & 1.4 & 0 \\ 0 & 2.4 & 1.0 \end{bmatrix}$$

$$\begin{cases} x_r = 1.5\sin(2\pi t/50) \\ y_r = 0.5\sin(4\pi t/50) \end{cases} \tag{4.26}$$

For the PDSM control, the limits of the velocities commands of the follower robot are given as follow:

$$\begin{cases} \nu_{f,max} = -\nu_{f,min} = 0.4m/s \\ \omega_{f,max} = -\omega_{f,min} = 1.8Rad/s \end{cases} \tag{4.27}$$

While the kinematic input disturbances defined in (4.3) is selected as follow:

$$\Delta = \begin{bmatrix} \delta_\nu \\ \delta_\omega \end{bmatrix} = \begin{bmatrix} .01sin(t) \\ .01cos(t) \end{bmatrix} \tag{4.28}$$

### 4.4.1 Formation control using the DSM control

In this simulation example, the discrete predictive sliding mode controller (4.25) is used to control the formation, the leader robot is assumed to be moving in a 8-shape trajectory produced by (4.26). The required separation distance is chosen as $L_d = 0.15$ m and the bearing angle is selected as $\phi_d = 3\pi/2$, while the initial robots posture are given as: $q_l = [0\ 0\ \pi/4]^T$ and $q_f = [0.25\ 1.5\ -\pi/4]^T$.

The real-time trajectories for both robots are shown in Figure 4.2 . The follower robot tracking errors and its velocities commands are shown in Figure 4.3 and Figure 4.4, respectively.

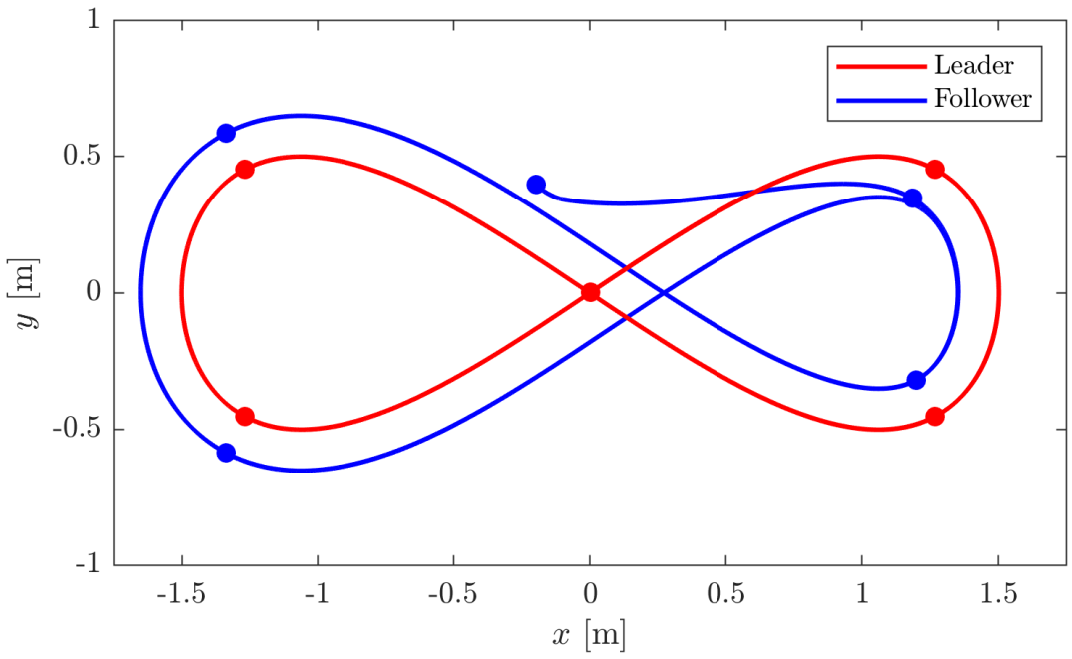


Figure. 4.2: Two robot leader follower formation, based on the discrete predictive sliding mode DPSM control.

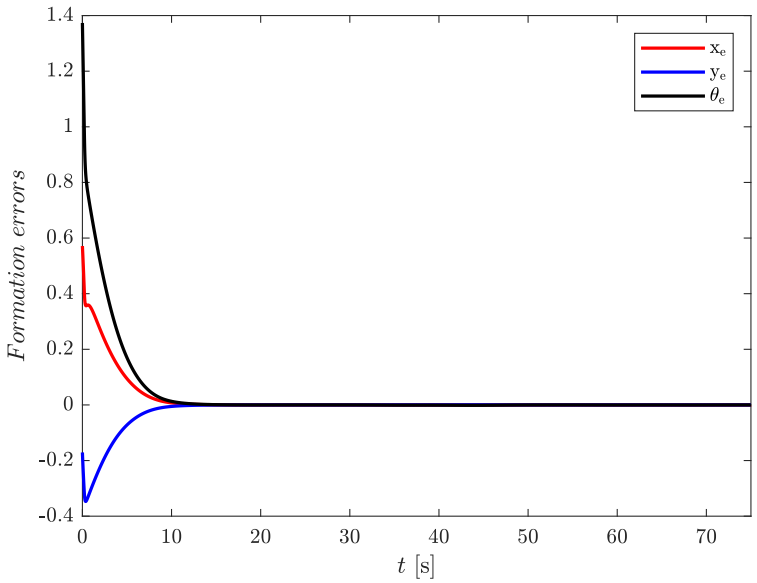


Figure. 4.3: Formation tracking error for the follower using the discrete predictive sliding mode DPSM control controller.

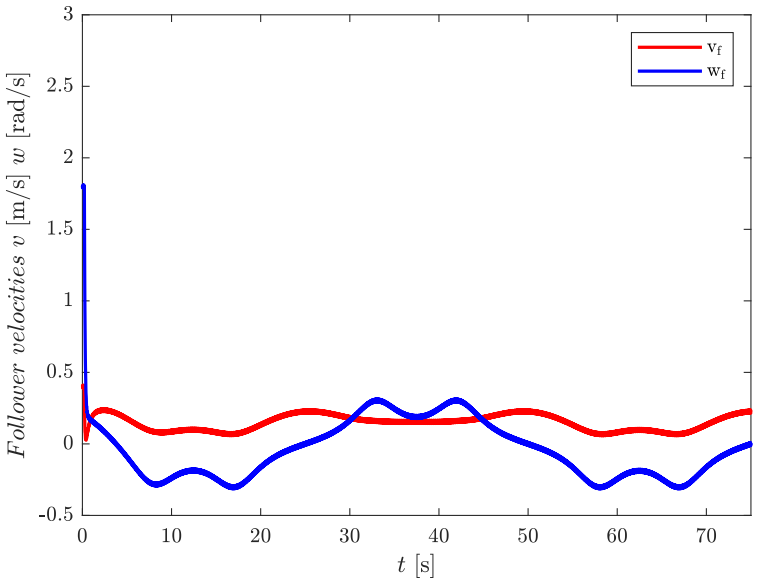


Figure. 4.4: Control inputs of the follower robot controlled by the discrete predictive sliding mode DPSM method.

### 4.4.2 Comparison between DSM and DPSM control methods

This section presents a comparison between the discrete sliding mode DSM control in (4.17) and the discrete predictive sliding mode DPSM control in (4.25). In this example, the leader robot is following a circular trajectory given by equation (4.29) with a constant angular velocity $\omega_l = 1$ Rad/s and a constant linear velocity $\nu_l = 1$ m/s. The initial follower robot position is selected as $q_f = [1.2 \ -1.1 \ \pi/4]^T$ and the initial leader posture is $q_l = [0 \ 0 \ \pi/2]^T$, while the required orientation angle and distance are chosen as $L_d = 1$ m and $\phi_d = 4\pi/3$ Rad.

$$\begin{cases} x_r = -1 + \cos(2\pi t/50) \\ y_r = \sin(2\pi t/50) \end{cases} \tag{4.29}$$

Figure 4.5, shows the formation trajectories based on both DSM and DPSM control schemes. While Figure 4.6 depict a comparison between the formation tracking errors, and the control inputs of the follower robot using the suggested control techniques are illustrated in Figure 4.7.

To compare the formation tracking performances, five error indexes are employed. Namely, mean square error $MSE = \frac{1}{T}\sum_1^T E_f(t)^2$, integral square error $ISE = \int_0^T E_f(t)^2 dt$, integral time square error $ITSE = \int_0^T tE_f(t)^2 dt$, integral time absolute error $ITAE = \int_0^T t|E_f(t)|dt$, and integral absolute error $IAE = \int_0^T |E_f(t)|dt$. Where $E_f(t)$ is given in (4.30) and $T$ is the time of simulation.

$$E_f(t) = x_e(t)^2 + y_e(t)^2 + \theta_e(t)^2 \tag{4.30}$$

The obtained results of the comparison between the formation tracking performances are listed in Table 4.1.

Table 4.1: Comparison between the formation tracking performances .

| | MSE | ISE | ITSE | IAE | ITAE |
|---|---|---|---|---|---|
| DSM | 0.0155 | 0.1211 | 0.0279 | 0.2548 | 0.0667 |
| PDSM | 0.0061 | 0.0463 | 0.0068 | 0.1528 | 0.0362 |

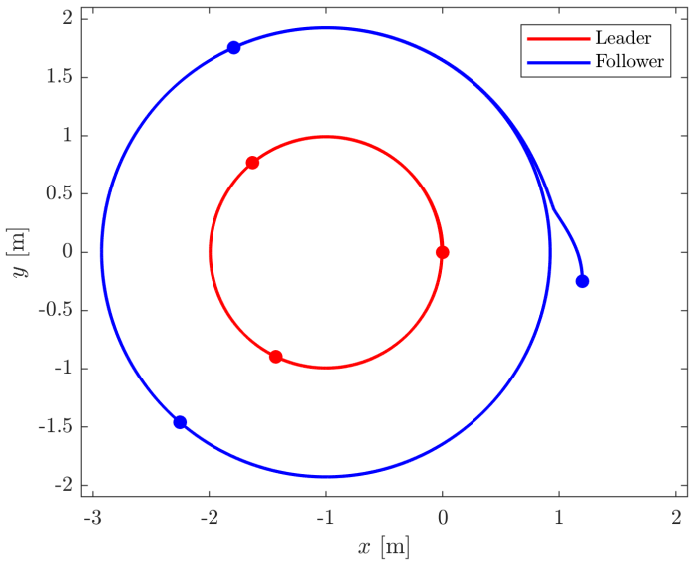


(a)

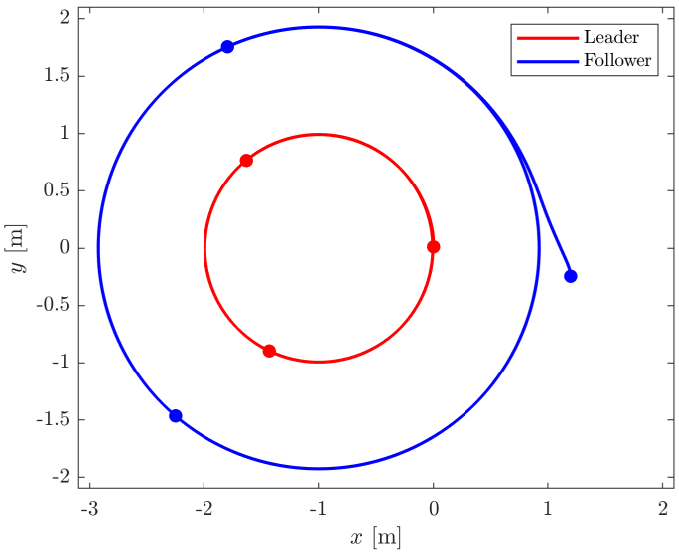


(b)

Figure. 4.5: Comparison between the formation trajectories, (a) using the discrete sliding mode DSM controller, (b) based on the discrete predictive sliding mode PDSM controller.

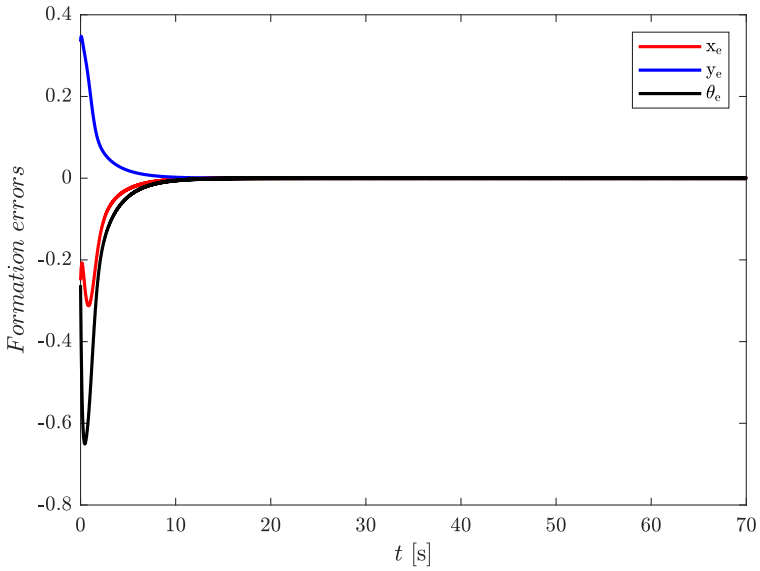


(a)

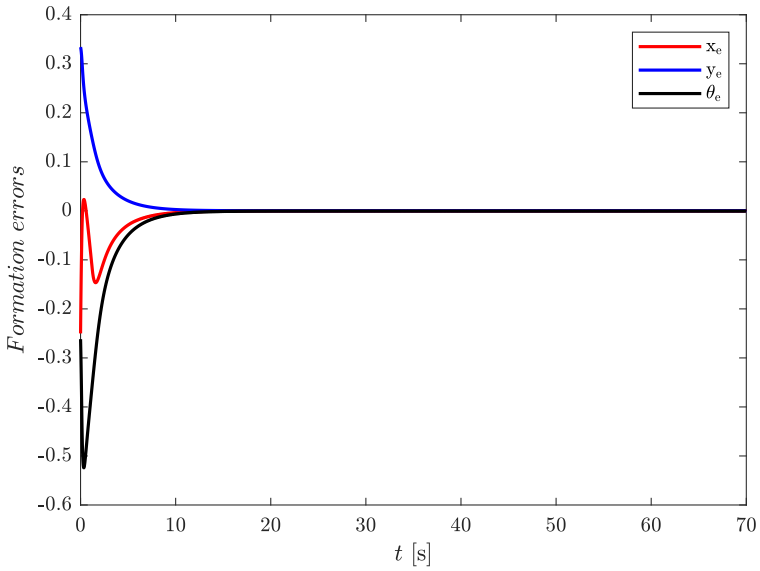


(b)

Figure. 4.6: Comparison between the tracking errors of the follower robot, (a) using the discrete sliding mode DSM controller, (b) based on the discrete predictive sliding mode PDSM controller.

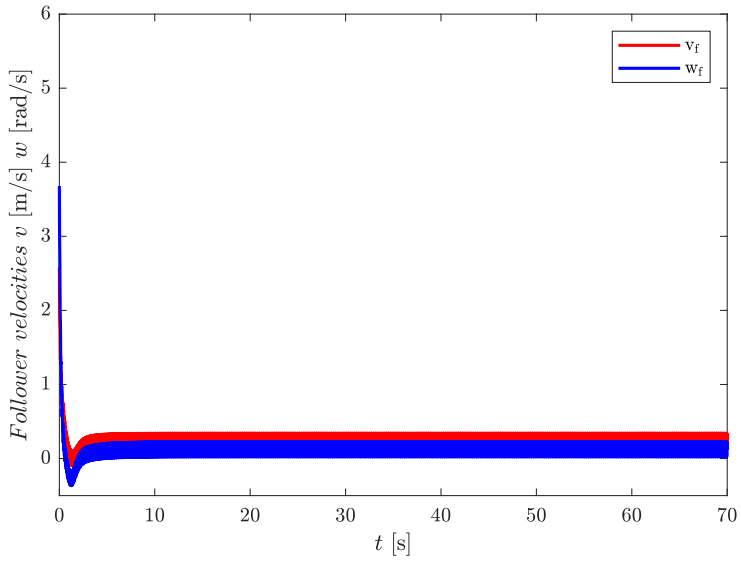


(a)

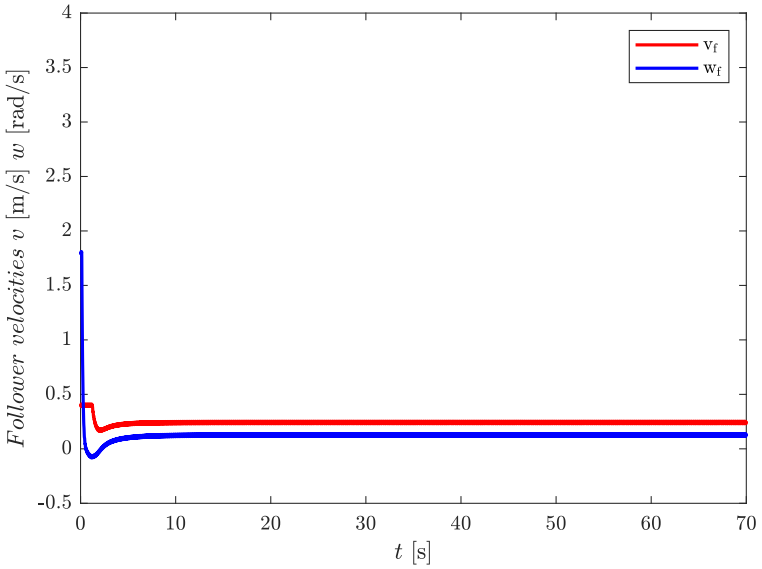


(b)

Figure. 4.7: Comparison between the velocities signals of the follower robots, (a) using the discrete sliding mode DSM controller, (b) based on the discrete predictive sliding mode PDSM controller.

In the first example, the simulation results of the leader-follower formation in an 8-shape trajectory is successfully performed. As shown in Figure 4.2, the follower robot effectively follows the leader, maintaining the required distance and keeping the desired heading angle. The tracking errors of the follower robot steadily decreases until it reaches zero in the presence of the input disturbances, as seen in Figure 4.3. Additionally, Figure 4.4 illustrate that the robot velocities adhere to the imposed constraints without any chattering.

The comparison between the formation trajectories in Figure 4.5 shows that the formation problem is successfully solved based on both proposed control strategies, where the tracking errors gradually reach the origin over time as depicted in Figure 4.6. However, from the control laws of the follower robots illustrated in Figure 4.7, it can be noted that the DPSM control scheme can generate a chattering free control signals that respect the physical input limits of the robot. Moreover, the analysis of the tracking performances in Table 4.1 show that DPSM control technique has a better formation tracking accuracy when compared to the DSM control strategy.

To summarize, the above simulation outcomes indicate that the proposed predictive sliding mode DPSM controller can perform an accurate formation tracking with a practical and chattering free control inputs.

## 4.5 Conclusion

The leader-follower-based formation control for wheeled nonholonomic mobile robots has been addressed in this chapter. Initially, the trajectory following problem was expanded into a formation control problem. Then, by the utilization of linear formation tracking error dynamics, we have designed a discrete sliding mode controller to guide the follower robots in maintaining their formation relative to the leader and achieving the desired spatial geometric configuration. Furthermore, to optimize control efforts and mitigate the challenging chattering phenomenon, we integrated a discrete model predictive control DMPC with the DSM approach. The suggested method efficacy was demonstrated through simulation results and comparative studies.

# CONCLUSION AND FUTURE WORK

In this thesis, the problem of formation control of multiple nonholonomic mobile robots has been addressed, the main aim was the development of new adaptive and robust control laws for the robots that can coordinate their movement to efficiently establish and sustain a desired geometric configuration, while accurately following a predefined paths. And with taking into account the motion constraints subjected to the kinematics of this types of robots and the practical challenges posed by the uncertainties and disturbances commonly encountered in their dynamics.

In this dissertation, different types of control methods has been used together with some formation control approaches in order to achieve the formation control of nonholonomic wheeled mobile robots with a satisfactory and effective performance. The accomplished work can be summarized as follows:

- ✓ A novel robust and stable torque controller has been designed for the formation control of multi nonholonomic wheeled mobile robots, using the leader follower approach and based on both kinematic and dynamic model of the robots. The suggested controller is developed by utilizing a combination of integral sliding mode control ISM, fractional calculus FO and fuzzy logic control. The main objective of this control scheme is to make the follower robots to follow their leader while forming a specific geometric shape under the presence of system un-modeled dynamics, parameter variation and disturbances. According to the simulation and comparison outcomes, the proposed control torques can ensure a chattering free, robust and rapid formation tracking when it compared to the traditional sliding mode controllers.

- ✓ An adaptive distributed formation control laws have been derived to coordinate the movement of swarm of nonholonomic wheeled robots into a predefined formations. First, the graph theory is employed to model the interaction between the robots in the formation in distributed manner, where the relative heading angle and distance between the follower robots and the leader are not anymore required in the control scheme design process. Then, the FTSMC fast terminal sliding Mode control is mixed with fractional calculus theory to derive a robust torque controllers for each robot in order to establish a fast and finite-time convergence toward the required formation pattern. Moreover, An adaptive mechanism is proposed to account the presence of bounded disturbances and uncertainties. the suggested torque controller is compared to the second order consensus algorithm SOCA and the traditional distributed sliding mode control DSMC. The findings showcase the efficacy of the proposed controller.

- ✓ A kinematic leader-follower formation controller has been designed to control the coordination of a team of mobile robots into a desired formation configurations. First, the trajectory tracking problem was transformed into a leader-follower formation problem. Then, a discrete model predictive control DMPC is employed alongside with discrete sliding mode DSM control to drive the follower robots in the formation to track the set of trajectories generated by their leader. Where the use of discrete sliding mode control can ensure robustness against the system kinematic disturbances, while the utilization of model predictive control lead to an improved trajectory tracking and formation maintenance with a constrained control inputs. The simulation outcomes underscore the effectiveness and potential of the proposed control approach in practical scenarios,

There are some challenging open topics to the problems studied in this thesis:

- ✓ In this dissertation, the proposed control algorithms has been examined only through simulation results to confirm the theoretical findings. Hence, in future work, we plan to implement our developed control inputs on real nonholonomic wheeled mobile robots to experimentally validate our theory results.

- ✓ In real-world applications, one of the most significant challenges in formation control algorithms for nonholonomic robots is avoiding collision between the robots during the formation. As well as the dynamic and static obstacles avoidance in unknown environment. Therefore, in future work we shall take into account the issue of formation control with collision and obstacle avoidance.

- ✓ We addressed in this thesis, the formation control of homogeneous wheeld mobile robots where we assumed that all the robots has the same dynamics. However, in practice the robots could have different dynamics sometimes. Hence, Development of formation control algorithms for heterogeneous robots can be investigated in future work.

# REFERENCES


[1] Q. Xu, M. Cai, K. Li, B. Xu, J. Wang, and X. Wu, "Coordinated formation control for intelligent and connected vehicles in multiple traffic scenarios," *IET Intelligent Transport Systems*, vol. 15, no. 1, pp. 159–173, 2021.

[2] M. Carpentiero, L. Gugliermetti, M. Sabatini, and G. B. Palmerini, "A swarm of wheeled and aerial robots for environmental monitoring," in *2017 IEEE 14th international conference on networking, sensing and control (ICNSC)*, pp. 90–95, IEEE, 2017.

[3] A. Yamashita, J. Sasaki, J. Ota, and T. Arai, "Cooperative manipulation of objects by multiple mobile robots with tools," in *Proceedings of the 4th Japan-France/2nd Asia-Europe congress on mechatronics*, vol. 310, p. 315, 1998.

[4] T. Recker, M. Heinrich, and A. Raatz, "A comparison of different approaches for formation control of nonholonomic mobile robots regarding object transport," *Procedia CIRP*, vol. 96, pp. 248–253, 2021.

[5] J. Hu, H. Niu, J. Carrasco, B. Lennox, and F. Arvin, "Voronoi-based multi-robot autonomous exploration in unknown environments via deep reinforcement learning," *IEEE Transactions on Vehicular Technology*, vol. 69, no. 12, pp. 14413–14423, 2020.

[6] C. Lytridis, V. G. Kaburlasos, T. Pachidis, M. Manios, E. Vrochidou, T. Kalampokas, and S. Chatzistamatis, "An overview of cooperative robotics in agriculture," *Agronomy*, vol. 11, no. 9, p. 1818, 2021.

[7] V. Arunkumar, D. Rajasekar, and N. Aishwarya, "A review paper on mobile robots applications in search and rescue operations," *Advances in Science and Technology*, vol. 130, pp. 65–74, 2023.

[8] Y. H. Choi and D. Kim, "Distance-based formation control with goal assignment for global asymptotic stability of multi-robot systems," *IEEE Robotics and Automation Letters*, vol. 6, no. 2, pp. 2020–2027, 2021.

[9] R. W. Beard, J. Lawton, and F. Y. Hadaegh, "A coordination architecture for spacecraft formation control," *IEEE Transactions on control systems technology*, vol. 9, no. 6, pp. 777–790, 2001.

[10] S. Monteiro and E. Bicho, "Attractor dynamics approach to formation control: theory and application," *Autonomous Robots*, vol. 29, pp. 331–355, 2010.

[11] R. Kuppan Chetty, M. Singaperumal, and T. Nagarajan, "Behavior based multi robot formations with active obstacle avoidance based on switching control strategy," in *Advanced Materials Research*, vol. 433, pp. 6630–6635, Trans Tech Publ, 2012.

[12] G. Antonelli, F. Arrichiello, F. Caccavale, and A. Marino, "Decentralized time-varying formation control for multi-robot systems," *The International Journal of Robotics Research*, vol. 33, no. 7, pp. 1029–1043, 2014.

[13] J. Alonso-Mora, S. Baker, and D. Rus, "Multi-robot formation control and object transport in dynamic environments via constrained optimization," *The International Journal of Robotics Research*, vol. 36, no. 9, pp. 1000–1021, 2017.

[14] J. Alonso-Mora, E. Montijano, T. Nägeli, O. Hilliges, M. Schwager, and D. Rus, "Distributed multi-robot formation control in dynamic environments," *Autonomous Robots*, vol. 43, pp. 1079–1100, 2019.

[15] A. Khan, E. Tolstaya, A. Ribeiro, and V. Kumar, "Graph policy gradients for large scale robot control," in *Conference on robot learning*, pp. 823–834, PMLR, 2020.

[16] N. Hacene and B. Mendil, "Behavior-based autonomous navigation and formation control of mobile robots in unknown cluttered dynamic environments with dynamic target tracking," *International Journal of Automation and Computing*, pp. 1–21, 2021.

[17] R. Brooks, "A robust layered control system for a mobile robot," *IEEE journal on robotics and automation*, vol. 2, no. 1, pp. 14–23, 1986.

[18] T. Balch and R. C. Arkin, "Behavior-based formation control for multirobot teams," *IEEE transactions on robotics and automation*, vol. 14, no. 6, pp. 926–939, 1998.

[19] D. Xu, X. Zhang, Z. Zhu, C. Chen, and P. Yang, "Behavior-based formation control of swarm robots," *mathematical Problems in Engineering*, vol. 2014, 2014.

[20] G. Lee and D. Chwa, "Decentralized behavior-based formation control of multiple robots considering obstacle avoidance," *Intelligent Service Robotics*, vol. 11, no. 1, pp. 127–138, 2018.

[21] T. Van Den Broek, N. Van De Wouw, and H. Nijmeijer, "A virtual structure approach to formation control of unicycle mobile robots," *Eindhoven University of Technology, the Netherlands, Tech. Rep. DCT*, vol. 2009, 2009.

[22] A. Sadowska, T. v. den Broek, H. Huijberts, N. van de Wouw, D. Kostić, and H. Nijmeijer, "A virtual structure approach to formation control of unicycle mobile robots using mutual coupling," *International journal of control*, vol. 84, no. 11, pp. 1886–1902, 2011.

[23] C. B. Low, "A flexible virtual structure formation keeping control design for nonholonomic mobile robots with low-level control systems, with experiments," in *2014 IEEE international symposium on intelligent control (ISIC)*, pp. 1576–1582, IEEE, 2014.

[24] C. B. Low, "Adaptable virtual structure formation tracking control design for nonholonomic tracked mobile robots, with experiments," in *2015 IEEE 18th International Conference on Intelligent Transportation Systems*, pp. 1868–1875, IEEE, 2015.

[25] Q. Qin, T.-S. Li, C. Liu, C. Philip Chen, and M. Han, "Virtual structure formation control via sliding mode control and neural networks," in *Advances in Neural Networks-ISNN 2017: 14th International Symposium, ISNN 2017, Sapporo, Hakodate, and Muroran, Hokkaido, Japan, June 21–26, 2017, Proceedings, Part II 14*, pp. 101–108, Springer, 2017.

[26] N. Nfaileh, K. Alipour, B. Tarvirdizadeh, and A. Hadi, "Formation control of multiple wheeled mobile robots based on model predictive control," *Robotica*, vol. 40, no. 9, pp. 3178–3213, 2022.

[27] K.-H. Tan and M. A. Lewis, "Virtual structures for high-precision cooperative mobile robotic control," in *Proceedings of IEEE/RSJ International Conference on Intelligent Robots and Systems. IROS'96*, vol. 1, pp. 132–139, IEEE, 1996.

[28] L. Dong, Y. Chen, and X. Qu, "Formation control strategy for nonholonomic intelligent vehicles based on virtual structure and consensus approach," *Procedia engineering*, vol. 137, pp. 415–424, 2016.

[29] L. Chen and M. Baoli, "A nonlinear formation control of wheeled mobile robots with virtual structure approach," in *2015 34th Chinese Control Conference (CCC)*, pp. 1080–1085, IEEE, 2015.

[30] X. Chen, F. Huang, Y. Zhang, Z. Chen, S. Liu, Y. Nie, J. Tang, and S. Zhu, "A novel virtual-structure formation control design for mobile robots with obstacle avoidance," *Applied Sciences*, vol. 10, no. 17, p. 5807, 2020.

[31] Z. Yang, S. Zhu, C. Chen, G. Feng, and X. Guan, "Leader-follower formation control of nonholonomic mobile robots with bearing-only measurements," *Journal of the Franklin Institute*, vol. 357, no. 3, pp. 1628–1643, 2020.

[32] J. Hirata-Acosta, J. Pliego-Jiménez, C. Cruz-Hernádez, and R. Martínez-Clark, "Leader-follower formation control of wheeled mobile robots without attitude measurements," *Applied Sciences*, vol. 11, no. 12, p. 5639, 2021.

[33] S. Moorthy and Y. H. Joo, "Formation control and tracking of mobile robots using distributed estimators and a biologically inspired approach," *Journal of Electrical Engineering & Technology*, pp. 1–14, 2022.

[34] X. Huang, Z. Li, and F. L. Lewis, "Cost-effective distributed ftfc for uncertain nonholonomic mobile robot fleet with collision avoidance and connectivity preservation," *Journal of Automation and Intelligence*, vol. 2, no. 1, pp. 42–50, 2023.

[35] J. P. Desai, J. P. Ostrowski, and V. Kumar, "Modeling and control of formations of nonholonomic mobile robots," *IEEE transactions on Robotics and Automation*, vol. 17, no. 6, pp. 905–908, 2001.

[36] Z. Peng, G. Wen, A. Rahmani, and Y. Yu, "Leader–follower formation control of nonholonomic mobile robots based on a bioinspired neurodynamic based approach," *Robotics and autonomous systems*, vol. 61, no. 9, pp. 988–996, 2013.

[37] X. Liang, H. Wang, Y.-H. Liu, W. Chen, and T. Liu, "Formation control of nonholonomic mobile robots without position and velocity measurements," *IEEE Transactions on Robotics*, vol. 34, no. 2, pp. 434–446, 2017.

[38] Z. Miao, Y.-H. Liu, Y. Wang, G. Yi, and R. Fierro, "Distributed estimation and control for leader-following formations of nonholonomic mobile robots," *IEEE Transactions on Automation Science and Engineering*, vol. 15, no. 4, pp. 1946–1954, 2018.

[39] S.-L. Dai, S. He, X. Chen, and X. Jin, "Adaptive leader–follower formation control of nonholonomic mobile robots with prescribed transient and steady-state performance," *IEEE Transactions on Industrial Informatics*, vol. 16, no. 6, pp. 3662–3671, 2019.

[40] X. Liang, H. Wang, Y.-H. Liu, Z. Liu, and W. Chen, "Leader-following formation control of nonholonomic mobile robots with velocity observers," *IEEE/ASME Transactions on Mechatronics*, vol. 25, no. 4, pp. 1747–1755, 2020.

[41] K.-K. Oh, M.-C. Park, and H.-S. Ahn, "A survey of multi-agent formation control," *Automatica*, vol. 53, pp. 424–440, 2015.

[42] E. D. Ferreira-Vazquez, E. G. Hernández-Martínez, J.-J. Flores-Godoy, G. Fernandez-Anaya, and P. Paniagua-Contro, "Distance-based formation control using angular information between robots," *Journal of Intelligent & Robotic Systems*, vol. 83, pp. 543–560, 2016.

[43] Z. Chen, C. Jiang, and Y. Guo, "Distance-based formation control of a three-robot system," in *2019 Chinese Control And Decision Conference (CCDC)*, pp. 5501–5507, IEEE, 2019.

[44] F. Sahebsara and M. de Queiroz, "Distance-based formation maneuvering of mobile robots with static obstacles," in *2022 IEEE Conference on Control Technology and Applications (CCTA)*, pp. 470–475, IEEE, 2022.

[45] C.-S. Lee, U.-S. Suh, K.-M. Lee, I.-H. Whang, and W.-S. Ra, "Practical distance-based multi-robot formation control using low-cost ultrasonic source tracker," *Journal of Electrical Engineering & Technology*, pp. 1–18, 2023.

[46] A. Sanchez-Sanchez, E. Hernandez-Martinez, J. González-Sierra, M. Ramírez-Neria, J. Flores-Godoy, E. Ferreira-Vazquez, and G. Fernandez-Anaya, "Leader-follower power-based formation control applied to differential-drive mobile robots," *Journal of Intelligent & Robotic Systems*, vol. 107, no. 1, p. 6, 2023.

[47] Z. Peng, S. Yang, G. Wen, A. Rahmani, and Y. Yu, "Adaptive distributed formation control for multiple nonholonomic wheeled mobile robots," *Neurocomputing*, vol. 173, pp. 1485–1494, 2016.

[48] Z. Peng, G. Wen, S. Yang, and A. Rahmani, "Distributed consensus-based formation control for nonholonomic wheeled mobile robots using adaptive neural network," *Nonlinear Dynamics*, vol. 86, pp. 605–622, 2016.

[49] S. Yang, Y. Cao, Z. Peng, G. Wen, and K. Guo, "Distributed formation control of nonholonomic autonomous vehicle via rbf neural network," *Mechanical Systems and Signal Processing*, vol. 87, pp. 81–95, 2017.

[50] X. Chu, Z. Peng, G. Wen, and A. Rahmani, "Distributed formation tracking of multi-robot systems with nonholonomic constraint via event-triggered approach," *Neurocomputing*, vol. 275, pp. 121–131, 2018.

[51] B. Kada, A. S. Balamesh, K. A. Juhany, and I. M. Al-Qadi, "Distributed cooperative control for nonholonomic wheeled mobile robot systems," *International Journal of Systems Science*, vol. 51, no. 9, pp. 1528–1541, 2020.

[52] M.-C. Park and H.-S. Ahn, "Displacement estimation by range measurements and application to formation control," in *2015 IEEE International Symposium on Intelligent Control (ISIC)*, pp. 888–893, IEEE, 2015.

[53] X. Liu, S. S. Ge, and C.-H. Goh, "Vision-based leader–follower formation control of multiagents with visibility constraints," *IEEE Transactions on Control Systems Technology*, vol. 27, no. 3, pp. 1326–1333, 2018.

[54] Q. Yao, S. Liu, and N. Huang, "Displacement-based formation control with phase synchronization in a time-invariant flow field," in *2018 IEEE 8th Annual International Conference on CYBER Technology in Automation, Control, and Intelligent Systems (CYBER)*, pp. 486–491, IEEE, 2018.

[55] R. S. Sharma, A. Mondal, and L. Behera, "Tracking control of mobile robots in formation in the presence of disturbances," *IEEE Transactions on Industrial Informatics*, vol. 17, no. 1, pp. 110–123, 2020.

[56] H. G. de Marina, "Maneuvering and robustness issues in undirected displacement-consensus-based formation control," *IEEE Transactions on Automatic Control*, vol. 66, no. 7, pp. 3370–3377, 2020.

[57] H. Li, H. Chen, and X. Wang, "Relative displacement measurement based affine formation tracking control for nonholonomic kinematic agents," in *2022 IEEE International Conference on Robotics and Biomimetics (ROBIO)*, pp. 195–200, IEEE, 2022.

[58] H. M. Güzey, T. Dierks, S. Jagannathan, and L. Acar, "Hybrid consensus-based control of nonholonomic mobile robot formation," *Journal of Intelligent & Robotic Systems*, vol. 88, pp. 181–200, 2017.

[59] M. Maghenem, A. Loría, E. Nuno, and E. Panteley, "Consensus-based formation control of networked nonholonomic vehicles with delayed communications," *IEEE Transactions on Automatic Control*, vol. 66, no. 5, pp. 2242–2249, 2020.

[60] T. Hernández, A. Loria, E. Nuño, and E. Panteley, "Consensus-based formation control of nonholonomic robots without velocity measurements," in *2020 European Control Conference (ECC)*, pp. 674–679, IEEE, 2020.

[61] J. G. Romero, E. Nuño, and C. I. Aldana, "Robust pid consensus-based formation control of nonholonomic mobile robots affected by disturbances," *International Journal of Control*, pp. 1–9, 2021.

[62] J. G. Romero, E. Nuño, E. Restrepo, and I. Sarras, "Global consensus-based formation control of nonholonomic mobile robots with time-varying delays and without velocity measurements," *IEEE Transactions on Automatic Control*, 2023.

[63] M. H. Yamchi and R. M. Esfanjani, "Distributed predictive formation control of networked mobile robots subject to communication delay," *Robotics and Autonomous Systems*, vol. 91, pp. 194–207, 2017.

[64] H. Xiao and C. P. Chen, "Leader-follower consensus multi-robot formation control using neurodynamic-optimization-based nonlinear model predictive control," *IEEE access*, vol. 7, pp. 43581–43590, 2019.

[65] W. Shang, H. Zhu, Y. Pan, X. Li, and D. Zhang, "A distributed model predictive control for multiple mobile robots with the model uncertainty," *Discrete Dynamics in Nature and Society*, vol. 2021, pp. 1–22, 2021.

[66] H. Xiao and C. P. Chen, "Time-varying nonholonomic robot consensus formation using model predictive based protocol with switching topology," *Information Sciences*, vol. 567, pp. 201–215, 2021.

[67] J. Wei and B. Zhu, "Model predictive control for trajectory-tracking and formation of wheeled mobile robots," *Neural Computing and Applications*, vol. 34, no. 19, pp. 16351–16365, 2022.

[68] C. Shinde, K. Das, S. Kumar, and L. Behera, "Distributed reinforcement learning based optimal controller for mobile robot formation," in *2018 European Control Conference (ECC)*, pp. 2800–2805, IEEE, 2018.

[69] C. Jiang, Z. Chen, and Y. Guo, "Learning decentralized control policies for multi-robot formation," in *2019 IEEE/ASME International Conference on Advanced Intelligent Mechatronics (AIM)*, pp. 758–765, IEEE, 2019.

[70] X. Zhang, Y. Peng, W. Pan, X. Xu, and H. Xie, "Barrier function-based safe reinforcement learning for formation control of mobile robots," in *2022 International Conference on Robotics and Automation (ICRA)*, pp. 5532–5538, IEEE, 2022.

[71] G. Khodamipour, S. Khorashadizadeh, and M. Farshad, "Adaptive formation control of leader-follower mobile robots using reinforcement learning and the fourier series expansion," *ISA transactions*, 2023.

[72] K. Oldham and J. Spanier, *The fractional calculus theory and applications of differentiation and integration to arbitrary order*. Elsevier, 1974.

[73] S. Das, *Functional fractional calculus*. Springer Science & Business Media, 2011.

[74] G. Klancar, A. Zdesar, S. Blazic, and I. Skrjanc, *Wheeled mobile robotics: from fundamentals towards autonomous systems*. Butterworth-Heinemann, 2017.

[75] H.-M. Wu, M. Karkoub, and C.-L. Hwang, "Mixed fuzzy sliding-mode tracking with backstepping formation control for multi-nonholonomic mobile robots subject to uncertainties," *Journal of Intelligent & Robotic Systems*, vol. 79, no. 1, pp. 73–86, 2015.

[76] D. Qian, S. Tong, J. Guo, and S. Lee, "Leader-follower-based formation control of nonholonomic mobile robots with mismatched uncertainties via integral sliding mode," *Proceedings of the Institution of Mechanical Engineers, Part I: Journal of Systems and Control Engineering*, vol. 229, no. 6, pp. 559–569, 2015.

[77] M. Asif, M. J. Khan, and A. Y. Memon, "Integral terminal sliding mode formation control of non-holonomic robots using leader follower approach," *Robotica*, vol. 35, no. 7, pp. 1473–1487, 2017.

[78] Y. Zhao, Y. Zhang, and J. Lee, "Lyapunov and sliding mode based leader-follower formation control for multiple mobile robots with an augmented distance-angle strategy," *International Journal of Control, Automation and Systems*, vol. 17, no. 5, pp. 1314–1321, 2019.

[79] C.-Y. Chen, T.-H. S. Li, Y.-C. Yeh, and C.-C. Chang, "Design and implementation of an adaptive sliding-mode dynamic controller for wheeled mobile robots," *Mechatronics*, vol. 19, no. 2, pp. 156–166, 2009.

[80] H. Xiao, Z. Li, and C. P. Chen, "Formation control of leader–follower mobile robots' systems using model predictive control based on neural-dynamic optimization," *IEEE Transactions on Industrial Electronics*, vol. 63, no. 9, pp. 5752–5762, 2016.

[81] T. Eren, "Formation shape control based on bearing rigidity," *International Journal of Control*, vol. 85, no. 9, pp. 1361–1379, 2012.

[82] R. R. Nair, H. Karki, A. Shukla, L. Behera, and M. Jamshidi, "Fault-tolerant formation control of nonholonomic robots using fast adaptive gain nonsingular terminal sliding mode control," *IEEE Systems Journal*, vol. 13, no. 1, pp. 1006–1017, 2018.

[83] O. W. Abdulwahhab and N. H. Abbas, "Design and stability analysis of a fractional order state feedback controller for trajectory tracking of a differential drive robot," *International Journal of Control, Automation and Systems*, vol. 16, no. 6, pp. 2790–2800, 2018.

[84] Y. Xie, X. Zhang, W. Meng, S. Zheng, L. Jiang, J. Meng, and S. Wang, "Coupled fractional-order sliding mode control and obstacle avoidance of a four-wheeled steerable mobile robot," *ISA transactions*, vol. 108, pp. 282–294, 2021.

[85] K. Singhal, V. Kumar, and K. Rana, "Robust trajectory tracking control of non-holonomic wheeled mobile robots using an adaptive fractional order parallel fuzzy pid controller," *Journal of the Franklin Institute*, 2022.

[86] R. Cajo, M. Guinaldo, E. Fabregas, S. Dormido, D. Plaza, R. De Keyser, and C. Ionescu, "Distributed formation control for multiagent systems using a fractional-order proportional–integral structure," *IEEE Transactions on Control Systems Technology*, vol. 29, no. 6, pp. 2738–2745, 2021.

[87] K. K. Ayten, M. H. Çiplak, and A. Dumlu, "Implementation a fractional-order adaptive model-based pid-type sliding mode speed control for wheeled mobile robot," *Proceedings of the Institution of Mechanical Engineers, Part I: Journal of Systems and Control Engineering*, vol. 233, no. 8, pp. 1067–1084, 2019.

[88] D. Baleanu, K. Diethelm, E. Scalas, and J. J. Trujillo, *Fractional calculus: models and numerical methods*, vol. 3. World Scientific, 2012.

[89] K. H. Kowdiki, R. K. Barai, and S. Bhattacharya, "Autonomous leader-follower formation control of non-holonomic wheeled mobile robots by incremental path planning and sliding mode augmented tracking control," *International Journal of Systems, Control and Communications*, vol. 10, no. 3, pp. 191–217, 2019.

[90] H. Xiao, C. P. Chen, G. Lai, D. Yu, and Y. Zhang, "Integrated nonholonomic multi-robot consensus tracking formation using neural-network-optimized distributed model predictive control strategy," *Neurocomputing*, vol. 518, pp. 282–293, 2023.

[91] W. Wang, J. Huang, C. Wen, and H. Fan, "Distributed adaptive control for consensus tracking with application to formation control of nonholonomic mobile robots," *Automatica*, vol. 50, no. 4, pp. 1254–1263, 2014.

[92] S. Moorthy and Y. H. Joo, "Distributed leader-following formation control for multiple nonholonomic mobile robots via bioinspired neurodynamic approach," *Neurocomputing*, vol. 492, pp. 308–321, 2022.

[93] S. I. Han, "Prescribed consensus and formation error constrained finite-time sliding mode control for multi-agent mobile robot systems," *IET Control Theory & Applications*, vol. 12, no. 2, pp. 282–290, 2018.

[94] C.-C. Tsai, Y.-X. Li, and F.-C. Tai, "Backstepping sliding-mode leader-follower consensus formation control of uncertain networked heterogeneous nonholonomic wheeled mobile multirobots," in *2017 56th Annual Conference of the Society of Instrument and Control Engineers of Japan (SICE)*, pp. 1407–1412, IEEE, 2017.

[95] R. Rahmani, H. Toshani, and S. Mobayen, "Consensus tracking of multi-agent systems using constrained neural-optimiser-based sliding mode control," *International Journal of Systems Science*, vol. 51, no. 14, pp. 2653–2674, 2020.

[96] J. Wang, H. Wang, M. Zhou, and S. Ju, "Distributed fault-tolerant formation control of nonholonomic mobile robots with ssa parameter optimization," in *Intelligent Networked Things: 5th China Conference, CINT 2022, Urumqi, China, August 7-8, 2022, Revised Selected Papers*, pp. 221–234, Springer, 2023.

[97] R. Afdila, F. Fahmi, and A. Sani, "Distributed formation control for groups of mobile robots using consensus algorithm," *Bulletin of Electrical Engineering and Informatics*, vol. 12, no. 4, pp. 2095–2104, 2023.

[98] N. Le-Dung, P. Huynh-Lam, N. Hoang-Giap, and N. Tan-Luy, "Event-triggered distributed robust optimal control of nonholonomic mobile agents with obstacle avoidance formation, input constraints and external disturbances," *Journal of the Franklin Institute*, vol. 360, no. 8, pp. 5564–5587, 2023.

[99] Y.-H. Chang, C.-Y. Yang, W.-S. Chan, H.-W. Lin, and C.-W. Chang, "Adaptive fuzzy sliding-mode formation controller design for multi-robot dynamic systems.," *International Journal of Fuzzy Systems*, vol. 16, no. 1, 2014.

[100] X. Chu, Z. Peng, G. Wen, and A. Rahmani, "Robust fixed-time consensus tracking with application to formation control of unicycles," *IET Control Theory & Applications*, vol. 12, no. 1, pp. 53–59, 2018.

[101] Y. Cheng, R. Jia, H. Du, G. Wen, and W. Zhu, "Robust finite-time consensus formation control for multiple nonholonomic wheeled mobile robots via output feedback," *International Journal of Robust and Nonlinear Control*, vol. 28, no. 6, pp. 2082–2096, 2018.

[102] Y.-H. Chang, C.-W. Chang, C.-L. Chen, and C.-W. Tao, "Fuzzy sliding-mode formation control for multirobot systems: design and implementation," *IEEE Transactions on Systems, Man, and Cybernetics, Part B (Cybernetics)*, vol. 42, no. 2, pp. 444–457, 2011.

[103] T.-L. Liao, J.-J. Yan, and W.-S. Chan, "Distributed sliding-mode formation controller design for multirobot dynamic systems," *Journal of Dynamic Systems, Measurement, and Control*, vol. 139, no. 6, p. 061008, 2017.

[104] B. R. W. REN W, "Distributed consensus in multi-vehicle cooperative control: theory and applications," *Springer, London*, 2007.

[105] X. Yu and L. Liu, "Leader-follower formation of vehicles with velocity constraints and local coordinate frames," *Science China Information Sciences*, vol. 60, pp. 1–15, 2017.

[106] G. Wen, C. P. Chen, Y.-J. Liu, and Z. Liu, "Neural network-based adaptive leader-following consensus control for a class of nonlinear multiagent state-delay systems," *IEEE transactions on cybernetics*, vol. 47, no. 8, pp. 2151–2160, 2016.

[107] C.-E. Ren, L. Chen, and C. P. Chen, "Adaptive fuzzy leader-following consensus control for stochastic multiagent systems with heterogeneous nonlinear dynamics," *IEEE Transactions on Fuzzy Systems*, vol. 25, no. 1, pp. 181–190, 2016.

[108] C.-E. Ren and C. P. Chen, "Sliding mode leader-following consensus controllers for second-order non-linear multi-agent systems," *IET Control Theory & Applications*, vol. 9, no. 10, pp. 1544–1552, 2015.

[109] J. Chen, D. Sun, J. Yang, and H. Chen, "Leader-follower formation control of multiple non-holonomic mobile robots incorporating a receding-horizon scheme," *The International Journal of Robotics Research*, vol. 29, no. 6, pp. 727–747, 2010.

[110] S. Lin, R. Jia, M. Yue, and Y. Xu, "On composite leader–follower formation control for wheeled mobile robots with adaptive disturbance rejection," *Applied Artificial Intelligence*, vol. 33, no. 14, pp. 1306–1326, 2019.

[111] D. Shen, W. Sun, and Z. Sun, "Adaptive pid formation control of nonholonomic robots without leader's velocity information," *ISA transactions*, vol. 53, no. 2, pp. 474–480, 2014.

[112] H. Iima and Y. Kuroe, "Swarm reinforcement learning methods improving certainty of learning for a multi-robot formation problem," in *2015 IEEE Congress on Evolutionary Computation (CEC)*, pp. 3026–3033, IEEE, 2015.

[113] W. Zheng and Y. Jia, "Leader-follower formation control of mobile robots with sliding mode.," *J. Robotics Netw. Artif. Life*, vol. 4, no. 1, pp. 10–13, 2017.

[114] M. Defoort, T. Floquet, A. Kokosy, and W. Perruquetti, "Sliding-mode formation control for cooperative autonomous mobile robots," *IEEE Transactions on Industrial Electronics*, vol. 55, no. 11, pp. 3944–3953, 2008.

[115] W. J. N. Goto and N. Martins, "Leader-follower formation tracking for differential-drive wheeled mobile robots with uncertainties and disturbances based on immune fuzzy quasi-sliding mode control," 2023.

[116] D. Elayaperumal and Y. H. Joo, "Robust swarm formation for multiple nonholonomic two-wheeled mobile robots using leader–follower approach via sliding mode controller and neural dynamic model," *Journal of Electrical Engineering & Technology*, vol. 18, no. 3, pp. 2245–2252, 2023.

[117] D. Gu and H. Hu, "A model predictive controller for robots to follow a virtual leader," *Robotica*, vol. 27, no. 6, pp. 905–913, 2009.

[118] S.-M. Lee, H. Kim, H. Myung, and X. Yao, "Cooperative coevolutionary algorithm-based model predictive control guaranteeing stability of multirobot formation," *IEEE Transactions on Control Systems Technology*, vol. 23, no. 1, pp. 37–51, 2014.

[119] H. Xiao and C. P. Chen, "Leader-follower multi-robot formation system using model predictive control method based on particle swarm optimization," in *2017 32nd Youth Academic Annual Conference of Chinese Association of Automation (YAC)*, pp. 480–484, IEEE, 2017.

[120] N. A. Martins, E. S. Elyoussef, D. W. Bertol, E. R. De Pieri, U. F. Moreno, and E. B. Castelan, "Nonholonomic mobile robot with kinematic disturbances in the trajectory tracking: a variable structure controller," *Learning and Nonlinear Models*, vol. 8, no. 1, pp. 23–40, 2010.

[121] K. L. Besseghieur, R. Trębiński, W. Kaczmarek, and J. Panasiuk, "Leader-follower formation control for a group of ros-enabled mobile robots," in *2019 6th International Conference on Control, Decision and Information Technologies (CoDIT)*, pp. 1556–1561, IEEE, 2019.

[122] Y. Kanayama, Y. Kimura, F. Miyazaki, and T. Noguchi, "A stable tracking control method for a non-holonomic mobile robot.," in *IROS*, pp. 1236–1241, 1991.

[123] G. Klančar and I. Škrjanc, "Tracking-error model-based predictive control for mobile robots in real time," *Robotics and autonomous systems*, vol. 55, no. 6, pp. 460–469, 2007.

[124] W. Gao, Y. Wang, and A. Homaifa, "Discrete-time variable structure control systems," *IEEE transactions on Industrial Electronics*, vol. 42, no. 2, pp. 117–122, 1995.